

DISS. ETH Nr. 20345

NOVEL IMMUNOCYTOKINES FOR CANCER THERAPY

A dissertation submitted to the

ETH Zürich

for the degree of

Doctor of Sciences

presented by

NADINE PASCHE

MSc Pharmaceutical Sciences, ETH Zürich

Born November 2, 1984

Citizen of Ferlens (VD)

accepted on the recommendation of

Prof. Dr. Dario Neri, examiner

Prof. Dr. Cornelia Halin, co-examiner

2012

To my Family

and

To Mattia

Table of Contents

1. Summary	8
2. Introduction	14
2.1. Intact and armed antibodies in cancer therapy	14
2.2. Cytokines in cancer therapy	16
2.3. Extracellular matrix components as tumor-associated antigens	17
2.4. Immunocytokines: a promising class of armed antibodies	18
2.5. Immunocytokines formats and biodistribution data	19
2.6. Selected preclinical findings	21
2.6.1. Monotherapy	21
2.6.2. Combination therapy	27
2.7. Immunocytokines in clinical development	28
2.8. Promising immune modulators for immunocytokine development	31
2.8.1. Interleukin 7	31
2.8.2. Interleukin 12	32
2.8.3. Interleukin 17	34
2.8.4. Interleukin 18	36
2.9. Aim of the thesis	37
3. Results	39
3.1. Immunocytokines based on murine Interleukin 7	39
3.1.1. Cloning and characterization of F8-mIL7	39
3.1.1.1. Cloning and expression	39
3.1.1.2. In vitro characterization	40
3.1.1.2.1. SDS-PAGE	40
3.1.1.2.2. Size exclusion chromatography	41
3.1.1.2.3. BIAcore analysis	41
3.1.1.2.4. Immunofluorescence analysis on tumor sections	42
3.1.1.3. In vivo characterization	42

3.1.1.3.1.	Biodistribution studies on F9 teratocarcinoma bearing immunocompetent and athymic mice	42
3.1.1.3.2.	Therapeutic properties on F9 teratocarcinoma bearing immunocompetent and athymic mice	44
3.1.2.	Cloning and characterization of novel formats for mIL7-based immunocytokines	45
3.1.2.1.	Cloning and expression	45
3.1.2.2.	In vitro characterization	46
3.1.2.2.1.	SDS-PAGE	46
3.1.2.2.2.	Size exclusion chromatography of F8-mIL7-F8 and KSF-mIL7-KSF	48
3.1.2.2.3.	BIAcore analysis of F8-mIL7-F8	48
3.1.2.2.4.	F8-mIL7-F8 and KSF-mIL7-KSF immunofluorescence analysis on tumor sections	49
3.1.2.2.5.	F8-mIL7-F8 and KSF-mIL7-KSF stability	49
3.1.2.2.6.	F8-mIL7-F8 and KSF-mIL7-KSF bioactivity assay	50
3.1.2.3.	In vivo characterization of F8-mIL7-F8 and KSF-mIL7-KSF	50
3.1.2.3.1.	Biodistribution studies on F9 teratocarcinoma bearing immunocompetent mice	50
3.1.2.3.2.	Therapeutic properties on F9 teratocarcinoma bearing immunocompetent mice	51
3.2.	Immunocytokine based on murine Interleukin 17	53
3.2.1.	Cloning and characterization of F8-mIL17	53
3.2.1.1.	Cloning and expression	53
3.2.1.2.	In vitro characterization	54
3.2.1.2.1.	SDS-PAGE	54
3.2.1.2.2.	Size exclusion chromatography	55
3.2.1.2.3.	BIAcore analysis on EDA coated chip	55
3.2.1.2.4.	Bioactivity assay	56
3.2.1.2.5.	Immunofluorescence analysis on tumor sections	56
3.2.2.	In vivo characterization	57
3.2.2.1.	Biodistribution studies in F9 teratocarcinoma bearing immunocompetent and athymic mice	57

3.2.2.2. Therapeutic properties in F9 teratocarcinoma bearing immunocompetent and athymic mice	58
3.2.2.3. Infiltration studies in F9 teratocarcinoma bearing immunocompetent mice	59
3.2.2.4. Blood vessels density studies in F9 teratocarcinoma bearing immunocompetent mice	61
3.3. Immunocytokines based on murine Interleukin 18	62
3.3.1. Cloning and characterization of F8-mIL18	62
3.3.1.1. Cloning and expression	62
3.3.1.2. In vitro characterization	62
3.3.1.2.1. SDS-PAGE	62
3.3.1.2.2. Size exclusion chromatography	63
3.3.1.2.3. BIAcore analysis on EDA coated chip	64
3.3.1.2.4. Immunofluorescence analysis on tumor sections	64
3.3.1.3. In vivo characterization	65
3.3.1.3.1. Biodistribution studies on F9 teratocarcinoma bearing immunocompetent and athymic mice	65
3.3.1.3.2. Therapeutic properties on F9 teratocarcinoma bearing immunocompetent and athymic mice	66
3.3.2. Cloning and characterization of mIL18	68
3.3.3. Cloning and characterization of cysteine to serine mutants of F8-mIL18	68
3.3.4. Cloning and characterization of novel formats for mIL18-based immunocytokines	70
3.3.4.1. Cloning and expression of F8-mIL18 with 6 amino acids linker	70
3.3.4.2. Cloning, expression and in vitro characterization of F8-mIL18-F8	71
3.3.4.2.1. Cloning and expression	71
3.3.4.2.2. SDS-PAGE	72
3.3.4.2.3. Size exclusion chromatography	73
3.3.4.3. Cloning, expression and in vitro characterization of mIL18-F8	73
3.3.4.3.1. Cloning and expression	73
3.3.4.3.2. SDS-PAGE	74
3.3.4.3.3. Size exclusion chromatography	75

3.4. Immunocytokines based on murine Interleukin 12	77
3.4.1. Cloning and expression of mL12-F8-F8 and mL12-KSF-KSF	77
3.4.2. In vitro characterization of mL12 fusion proteins	78
3.4.2.1. SDS-PAGE	78
3.4.2.2. Size exclusion chromatography	79
3.4.2.3. BIAcore analysis on EDA coated chip	79
3.4.2.4. Immunofluorescence analysis on tumor sections	80
3.4.2.5. Stability	80
3.4.2.6. Blood binding assay	81
3.4.3. In vivo characterization	81
3.4.3.1. Biodistribution studies on F9 teratocarcinoma bearing immunocompetent mice	81
3.4.3.2. Therapeutic properties	82
3.4.3.2.1. F9 teratocarcinoma bearing immunocompetent mice	82
3.4.3.2.1.1. mL12-F8-F8 as monotherapy	82
3.4.3.2.1.2. mL12-F8-F8 intratumoral injections	83
3.4.3.2.1.3. Combination therapies	84
3.4.3.2.1.3.1. mL12-F8-F8 and F8-IL2	84
3.4.3.2.1.3.2. mL12-F8-F8 and paclitaxel	86
3.4.3.2.2. Combination therapy of mL12-F8-F8 and Paclitaxel on CT26 teratocarcinoma bearing immunocompetent mice	88
4. Materials and methods	90
4.1. Cell lines and animals	90
4.2. Cloning of fusion proteins	90
4.2.1. Cloning of murine Interleukin 7 based immunocytokines	90
4.2.2. Cloning of murine Interleukin 17 based immunocytokine	92
4.2.3. Cloning of murine Interleukin 18 based immunocytokines	92
4.2.4. Cloning of murine Interleukin 12 based immunocytokines	95
4.3. Expression, purification and characterization of immunocytokines	96
4.4. Western blot analysis	97
4.5. Deglycosilation	97

4.6. Stability	98
4.7. Bioactivity assays	98
4.7.1. Murine Interleukin 7 bioactivity assay	98
4.7.2. Murine Interleukin 17 bioactivity assay	98
4.8. Immunofluorescence analysis on tumor sections	99
4.9. Quantitative biodistribution studies	99
4.9.1. Murine Interleukin 7 based immunocytokines	99
4.9.2. Murine Interleukin 17 based immunocytokine	100
4.9.3. Murine Interleukin 18 based immunocytokines	100
4.9.4. Murine Interleukin 12 based immunocytokines	100
4.10. Syngeneic tumor mouse models in immunocompetent and athymic mice	100
4.10.1. Murine Interleukin 7 based immunocytokines	101
4.10.2. Murine Interleukin 17 based immunocytokine	101
4.10.3. Murine Interleukin 18 based immunocytokines	101
4.10.4. Murine Interleukin 12 based immunocytokines	101
5. Discussion	103
6. Conclusions and outlook	107
7. References	110
8. Curriculum vitae	125
9. Acknowledgments	128

1. SUMMARY

Several cytokines have been investigated in clinical trials, based on their potent therapeutic activity observed in animal models of cancer and other diseases. However, substantial toxicities are often observed at low doses, thus preventing escalation to therapeutically active regimens. The use of recombinant antibodies or antibody fragments as delivery vehicles promises to greatly enhance the therapeutic index of pro-inflammatory cytokines.

Antibody-mediated pharmacodelivery strategies have been reported for many cytokines, including Interleukin 2 (IL2), Interleukin 10 (IL10), Interleukin 12 (IL12), Interleukin 15 (IL15), Granulocyte macrophage colony stimulating factor (GM-CSF), Interferon alpha (IFN α), Interferon gamma (IFN γ) and Tumor necrosis factor (TNF).

Indeed, a number of antibody-cytokine fusion proteins (“immunocytokines”) have been moved to clinical trials using, in most cases, antibodies specific to splice isoforms of fibronectin or of tenascin-C. These components of the modified sub-endothelial tumor extracellular matrix are strongly expressed in the cancer neo-vasculature and stroma, but are virtually undetectable in normal adult tissues. Clinical development programs in oncology have so far focused on the pro-inflammatory cytokines IL2, IL12 and TNF as active payloads.

In this thesis, I describe the design, production and characterization of several novel immunocytokines, based on the fusion of the clinical-stage F8 antibody (specific to the alternatively spliced EDA domain of fibronectin, a marker of tumor neo-vasculature) with murine Interleukin 7 (mIL7), Interleukin 12 (mIL12), Interleukin 17 (mIL17) and Interleukin 18 (mIL18).

Murine IL7 is an immunomodulatory protein which has previously shown anti-cancer activity in preclinical models and whose human counterpart is currently being investigated in clinical trials. The sequential fusion of the antibody fragment scFv(F8) in diabody format with mIL7 yielded an immunocytokine (termed “F8-mIL7”) of insufficient pharmaceutical quality and in vivo tumor targeting performance, with a striking dose dependence on tumor targeting selectivity. By contrast, a novel immunocytokine design (termed “F8-mIL7-F8”), in which two scFv moieties were fused at the N- and C-terminus of murine IL7, yielded a protein of

excellent pharmaceutical quality and with improved tumor-targeting performance. Both F8-mIL7 and F8-mIL7-F8 could induce tumor growth retardation in immunocompetent mice, but were not able to eradicate F9 tumors. The combination of F8-mIL7-F8 with paclitaxel led to improved therapeutic results, which were significantly better compared to those obtained with saline treatment.

There has been a long controversy as to whether IL17 has an impact on tumor growth. In order to assess whether IL17 may affect tumor growth, it would be convenient to achieve high levels of this pro-inflammatory cytokine at the tumor neo-vasculature, since IL17 is known to promote angiogenesis. We have generated and tested *in vivo* a fusion protein, consisting of the F8 antibody and of mIL17. The resulting immunocytokine (termed F8-mIL17) was shown to selectively localize at the tumor neo-vasculature and to vigorously promote tumor angiogenesis, without however reducing or enhancing tumor growth rate both in immunocompetent and in immunodeficient mice.

Murine IL18 is a pro-inflammatory cytokines which promotes IFN γ production. As already observed with mIL7, the sequential fusion of the antibody fragment scFv(F8) in diabody format with mIL18 yielded an immunocytokine (termed "F8-mIL18") of insufficient pharmaceutical quality. Nevertheless, the fusion proteins showed impressive *in vivo* tumor targeting performance and promising therapeutic effects. Different immunocytokines were cloned and expressed; including cysteines to serines mutants, changes in linkers and design of novel formats (F8-mIL18-F8, mIL18-F8). None of these approaches led to the development of a mIL18-based immunocytokine with decent pharmaceutical quality.

The heterodimeric nature of IL12 makes it compatible with a large variety of different immunocytokine formats. We found that the sequential fusion of IL12 as a single polypeptide with two F8 antibodies in scFv format, using suitable linkers, allowed the preparation of an immunocytokine of good pharmaceutical quality, capable of selective localization on the tumor neo-vasculature *in vivo*, as judged by quantitative biodistribution analysis with radioiodinated protein preparations. The resulting protein, termed IL12-F8-F8, potently inhibited tumor growth in immunocompetent syngeneic models of cancer, but did not lead to disease eradication when used alone or in combination with the Interleukin-2-based immunocytokine F8-IL2. By contrast, the combination of IL12-F8-F8 with paclitaxel led to pronounced tumor growth retardation and to the cure of a subset of tumor-bearing mice, with a treatment modality which was well tolerated.

In this thesis, progress was made towards the development of novel immunocytokine formats, characterized by improved pharmaceutical quality and pharmacokinetic properties, including disease-homing performance. Choosing the right biological payload represents a crucial decision for the development of immunocytokines. For this reason, the investigation of four different cytokines as antibody fusion partners allowed us to observe their relative benefits, in terms of therapeutic performance, disease-homing behavior and pharmaceutical quality. When given as monotherapy, immunocytokines did not mediate complete cures of cancer in the animal models tested. However, combination therapies with IL12-based immunocytokines have resulted in long-lasting tumor eradications, which cannot be achieved by conventional chemotherapy.

RIASSUNTO

Le citochine hanno dimostrato una potente attività terapeutica in modelli animali di cancro ed altre malattie. Per questo motivo molte di loro sono già state esaminate in studi clinici. Purtroppo, già a dosi basse, molto spesso vengono osservate considerevoli tossicità che impediscono l'aumento della dose fino a regimi terapeuticamente attivi. L'uso di anticorpi ricombinanti o frammenti di anticorpi come veicoli può migliorare significativamente l'indice terapeutico delle citochine proinfiammatorie.

Molte citochine sono già state fuse ad anticorpi, creando le cosiddette "immunocitochine", in modo da ottenere una localizzazione selettiva del farmaco al sito tumorale. In particolare sono state prese in esame interleuchina 2 (IL2), interleuchina 10, interleuchina 12 (IL12), interleuchina 15, il fattore stimolante le colonie granulocitarie-macrofagiche, interferone alfa, interferone gamma (IFN γ) e il fattore di necrosi tumorale (TNF).

Alcune di queste citochine sono state testate in studi clinici, nella maggior parte dei casi l'anticorpo usato è specifico per alcuni domini frutto di splicing alternativo della fibronectina o della tenascina C. Questi componenti della matrice extracellulare modificata del subendotelio tumorale sono fortemente espressi nella neovascolatura e nello stroma canceroso, ma non sono praticamente rilevabili nel tessuto adulto sano. Lo sviluppo clinico di immunocitochine nell'ambito oncologico si è fino ad ora incentrato nell'uso delle citochine proinfiammatorie IL2, IL12 e TNF quali componenti attivi di queste nuove proteine.

In questa tesi sono descritti la concezione, la produzione e la caratterizzazione di alcune nuove immunocitochine basate sulla fusione dell'anticorpo F8 (specifico per il dominio EDA della fibronectina, risultante da uno splicing alternativo e pertanto un antigene specifico dell neovascolatura tumorale), già studiato in clinica, con interleuchina 7 murina (mIL7), interleuchina 12 murina (mIL12), interleuchina 17 murina (mIL17) e interleuchina 18 murina (mIL18).

La citochina mIL7 regola il sistema immunitario e ha mostrato proprietà antitumorali in modelli animali preclinici, inoltre, la sua equivalente umana è attualmente oggetto di studio in clinica. La fusione sequenziale del frammento anticorpale scFv(F8) nel cosiddetto formato "diabody" con mIL7 ha prodotto un'immunocitochina (chiamata "F8-mIL7") di insufficiente qualità farmaceutica e scarsa capacità di localizzazione nella regione tumorale associata ad una marcata correlazione tra il profilo di distribuzione e la

dose amministrata. Al contrario, la nuova immunocitochina F8-mIL7-F8, basata su un design completamente nuovo del formato dove due scFv sono fusi rispettivamente all'N- e al C-terminus di mIL7, possiede un'eccellente qualità farmaceutica combinata con una migliore accumulazione a livello tumorale. Entrambe le proteine di fusione, F8-mIL7 e F8-mIL7-F8, sono in grado di ritardare la crescita tumorale in topi immunocompetenti ma non riescono ad eradicare il teratocarcinoma F9. L'amministrazione combinata di F8-mIL7-F8 con paclitaxel ha mostrato dei migliori risultati terapeutici, con un ritardo nella crescita significativo rispetto al gruppo di controllo iniettato con soluzione salina.

L'effetto di interleuchina 17 sulla crescita tumorale è da lungo oggetto di una controversia. Per poter capire se IL17 influisce o meno sulla proliferazione delle cellule tumorali sarebbe utile raggiungere un'alta concentrazione di citochina infiammatoria nella regione neovascolare del tumore, considerando che IL17 è conosciuta in quanto agente proangiogenico. È stata prodotta e testata in vivo un'immunocitochina composta dall'anticorpo scFv(F8) e da mIL17 (F8-mIL17). La proteina è in grado di localizzarsi selettivamente nella neovascolatura tumorale e di promuovere vigorosamente l'angiogenesi nella zona cancerosa, senza però modificare la crescita tumorale né in topi immunocompetenti né in topi immunodeficienti.

La citochina proinfiammatoria mIL18 stimola la produzione di IFN γ . Come già osservato per mIL7, la fusione sequenziale del frammento anticorpale scFv(F8) nel formato diabody con mIL18 ha prodotto un'immunocitochina (F8-mIL18) di scarsa qualità farmaceutica. Ciononostante, la proteina ha mostrato una notevole accumulazione selettiva al sito tumorale e una promettente attività terapeutica. Diverse immunocitochine basate su mIL18 sono state clonate ed espresse; in particolare sono state prodotte forme mutanti di mIL18 dove le cisteine sono state sostituite da serine, il linker tra anticorpo e citochina è stato accorciato e nuovi formati sono stati analizzati (F8-mIL18-F8, mIL18-F8). Nessuno di questi approcci è stato in grado di generare un'immunocitochina con una qualità farmaceutica decente.

Grazie alla sua natura eterodimerica, IL12 è un partner ideale per la creazione di nuove immunocitochine, in quanto permette la realizzazioni di diversi formati alternativi. La fusione sequenziale di IL12 con due scFv(F8) come singola catena polipeptidica usando dei linker idonei, permette la produzione di un'immunocitochina (mIL12-F8-F8) di buona qualità farmaceutica e capace di accumularsi nella neovascolatura tumorale in vivo. Questa nuova immunocitochina basata su IL12 è in grado di ritardare considerevolmente la crescita tumorale in modelli di cancro singenici impiantati in topi immunocompetenti, ma se amministrata da sola o in combinazione con l'immunocitochina basata sulla fusione di F8 con IL2 non

riesce ad eradicare il tumore. Al contrario, se combinata con paclitaxel, mIL12-F8-F8 ha mostrato una pronunciata inibizione della crescita tumorale e la cura completa di alcuni topi, con un ciclo di trattamento ben tollerato.

In questa tesi sono stati fatti progressi riguardo lo sviluppo di immunocitochine con nuovi formati, i quali presentano miglioramenti in termini di qualità farmaceutica e proprietà farmacocinetiche, includendo la capacità di localizzarsi al sito tumorale.

Scegliere la citochina più appropriata è una decisione cruciale durante lo sviluppo di un'immunocitochina. Per questo motivo, lo studio di quattro differenti interleuchine come partner per la fusione con un frammento anticorpale, ci ha permesso di osservare i loro relativi meriti in termini di performance terapeutica, capacità di localizzazione nel tumore e qualità farmaceutica.

Se usate come singoli agenti terapeutici, le immunocitochine non sono purtroppo in grado di curare completamente il cancro nei modelli animali da noi studiati. Combinando però immunocitochine basate su IL12 con agenti chemoterapici si sono ottenute delle eradicazioni dei tumori durature, risultato che non è possibile raggiungere con la chemioterapia convenzionale.

2. INTRODUCTION

2.1. INTACT AND ARMED ANTIBODIES IN CANCER THERAPY

The 'magic bullet' concept stated by Paul Ehrlich at the end of the nineteenth century, depicted antibodies as entities capable to specifically trace and kill tumor cells. Yet, the antibody era started only in the late 1970s when the generation of murine monoclonal antibodies (mAb) was described by Köhler and Milstein [1]. Unfortunately, the immune response of patients to antibodies of rodent origin, delayed their development as therapeutic agents by other ten years, when chimeric antibodies were generated [2,3].

In 1997 the US FDA approved the first therapeutic antibody, rituximab (Rituxan/MabThera, chimeric, anti-CD20 mAb), for the treatment of Non-Hodgkin's lymphoma (NHL) [4]. Rituximab is nowadays one of the most prominent blockbusters among all biopharmaceuticals. Together with trastuzumab (Herceptin, breast cancer overexpressing HER2, humanized anti-HER2 mAb), bevacizumab (Avastin, metastatic colorectal cancer, glioblastoma and metastatic renal carcinoma, humanized anti-VEGF (Vascular Endothelial Growth Factor) mAb) and cetuximab (Erbix, EGFR (Epithelial Growth Factor Receptor) expressing metastatic colorectal cancer, chimeric anti-EGF mAb) it generated \$18 billion in sales in 2009 [5].

Four more monoclonal antibodies are approved for the treatment of cancer including alemtuzumab (Mabcampath/Campath, chronic lymphocytic leukemia, humanized anti-CD52 mAb), panitumumab (Vectibix, EGFR-expressing colorectal cancer, human anti-EGFR mAb), ofatumumab (Arzerra, chronic lymphocytic leukemia, human anti-CD20 mAb) [5] and the recently approved ipilimumab (Yervoy, melanoma, human anti-CTLA4 mAb) [6].

Tumor specific antibodies can also be armed and used for the targeted delivery of toxic payloads to the site of disease, in order to minimize side effects while maximizing therapeutic performance. Cytokines, cytotoxic drugs, toxins or radionuclides have been conjugated to targeting antibodies or antibody fragments and have been evaluated in preclinical and clinical settings (**Fig. 2.1**) [7]. Five products were approved and four are available in the market. In particular, two radiolabeled mAb directed against CD20, tositumomab (Bexxar,

radiolabeled with iodine-131) and britumomab tiuxetan (Zevalin, radiolabeled with yttrium-90), are currently used for the treatment of non-Hodgkin's lymphoma. Catumaxomab (Removab) was recently approved and it is the first bispecific antibody available in the market. This chimeric mAb is specific for EpCAM (Epithelial Cell Adhesion Molecule) and CD3 antigen, it is indicated for the treatment of malignant ascites in patients suffering from EpCAM-positive carcinomas [5]. Brentuximab vedotin (Adcetris) was approved in 2011 for the treatment of Hodgkin's lymphoma and anaplastic large cell lymphoma, the anti-CD30 mAb is conjugated to the antimetabolic agent monomethyl auristatin E [8].

Gemtuzumab zogetacin (Mylotarg), a humanized anti-CD33 mAb conjugated with a toxic antibiotic (calicheamicin), was approved in 2000 and used for the treatment of acute myeloid leukemia. It was withdrawn in 2010 due to no objective benefit for the patients and an elevated rate of fatal adverse events[8].

Even though only four out of twelve mAb-based products approved for tumor therapy are conjugated to active moieties, the field of the targeted delivery of drugs represents a growing portion of the overall oncological sector.

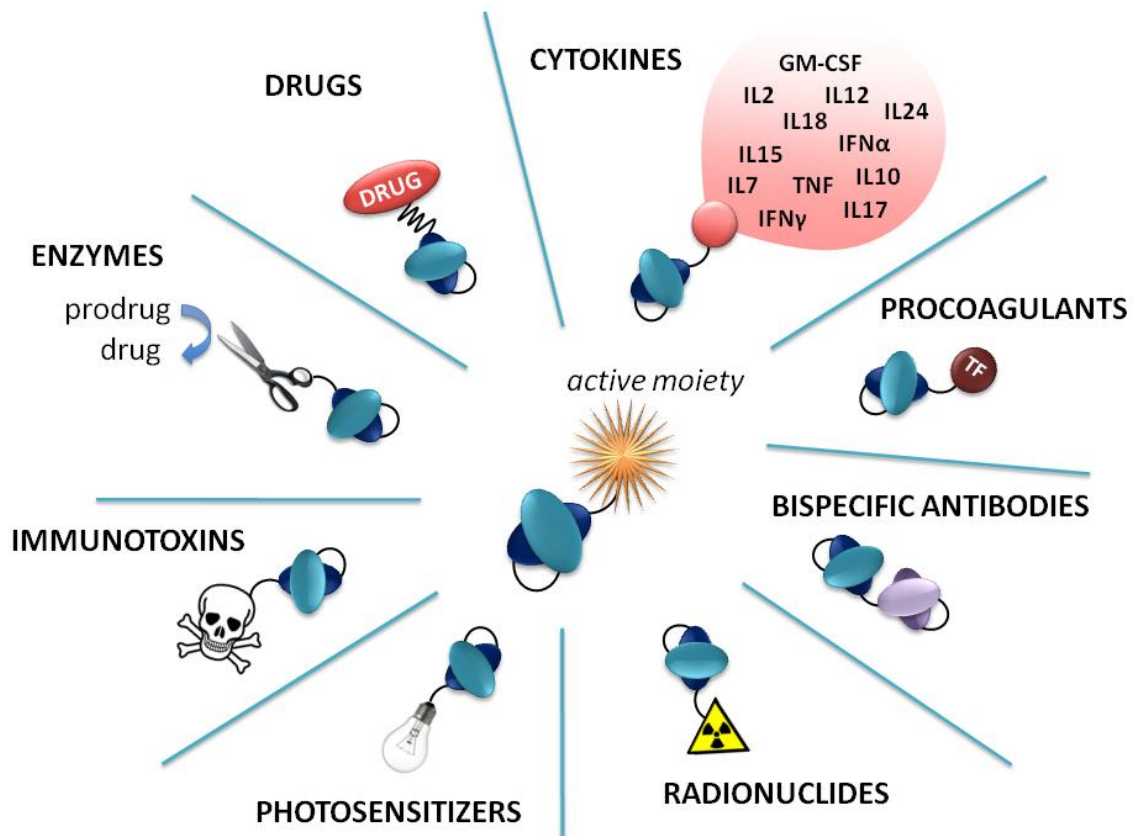


Fig. 2.1 Schematic representation of the antibody derivatives that can be use for targeted cancer therapy. Immunocytokines, immunocoagulants, bispecific antibody (e.g. anti CD3Ab), radioimmunoconjugates, antibody-photosensitizers conjugates, immunotoxins, ADEPT (Antibody-directed enzyme prodrug therapy), antibody-drug conjugates.

2.2. CYTOKINES IN CANCER THERAPY

Many cytokines have shown potent antitumor activities in preclinical experiments and represent promising agents for cancer therapy. However, despite encouraging results in animal models, only a few cytokines [e.g., Proleukin® (IL2), Roferon A® (IFN α 2a), Intron A® (IFN α 2b), Beromun® (TNF)], are approved as anticancer drugs. Current indications include metastatic renal cell cancer, malignant melanoma, hairy cell leukemia, chronic myeloid lymphoma, sarcoma and multiple myeloma, alone or in combination with chemotherapy. Additionally, certain cytokines are used in the clinical practice for the treatment of viral and of bacterial infections [5], while anti-inflammatory cytokines may confer a benefit to patients suffering from chronic inflammatory conditions.

While in preclinical models of cancer certain cytokines can mediate a complete tumor eradication, only a modest efficacy is often observed in the clinical setting. What are the reasons for such a striking difference between preclinical experiments and clinical trials?

In many cases, striking therapeutic results were obtained by intratumoral or peritumoral application of cytokines, intratumoral implantation of cytokine producing cells or cytokine gene transfection of cancer cells before implantation [9-13]. These modalities are rarely applicable in the clinical setting and are typically not efficacious in the case of disseminated disease. By contrast, the systemic administration of cytokines rarely induces complete cures [11,14-16]. Considerable toxicities can be observed at low doses, which prevent escalation to therapeutically active regimens [17].

2.3. EXTRACELLULAR MATRIX COMPONENTS AS TUMOR-ASSOCIATED ANTIGENS

Antigens expressed on the extracellular matrix of tumor blood vessels (i.e., markers of angiogenesis) are particularly attractive for the therapy of cancer, since new blood vessels are rarely found in the healthy human body but are characteristic features of tumors. Markers expressed on pathological blood vessels are more easily reached *in vivo* by antibody-based therapeutic agents coming from the bloodstream. A number of markers of angiogenesis have been reported so far. For some of them, antibodies have been generated with proven ability to selectively localize at the tumor site following intravenous administration. The extra domain A (EDA) and extra domain B (EDB) domains of fibronectin (**Fig. 2.2A**) and the A1 domain of Tenascin-C (TnC A1) (**Fig. 2.2A**) possibly represent the most extensively studied markers of angiogenesis[18,19]. Three human monoclonal antibodies (F8, L19 and F16) have been raised against these antigens and have been investigated for their targeting performance as well as therapeutic potential as targeting vehicle in preclinical and clinical (L19-IL2, L19-TNF, F16-IL2, L19-131I, F16-131I) settings. These alternatively spliced domains of extracellular matrix components exhibit a broad pattern of expression in many different types of solid cancer and of lymphoma, while their expression in normal organs is mainly confined to the female reproductive system in the proliferative phase[20]. Advances in transcriptomic and proteomic technologies promise to improve our knowledge of the pathological neo-vasculature at the molecular level and to delivery novel targets for the generation of new antibody-based products for cancer therapy [21,22].

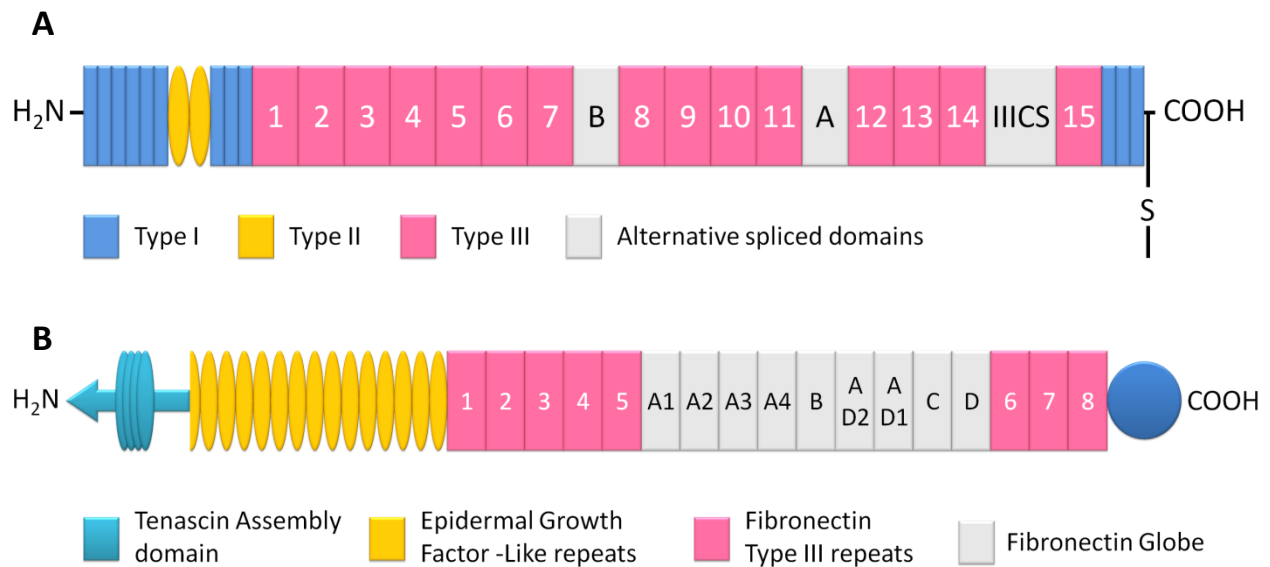


Fig. 2.2 (A) Model of the domain structure of a fibronectin monomer. The protein domains undergoing alternative splicing (i.e. EDB, EDA and IIICS) are indicated in white. The epitope recognized by L19 is located within the EDB region, whereas the F8 antibody targets the EDA repeat. (B) Structure of Tenascin-C. The F16 antibody is specific for the alternatively spliced A1 domain.

2.4. IMMUNOCYTOKINES: A PROMISING CLASS OF ARMED ANTIBODIES

It is well established that cytokines can achieve curative effects for cancer treatment, but only if high concentrations of localized drug in the tumor environment are administered. Since most cytokines do not preferentially localize at the tumor site after systemic administration [23], the targeted delivery of these immunostimulatory proteins could lead to an improved therapeutic index and to more potent therapeutic benefit with acceptable side effects. A prominent example is represented by the antibody-based targeted delivery of IL12, which allows to obtain therapeutic effects comparable to the ones observed by the cytokine alone but at a 20-fold lower administered dose [24].

Immunocytokines represent a novel class of biopharmaceuticals, which have a great potential for the therapy of cancer [7]. These products consist of a cytokine moiety fused to monoclonal antibodies or to an antibody fragment serving as delivery vehicle for the selective localization of the immunostimulatory payload at sites of disease.

2.5. IMMUNOCYTOKINES FORMATS AND BIODISTRIBUTION DATA

Several recombinant antibody formats can be considered for immunocytokine development (**Fig. 2.3**). They range from single-chain variable fragments (scFv) (MW (Molecular Weight) ~ 28 kDa) to full immunoglobulin G (IgG) (MW ~ 150 kDa) and may differ in terms of their valence. The IgG format has been used for immunocytokine development, in spite of the fact that the Fc (Constant Fragment) portion of the molecule could contribute to a long circulatory half-life and to the targeting of the cytokine moiety to cells bearing Fc receptors. Our group has preferred to focus on antibody fragments in scFv format, which can form monomers or non-covalent homodimers (“diabodies” [25]) depending on the cytokine fusion modality and the length of the linker connecting VH (Variable Heavy) and VL (Variable Light) chains. Diabodies are particularly suited cytokine partners for immunocytokine construction, as their bivalent nature contributes to a high binding avidity and since the resulting molecular weight is larger than the renal filtration threshold, thus mediating a rapid hepatobiliary clearance mechanism. Notably, tumor-targeting diabodies exhibit favorable tumor-to-organ ratios at early time points following intravenous administration, compared to other antibody formats [26,27].



Fig. 2.3 Schematic representation of seven different recombinant antibody formats, frequently used for immunocytokine development. The formats include Fab fragments (~50kDa) and the corresponding disulfide-linked homodimeric F(ab')₂ structure, which may contain the hinge region (~110kDa). The scFv represents the smallest portion of the antibody molecule which retains the binding affinity (though not the avidity) of the parental antibody. When short peptide linkers are used between VH and VL domain, homodimeric diabody structures (~55 kDa) can be generated. IgG, Immunoglobulin G. The scFv-Fc format consists of a scFv fused to the Fc portion of an IgG molecule (~110 kDa). A smaller version, named mini-antibody, Small Immune Protein or SIP uses the CH3 domain of an IgG or the εCH4 domain of an IgE antibody to mediate a stable homodimerization of scFv (~80 kDa).

(Adapted from: Pasche and Neri (2012) *Drug Discovery Today* [28])

A number of cytokines have been used for the production of fusion proteins with disease-targeting antibodies **Fig. 2.4** summarizes the immunocytokines which have been described in preclinical studies (i.e., *in vivo* biodistribution analysis and/or therapy), depicting the molecular format used for antibody-cytokine fusion. In most cases, antibodies have been genetically fused to cytokines and expressed in mammalian cells. In earlier works, however, chemical conjugates have been reported for TNF (ZME/TNF)[29] and IFN alpha (C2-2b-2b; 20-2b) [30,31]. The majority of preclinical studies with immunocytokines have been conducted in mouse models of cancer.








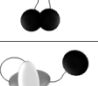




The choice of the cytokine, the antigen recognized by the antibody and the molecular format used for immunocytokine production influence the ability of this class of biopharmaceuticals to selectively localize at sites of disease. Ideally, the disease targeting performance of an immunocytokine should be assessed by quantitative biodistribution studies with radiolabeled protein preparations in animal models and by nuclear medicine techniques in patients. Three main classes of immunocytokines can be identified based on published biodistribution data:

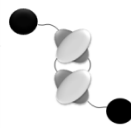

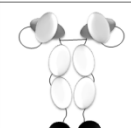


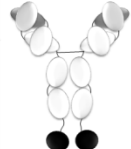
- (i) antibody-cytokine fusions which selectively localize at site of disease, with targeting performance which is largely independent of the dose used [in the mouse, this typically ranges between 1 – 100 μ g]. Prominent examples in this class include fusions based on IL2 or TNF [23,32].
- (ii) immunocytokines whose targeting performance varies as a function of the injected dose (usually, exhibiting better results at higher concentrations) Prominent examples in this class include fusions based on GM-CSF or IL7 [33,34].
- (iii) fusion proteins in which the cytokine moiety abrogates the disease targeting performance of the parental antibody. A prominent example is represented by IFN γ , which (upon fusion with the L19 antibody) targeted tumors only in mice which were deficient in IFN γ receptor, but not in wild-type mice [35].


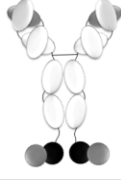
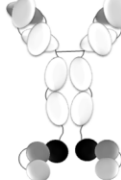

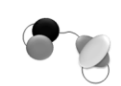


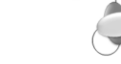
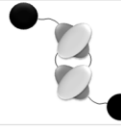

2.6. SELECTED PRECLINICAL FINDINGS

2.6.1. MONOTHERAPY

Fig. 2.4 schematically summarizes key findings related to the tumor homing properties and therapeutic performance of immunocytokines in mouse models of cancer. In some case (e.g., IL2), the human cytokine could be used for product development and preclinical evaluation, as the cytokine moiety cross-reacts with the murine receptor(s). In other cases (e.g., TNF and IL12), the murine cytokine should preferably be used, because of species barriers. Anticancer activity is classified in various categories, according to the tumor growth retardation observed in animal models. Furthermore, the Figure indicates whether a given fusion protein exhibited a superior therapeutic performance compared to closely related proteins used as negative control (NC). In most cases, these comparisons were performed with the cytokine alone or with immunocytokines having the same molecular format but antibodies of irrelevant specificity in the mouse. In some cases, especially when IgGs were fused to cytokines, therapeutic performance was compared to the activity of the corresponding unconjugated naked immunoglobulin. In few cases, tumor cells not expressing the antibody's antigen were used as negative control. As a general trend, whenever a selective accumulation of an immunocytokine was observed at the tumor site as a result of the targeting antibody moiety used, a strong therapeutic benefit was observed compared to immunocytokines of irrelevant specificity used as negative controls. The best therapeutic results were reported so far for IL2, IL12, IL15 and TNF, in line with the positive tumor uptake data observed in biodistribution studies.

Name	Format	Antigen	Tumor model	Targeting <i>in vivo</i>	Efficacy	Clinic	Refs
TNF alpha							
FAP-TNF		FAP	HT1080-FAP ⁺ s.c. ²	n.a.	+, > NC	no	168
G250-TNF		CA IX	NU-12 s.c. ² ; SK-RC17/52 s.c. ²	NU-12: (+) DD ^a	SK-RC17/52: ++, > NC	no	169
scFvMEL-TNF		gp240	A375 s.c. ²	(+)	+++ , > NC	no	155, 170
L19-TNF		EDB	F9 s.c. ¹ ; WEHI 164 s.c. ¹ ; C51 s.c. ¹	F9: ++	F9: +, > NC ; ++, > NC (<i>Melph</i>) WHEI 164, C51: +++ , > NC (<i>Melph</i>)	P. II	32, 43
MFE23-TNF		CEA	LS174T s.c. ²	++	n.a.	no	171
TNF-TNT3		DNA	LS174T s.c. ²	+	n.a.	no	172
TNF-FuP		EGFR	BLM s.c. ^{3,4}	(+) ³	+, ≈ NC ⁴	no	173
TNF-B1		LeY	MCF-7 s.c. ²	n.a.	+++ , > NC	no	174
ZME/TNF		gp240	A375 s.c. ²	(+) ^b	++ , > NC	no	29
GM-CSF							
L19-GMCSF		EDB	F9 s.c., i.v. ¹ ; C51 s.c., i.v. ¹	F9 s.c.: (+)/+ DD	F9 s.c.: +, > NC F9 i.v.; C51: +	no	33
Anti HER2/ <i>neu</i> IgG3-GMCSF		HER2/ <i>neu</i>	CT26 s.c. ¹ ; CT26 HER2 ⁺ s.c. ¹	HER2 ^{+/-} + ^c	HER2 ⁺ : +, > NC	no	175
CLL1-GMCSF		MHC II	ARH-77 ²	+ ^d	n.a.	no	176

Name	Format	Antigen	Tumor model	Targeting <i>in vivo</i>	Efficacy	Clinic	Refs	
Interleukin 2								
L19-IL2		EDB	F9 s.c. ^{1, 2} ; C51 s.c. ² ; N52 s.c. ² ; Ramos ³ s.c., i.v.; A20 s.c. ¹ , DoHH-2 s.c. ³	Fg2: ++ ^a Ramos s.c.: + A20: +	F9 ^{1, 2} , C51, N52: ++, > NC Ramos s.c., i.v.; DoHH-2: +, > NC; +++ (<i>Ritux.</i>)	P. II	23, 39	
F16-IL2		TnC A1	MDA-MB-231 s.c. ² ; U87MG s.c., orthot. ²	MDA: ++ U87 s.c.: ++	MDA: +, > NC; ++ (<i>Doxo /PTX</i>) U87: s.c. no effect; +++ (<i>TMZ</i>) orthot. +; ++ (<i>TMZ</i>)	P. Ib/II	37, 38	
F8-IL2		EDA	Caki-1 ²	+	+	no	42	
KS-IL2		EpCAM	CT26-KSA i.s., i.v., s.c. ¹ ; PC-3.MM2 i.v. ³ ; 4T1 ¹ s.c., i.v.; LCC s.c. ¹	CT26-KSA i.v.: + ^e	CT26-KSA: i.v, i.s. ++++, > NC; s.c. ++ (<i>PTX</i>) PC-3: ++++, > NC 4T1: s.c. +++ (<i>CP</i>); i.v. ++ (<i>CP</i>) LCC: ++ (<i>CP</i>)	P. I	16, 36, 177	
ch14.18-IL2		GD2	M21 i.v. ^{3, 4} , i.s. ³ , s.c. ² ; B16-GD2 i.v. ¹ , i.s. ¹ ; SK-N-AS i.s. ⁴ ; NX2S ¹ i.v., s.c. spon. met.	M21 s.c.: + M21 i.v. ³ /i.s.: + ^e B16-GD2: (+) ^f NX2S s.c.: +	M21 i.v. ⁴ : ++++, > NC B16-GD2: ++++, > NC SK-N-AS: ++++, > NC NX2S i.v.: ++++, > NC NX2S s.m.: ++++, > NC NX2S s.c.: +++ (<i>IL2</i>)	P. II	14, 15, 178 – 182	
ch225-IL2		EGF	M24met i.s. ⁴	n.a.	++++, > NC	no	178	
antiCD20-IL2		CD20	Daudi i.v. ^{3, 4}	n.a.	++++, > NC	no	154	
Anti HER2/ <i>neu</i> IgG3-IL2		HER2/ <i>neu</i>	CT26-HER2 ¹	n.a.	+, > NC	no	183	
CLL1-IL2		MHC II	ARH-77 ²	++ ^d	n.a.	no	176	
IL2-FuP		EGFR	BLM s.c. ^{3, 4}	+ ³	+ ⁴	no	173	
AntiCEA-IL2			CEA	MC-38, MC-38-CEA s.c. ⁷	+	++, > NC	no	184
FUMK1-IL2			MK1 (=EpCAM)	MKN-74 s.c. ⁴	n.a.	++, > NC	no	185
IL2-MOV19		αFR	CT26-αFR ¹ s.c., i.v.	g	s.c.: ++, > NC	no	186	
2aG4-IL2		PS	-	n.a.	Vaccine adjuvant!	no	187	
NHS-IL2LT		DNA	NX2S i.v. ¹ , LCC i.v. ¹	n.a.	IL2 is in a low toxicity form! ++, > NC	Phase I	188	

Name	Format	Antigen	Tumor model	Targeting <i>in vivo</i>	Efficacy	Clinic	Refs
Interleukin 12							
BC1-IL12		EDB	PC3mm2 ³ i.v., s.c.; A431 s.c. ³ ; HT29 s.c. ³	n.a.	PC3 i.v.: +++ PC3 s.c., HT29: +, > NC A431: +, ≈ NC	P. II	100
chTNT3-IL12		DNA	LS147T s.c. ² ; DU145 s.c. ⁴	LS147T: +	DU145: +, > NC	(NHS-IL12) P. I	189
KS-IL12			DU145 i.v. ⁴ ; CT26-Ep21 i.v. ³	n.a.	DU145: ++, > NC CT26: ++	no	190
KS-IL12/IL2		EpCAM	LCC-EpCAM s.c. ¹	n.a.	+++	no	44
mScIL-12-her2.IgG3		HER2/ <i>neu</i>	CT26-HER2 s.c. ^{1,5,6} , i.v. ¹ ; CT26 s.c. ¹	n.a.	CT26HER2: s.c. ¹ , i.v. ¹ ++, ≈ NC; s.c. ^{5,6} +, ≈ NC CT26: +, ≈ NC		191, 192
IL12-scFv(L19)			F9 s.c. ¹ ; C51 ¹ s.c., i.v.	F9: +	F9: ++, > NC; +++ (L19-TNF) C51: s.c. +, > NC; i.v. ++, > NC	no	24, 40, 98
IL12-SIP(L19)		EDB	F9 s.c. ¹	+	n.a.	no	98
L19p35/p40L19			F9 s.c. ¹	++	++	no	98
F8p35/p40F8		EDA	F9 s.c. ¹	++	n.a.	no	99
Interleukin 7							
F8-IL7		EDA	F9 s.c. ¹	-/(+) DD	+	no	34
F8-IL7-F8				+	+, ≈ NC	no	34

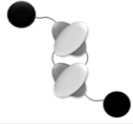

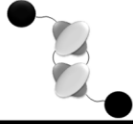
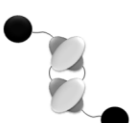

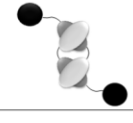
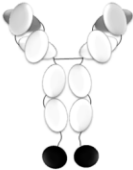




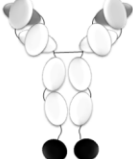
Name	Format	Antigen	Tumor model	Targeting <i>in vivo</i>	Efficacy	Clinic	Refs
Interleukin 15							
L19-IL15		EDB	F9 ¹ s.c., i.v.; C51 ¹ s.c., i.v.	F9: +	F9: s.c. +, > NC; i.v. ++ C51: s.c. +; i.v. +	no	33
Interleukin 17							
F8-IL17		EDA	F9 s.c. ¹	+	no effect	no	146
Interleukin 18							
F8-IL18		EDA	F9 s.c. ¹	+ / ++ DD	n.a.	no	N.P., D.N.; unpub.
Interleukin 10							
F8-IL10		EDA	F9 s.c. ¹	++	Rheumatoid arthritis, endometriosis	P. I	20, 162
L19-IL10		EDB	F9 s.c. ¹	++ ^h	Rheumatoid arthritis, psoriasis	no	160, 161
IFN alpha							
F8-IFN α		EDA	F9 s.c. ¹ ; Cloudman S91 s.c. ¹	F9: ++ S91: -/+ DD	+, \approx CN	no	145
CD20IgG3 IFN α		CD20	38C13-CD20 s.c. ¹ ; Daudi s.c. ²	n.a.	38C13: +++ , > NC Daudi: +++ , > NC	no	193
AntiHER2/ <i>neu</i> -IFN		HER2/ <i>neu</i>	38C13-HER2 ⁺ s.c. ¹	n.a.	+++ , > NC	no	194
C2-2b-2b		HLA-DR	Daudi i.v. ³ ; CAG i.v. ³	n. a.	Daudi: +++ , > NC CAG: +++	no	31
20-2b		CD20	Daudi i.v. ³ ; Raji i.v. ³ ; NAMALWA i.v. ³	n. a.	Daudi: +++ , > NC Raji, NAMALWA: +(+), > NC	no	30
IFN gamma							
L19-IFN γ		EDA	F9 s.c. ^{1,2,8} ; i.v. ¹ ; C51 s.c., i.v. ¹ ; CT26 s.c. ¹	F9 s.c.: + ^{1,2} , ++ ⁸	F9 s.c.: +, > NC F9 i.v.: ++ (L19-IL2, Doxo) C51; CT26 : -	no	35
TNT3- IFN γ		DNA	LS174T s.c. ² ; MAD109 s.c. ¹ ; RENCA i.v. ¹	LS174T: + MAD109: +	RENCA: ++ , > NC	no	172, 195

Fig. 2.4 Comprehensive summary of immunocytokines, which have been tested in animal models (in vivo biodistribution studies and/or therapy experiments). Name, molecular format, cognate antigen and tumor model(s) used are indicated. Targeting and therapy performance are schematically classified according to parameters indicated below. The Figure also indicates whether the product has been moved to clinical trials (Phase I or Phase II studies).

The animal models used in different publications (provided as References) were: 1) immunocompetent mice; 2) athymic mice; 3) SCID mice (lack of T and B cells); 4) SCID mice with human effector cells; 5) RAG2 KO mice; 6) SCID beige mice (lack of T, B and NK cells); 7) CEA transgenic mice; 8) IFN γ -R KO mice.

Targeting performance *in vivo* was classified on the basis of tumor to organ ratios observed for the majority of tested organs at 24h: - [< 1]; (+) [between 1 and 2]; + [between 2 and 10]; ++ [> 10]. Whenever experimental data did not allow this classification, results were presented on the basis of a) tumor to blood ratio at 24h; b) tumor to blood ratio at 72h; c) HER2⁺ tumor to HER2⁻ tumor ratio at 12h, tumor to blood ratio at 12h; d) tumor to organs ratio at 72h; e) metastatic organs to healthy organs ratio at 24h; f) metastatic organs to healthy organs ratio at 12h; g) accumulation in lung CT26-alphaFR positive tumor; h) targeting performance assessed in psoriatic mice [+] and arthritic mice [based on autoradiographic signals]. DD indicates dose dependence.

Therapy efficacy was defined as growth retardation (GR) compared to the saline group:

- [no GR]; + [GR $< 50\%$]; ++ [GR $> 50\%$]; +++ [cure]. Performance of the immunocytokine compared to the one of a negative control (NC, untargeted cytokine (fused to an irrelevant antibody or alone), naked antibody, tumors not expressing the antigen) was also assessed. > NC [superior performance of immunocytokine], \approx NC [comparable performance of immunocytokine and NC].

Abbreviations: FAP Fibroblast-activating protein, CA IX Carbonic anhydrase IX, CEA Carcinoembryonic antigen, HER2/neu Human epidermal growth factor receptor 2, MHC II Major histocompatibility complex, α FR Alpha folate receptor, PS Phosphatidylserine, HLA-DR Human leukocyte antigen DR, i.s. Intraspinal, DD Dose dependence, n.a. Not assessed. (*Adapted from: Pasche and Neri (2012) Drug Discovery Today [28]*)

2.6.2. COMBINATION THERAPY

Several studies have explored the combination of immunocytokines with other pharmacological agents, such as cytotoxic drugs [34,36-38] or intact immunoglobulins [39]. In general, immunocytokines appear to be ideal combination partners for established anti-cancer therapeutic agents, as they typically do not exhibit overlapping limiting toxicities with those associated with conventional chemotherapy (e.g., myelotoxicity, gastrointestinal, toxicity for kidney, liver or other organs). However, optimal combination partners have to be judiciously identified based on preclinical studies which analyze the influence of dosage, schedule and administration sequence on therapeutic outcome. Most pro-inflammatory immunocytokines activate the

endothelium and the resulting vascular leakage of fluids and proteins, drop in blood pressure and fever-like symptoms are compatible with the simultaneous administration of chemotherapeutic agents. The vasoactive properties of certain cytokines (most notably, IL2 and TNF) have been exploited in order to increase the uptake of other therapeutic agents at the tumor site [40,41].

A potentiation of Antibody-Dependent Cell Cytotoxicity (ADCC) has been observed in combination therapies with certain IgG therapeutics, since pro-inflammatory immunocytokines mediate the infiltration of many types of leukocytes into the tumor mass [38,42]. By contrast, to our knowledge, the combined use of immunocytokines with blocking antibodies (e.g., TNF or VEGF blockers) has not yet been reported.

In the recent past, the combined use of different immunocytokines has started to be explored, with encouraging preclinical results. For example, the combined use of L19-IL2 and L19-TNF, or L19-IL12 and L19-TNF has led to the eradication of tumors in immunocompetent mouse models of the disease, which could not be cured by the individual immunocytokines used as single agents [32,40,43].

Moreover, the fusion of two cytokines onto the same targeting antibody (KS-IL12/IL2) was able to eradicate LCC-EpCAM tumors. The therapeutic activity of novel immunocytokine was comparable to the one of the single immunocytokines (i.e. KS-IL12 and KS-IL2) injected simultaneously [44].

2.7. IMMUNOCYTOKINES IN CLINICAL DEVELOPMENT

Despite the large number of immunocytokines in preclinical development, only a few of them have entered clinical trials (**Fig. 2.5**). Interleukin 2 fusion proteins account for the most advanced immunocytokines in clinical development, in line with the fact that the unconjugated cytokine is routinely used for the therapy of patients with metastatic renal cell carcinoma or melanoma. The typical adverse events observed with IL2-based immunocytokines resemble the ones of recombinant IL2, including hypotension, fever, rigor, neuropathic pain, hypoxia, pruritus, allergic reactions, hypophosphatemia, thrombocytopenia, leucopenia and neutropenia.

compound	generic name	antibody format	antigen	indications	highest phase	organization
interleukin 2						
L19 – IL2	Darleukin	diabody	EDB of fibronectin	melanoma	phase II	Philogen
F16 – IL2	Teleukin	diabody	A1 domain of Tenascin C	breast cancer, lung cancer	phase II	Philogen
KS – IL2	EMD 273066	IgG	epithelial cell adhesion molecule	ovarian cancer, colorectal cancer, NSCL carcinoma, prostate cancer	phase I	Merck KGaA
Ch14.18 – IL2	EMD 273063	IgG	ganglioside GD2	melanoma, neuroblastoma	phase I/II	Merck KGaA
NHS – IL2 LT	EMD 521873	IgG	DNA/histone complexes	non-Hodgkin lymphoma, NSCL cancer	phase I	Merck KGaA
interleukin 12						
BC1 – IL12	AS1409	IgG	EDB of fibronectin	melanoma	phase I/II	Antisoma
NHS – IL12	MSB0010360	IgG	DNA/histone complexes	epithelial and mesenchymal malignant tumors	phase I	Merck KGaA
TNF alpha						
L19 - TNF	Fibromun	trimeric scFv	EDB of fibronectin	melanoma (isolated limb perfusion)	phase I/II	Philogen
interleukin 10						
F8 – IL10	Dekavil	diabody	EDA of fibronectin	arthritis	phase I	Philogen

Fig. 2.5 Immunocytokines in clinical development. Immunocytokines based on IL2, IL12, TNFalpha and IL10 are currently being investigated in clinical trials. Splice-isoforms of fibronectin and tenascin-C represent the most frequently used target antigens for cytokine delivery (i.e., 5 out of 9 immunocytokines currently in clinical trials).

(Adapted from: Pasche and Neri (2012) *Drug Discovery Today* [28])

L19-IL2 was studied in patients with metastatic renal cell carcinoma. A recommended dose could be identified (i.e. 22.5 mio IU/patient/day – 3 injections/week). Toxicities were manageable and reversible. Disease stabilization could be achieved in 83% of the metastatic renal cell carcinoma patients after the second cycle (i.e., 6 weeks). Median progression free survival was 8 months (1.5 – 30.5 months) [45].

More promising results have recently been reported for the combined use of L19-IL2 with dacarbazine in metastatic melanoma. After a dose escalation study in 10 patients, 22 additional patients were enrolled.

Toxicities were manageable and reversible. Efficacy could be evaluated in 29 out of the 32 patients. 28% of the patients had an objective response evaluable by “Response evaluation criteria in solid tumors” (RECIST), including one patient who experienced a Complete Response and who was still tumor free after 21 months. 61.5% of the patients treated at the recommended dose (n = 26) were still alive after 12 months, the median survival of pretreated melanoma patients is of about 6 to 9 months. A controlled phase IIb study (L19-IL2 + dacarbazine vs. dacarbazine alone) with 90 metastatic melanoma patients is currently in progress [46].

Disease stabilization was also achieved in 58% of melanoma patients receiving ch14.18-IL2 after the first cycle (i.e., 1 week). However, only 24% of total patients did not have any progression after the second cycle (i.e., 6 weeks). Phase II studies revealed that only 2 out of 9 melanoma patients receiving ch14.18-IL2 had a disease stabilization. No objective responses were observed [47,48].

In children with neuroblastoma treated with ch14.18-IL2, a recommended dose could be identified (i.e. 110mio IU/m² given over 3 days). Stable disease was achieved in 54% of the patients after two or more cycles (i.e., at least 6 weeks). In a subsequent Phase II trial, it was found that 22% of the patients having a disease evaluable only by metaiodobenzylguanidine (MIBG) scintigraphy and/or bone marrow histology (i.e., low tumor load) enjoyed a complete response lasting at least 9 months up to more than 35 months. Unfortunately, ch14.18-IL2 did not have any impact on bulky disease [49,50]. Additionally, a second immunocytokine (KS-IL2) has been studied in Phase I clinical trials [51].

In the case of non-targeted IL2, a variety of regimens have been used in the clinic, ranging from low-dose regimens at 75 Mio IU/week [52] to the intense regimens at 900 Mio IU/week (in young patients and in intensive care units) [53]. By contrast, IL2-based immunocytokines have so far been administered in the 67.5 - 110 Mio IU IL2 equivalents/week range [50,54], as companies have preferred to avoid the intensive care unit and develop a product broadly available to cancer patients. L19-IL2 and ch14.18-IL2 are administered as long infusions (1h, 4h) and have similar pharmacokinetics, with a terminal half-life of about 3 hours [48,54]; whereas KS-IL2 appears to have a prolonged half-life (4 – 6.7h) [51]. When Proleukin is administered as a short infusion (5 min), it displays a shorter half life (t_{1/2} distribution = 13min, elimination

= 85 min). However, when the same product is administered by subcutaneous (s.c.) injection, its terminal half-life is approximately 5 hours [55].

Two Interleukin-12 fusion proteins are also currently being evaluated in clinical trials. While NHS-IL12 is still in Phase I, results for a Phase I study with BC1-IL12 in melanoma and renal cell carcinoma patients have recently been reported. A recommended dose could be identified and two out of 13 patients experienced a partial response lasting 7 and 17 months before disease progression (i.e. 15 μ g/kg weekly) [56].

As therapeutic performance appears to correlate with tumor localization efficiency, it would be desirable to use nuclear medicine technique (e.g., PET (Positron Emission Tomography)) for the tomographic assessment of the tumor targeting properties of immunocytokine products in individual patients. Immuno-PET methodologies may be facilitated by the recent availability of clinical-grade iodine-124, a PET radionuclide with a half-life of 4 days, which matches the antibody residence at the tumor site [57]. Furthermore, microscopic analysis of biopsy samples may facilitate the assessment of targeting microheterogeneity and of leukocyte infiltration into the tumor mass. From a logistical point of view, however, it is still not easy to incorporate immuno-PET procedures and analysis of biopsies into the execution of clinical trials.

The individual response to treatment may depend not only on immunocytokine localization at the tumor site, but also on the immunological status of the patient. Most studies have so far reported the effect of the therapeutic immunocytokine on peripheral blood lymphocytes [54]. However, the recent discovery that cancer cells release peptides bound to soluble HLA-I (Human Leukocyte Antigen) molecules and that hundreds of these peptides can be identified by affinity capture and mass spectrometric analysis [58] indicates avenues for the non-invasive assessment of tumor-antigens which are displayed at the tumor site.

2.8. PROMISING IMMUNE MODULATORS FOR IMMUNOCYTOKINE DEVELOPMENT

Immunocytokines will find an increasing use in therapy of cancer. Progress in this field will crucially rely on the identification of accessible good-quality markers of pathology, on the engineering of suitable protein formats and on the judicious choice of suitable cytokines and combination partners. Here we present three cytokines that were never fused to an antibody for the therapy of cancer (i.e., IL7, IL17 and IL18) and a well known cytokine in the field of oncology that was already fused to targeting antibodies (IL 12).

2.8.1. INTERLEUKIN 7

Interleukin 7 is a pleiotropic cytokine with a central role for the modulation of T- and B-cells development, as well as for T-cell homeostasis. IL7 was first identified based on its ability to induce the growth of immature B lymphocytes [59,60]. Although human B-cell development does not appear to require IL7, immature human B cells proliferate in response to IL7 and IL7 treatment in mice leads to the expansion of immature B cells [61]. IL7 has been shown to induce the proliferation of thymocytes in culture [62] and to modulate T-cell activation [63,64], driving type 1 immune responses by the up-regulation of IL2 and the subsequent IFN γ production [65,66]. Furthermore, IL7 acts as a trophic factor for mature T cells, inhibiting cell death [67] and enhancing lytic activity in different cell types [61].

The anticancer activity of IL7 has been investigated in several animal models and with various experimental strategies. In a Renca renal cell carcinoma model, a dose dependent reduction (50% to 75%) in pulmonary metastases was observed following the systemic administration of recombinant human IL7 (hIL7) [68]. Moreover, several investigators have used gene therapy techniques to increase local production of IL7 in primary murine plasmacytoma [69], glioma [9] and melanoma [70]. In most cases, the tumor cells transfected with IL7 gene were rejected after implantation. Some investigators have also transduced IL7 into dendritic cells, which were subsequently injected in murine lung tumor models, leading to cancer regression and to protection against subsequent tumor challenges [13,71]. Recombinant human IL7 has recently been studied in a phase I clinical trial in 16 patients with various types of advanced metastatic cancer, showing to be well tolerated up to doses of 60 μ g/kg. Grade 1 to 2 constitutional symptoms developed 6 to 8 hours following administration, as well as mild local reactions with erythema, pruritus and

induration. Only two patients did not complete therapy because of toxicity. One developed rapidly reversible grade 3 liver enzyme and bilirubin elevation, while the other developed grade 3 chest pain and hypertension, with mild troponin levels increase. No objective responses were reported in the study [72].

Murine IL7 has a predicted molecular weight of 14.9 kDa but, due to N-glycosylation, exhibits a molecular mass for the active protein of 25 kDa [59]. Within the coding region of IL7, six cysteines (Cys) are involved in intramolecular disulfide bonds [59] and are conserved between mouse and man. Disulfide bond in hIL7 have been assigned based on the combination of MALDI mass spectroscopy and site-directed cysteine to serine mutational analyses. In vitro assays with IL7 mutants, based on the proliferation of 2E8 cells, indicated that the Cys3-Cys142 and Cys48-Cys93 disulfides are more important than Cys35-Cys130 for the biological activity of the protein [73].

2.8.2. INTERLEUKIN 12

Interleukin 12 is a 70kDa heterodimeric glycosylated cytokine composed by two subunits, named p35 and p40, covalently linked by a disulfide bridge [74]. IL12 is produced by antigen presenting cells, including macrophages, monocytes, neutrophils and a subset of B cells. This cytokine regulates the balance between Th1 and Th2 responses and is therefore a key regulator of cell-mediated immune responses. In particular, it plays a critical role in the promotion of Th1 responses [75-79] by (i) promoting differentiation of naïve T cells into IFN γ producing Th1 cells [75], (ii) co-stimulating the maximal secretion of IFN γ by Th1 cells [80] and (iii) stimulating the development of resting memory T cells into IFN γ producing Th1 cells [76]. IL12 also stimulates IFN γ secretion in NK cells, leading to the activation of phagocytic cells and to inflammation. Furthermore, IL12 promotes the differentiation of CD8 $^{+}$ cytotoxic T cells [81] and the reactivation and survival of CD4 $^{+}$ memory T cells [82]. Moreover, IL12 enhances the cytotoxic activity of NK cells and of CD8 $^{+}$ cytotoxic T cells [74]. Finally, IL12 directly stimulates early hematopoietic progenitor cells and promotes the proliferation and differentiation of bone marrow progenitors through synergy with other hematopoietic growth factors.

IL12 is a key cytokine acting on both innate and adaptive immune system. For this reason, multiple mechanisms have been reported for the anti-tumor activity of IL12 [83]. Following the induction of IFN γ production of a cascade of cytokines with pro-inflammatory, cytotoxic or cytostatic effects on tumor cells as well as anti-angiogenic molecules is observed. Moreover, the IL12-stimulated cytotoxic cells can directly act on cancer or endothelial cells [83].

The anti-tumor activity of IL12 has been investigated in several preclinical studies. Brunda and co-workers reported impressive therapeutic results in different models of cancer following the intraperitoneal administration of the cytokine, although no cures were achieved [84].

Despite the encouraging preclinical results, the administration of recombinant human IL12 in clinical trials in patients with cancer was associated with limited efficacy and with severe toxicity. The MTD (Maximal Tolerated Dose) for intravenous (i.v.) rhIL12 administration was found to be 500 ng/kg [85]. In a Phase II clinical trial, a slight change in the administration schedule caused the hospitalization of 12 out of 17 patients and the death of two of them, with only one partial response [17]. Different schedules and administration modalities were used in order to prevent severe toxicity, but they were associated with a lack of efficacy [86-93] (exception made for some particular types of cancer, such as cutaneous T-cell lymphoma, AIDS related Kaposi-sarcoma and non-Hodgkin's lymphoma, for which partial responses and complete responses could be observed [94-96]).

The systemic administration of untargeted rhIL12 at the MTD leads to an insufficient therapeutic concentration at the tumor site. For this reason, the use of tumor-targeting IL12-based immunocytokines has been proposed by our group and by others. Indeed, a large variety of molecular formats can be considered for IL12-based immunocytokines, since:

- (i) antibodies can be expressed as full immunoglobulins or as antibody fragments
- (ii) IL12 can be expressed as a single polypeptide, preserving the functionally-relevant intact N-terminus of the p40 subunit in a sequential p40-p35 fusion, or by attaching the individual subunits to different recombinant antibody moieties and letting them heterodimerize by disulfide bond formation

Our group has initially obtained promising therapeutic results with a sequential fusion of the p40 and p35 subunits with the tumor-targeting scFv(L19) [24,40], an antibody fragment specific to the alternatively-spliced EDB domain of fibronectin [97]. However, the tumor accumulation of this monomeric immunocytokine, as measured by quantitative biodistribution analysis, was less efficient compared to other dimeric or trimeric L19-based immunocytokines [23,32]. For this reason, alternative formats for the fusion of IL12 to tumor targeting antibodies were tested *in vitro* and *in vivo* [98,99]. These experiments showed that the fusion of one scFv moiety to each individual subunit of IL12 (i.e., fusion of both p40 and p35 to a scFv moiety) yielded heterodimeric immunocytokines with excellent tumor targeting properties in

biodistribution studies and with potent therapeutic activity. However, the GMP production of this heterodimeric cytokine is challenging, because of stability issues for stably-transfected cell lines and because of the propensity of the p40 and p35 subunits to homodimerize [99]. For this reason, our laboratory has continued to explore alternative formats for IL12-based immunocytokines, which would combine good pharmaceutical properties and efficient *in vivo* tumor targeting.

IL12 has also been fused to the C terminus of a humanized antibody (BC1) in IgG format [100], specific to a cryptic epitope on domain 7 of EDB-containing fibronectin [101]. The immunocytokine was investigated in a phase I clinical trial. The MTD was found to correspond to 15ug/kg and one partial response out of 13 treated patients was observed [56].

2.8.3. INTERLEUKIN 17

Interleukin 17 is the founding member of a new cytokine subfamily that includes seven ligands and five receptor subunits [102,103]. In 1993 the gene encoding IL17 was discovered in a rodent T cell library and termed CTLA-8 [102]. IL17 did not resemble to any known cytokine, but was recognized to have homology to an open reading frame encoded within *Herpesvirus Saimiri* [104]. A human IL17 homologue was identified that was also shown to be a T cell-derived factor with cytokine-like activity [105]. IL17 gene is located on chromosome 6 [102] and the protein is encoded by a polypeptide of 155 amino acids with an N-terminal leader sequence of 19 amino acids. There is one potential N-linked glycosylation site and six cysteine residues [105]. IL17 is a homodimeric cytokine that is secreted as a mixture of glycosylated (31kDa) and non-glycosylated (28kDa) protein [106].

IL 17 is mainly secreted by a new subset of T cells, termed Th17, which are similar to Th1 and Th2 cells [107]. Their development is driven by many different cytokines and IL23 is required for the pathogenicity and expansion of these cells [108]. Th17 cells are able to transfer autoimmune diseases. Apart from Th17 cells also CD8+ cells, $\gamma\delta$ + T cells and NKT cells are important sources of IL17 [109-111].

There are different mechanisms that contribute to suppress IL17 production or function. In particular, both Th1 and Th2 cytokines suppress Th17 development [112,113]; moreover, IL27 and IL2 also limit Th17 activity or development [114]. IL10, a well known anti-inflammatory cytokine, is also secreted by Th17 cells, but its production is counter-acted by IL23. This fact also explains the important role of IL23 in mediating autoimmunity in spite of the fact that it is not needed for Th17 differentiation [108].

IL17 activates the induction of cytokines (i.e. Interleukin 6 (IL6) and Granulocyte Colony-Stimulating Factor (G-CSF)) and of several chemokines in non-immune cells such as fibroblasts and epithelial cells [105,106]. Their expression stimulates neutrophil expansion and recruitment. For this reason IL17 is known to be a potent neutrophil activator.

The IL17 gene targets include also acute phase response genes and anti-microbial substances. For example lipocalin 2/24p3 expression is regulated by IL17, this acute phase protein binds to bacterial siderophore, iron-scavenging molecules necessary for bacterial survival [115]. Moreover, IL17 acts also in the expression of defensins, calgranulins and mucins, which have a direct antimicrobial activity [102].

IL17 was also found to promote autoimmune diseases. Elevated IL17 levels were found in rheumatoid arthritis, systemic lupus erythematosus and psoriasis patients [102]. Several studies in rodent models of rheumatoid arthritis (e.g. collagen-induced arthritis) indicate that IL17 may be a key cytokine in the disease pathogenesis. In particular anti-IL17 antibodies had a prominent anti-inflammatory effect [116,117] and IL17 KO mice did not develop collagen-induced arthritis [118].

IL17 is known to stimulate angiogenesis. In a study on Non-small Cell Lung Cancer (NSCLC) IL17 markedly increased the net angiogenic activity, by stimulating the production of several angiogenic CXC chemokines [119]. Numasaki et al. investigated the role of IL17 in neovascularization using tumor models and rat cornea assay. IL17 was found to promote angiogenesis via stimulation of vascular endothelial cell migration and induction of a variety of proangiogenic factors [120].

Regarding cancer, it is controversial whether IL17 favors or inhibits tumor growth [121]. Tumor cells transfected with the IL17 gene grew faster than untransfected cells when implanted in immunodeficient mice [119,122], but similar experiments performed with IL17 in immunocompetent mice gave ambiguous results [120,123]. Moreover, MC38 tumor implantation in IL17 knockout mice led to faster tumor growth in one laboratory [124] but not in a second laboratory, where the experiments were repeated [125].

2.8.4. INTERLEUKIN 18

Interleukin 18 is a proinflammatory cytokine that was discovered as an IFN γ inducing factor and which belongs to the IL1 family [126]. It is secreted as a biologically inactive precursor protein (pro-IL18) [127]. Its cleavage by the IL1 β converting enzyme yields the biologically active IL18 protein (18kDa) [128].

IL18 is produced by macrophages, dendritic cells, Kupffer cells, keratinocytes, osteoblasts, adrenal cortex cells, intestinal epithelial cells, microglial cells and synovial fibroblasts [129]. Macrophage stimulators such as LPS, exotoxins from gram-positive bacteria and other microbial products induces IL18 production [126]. IL18 acts on several cells, including T cells, B cells and NK cells. In particular, it enhances T and NK cells maturation, cytokine production and cytotoxicity, also by increasing FasL on NK cells. Moreover, it can induce Th1 or Th2 maturation depending on the presence of other cytokines and on the genetic background [129].

IL18 synergizes with other cytokines and induces the production of Interleukin 4 (IL4), IL6, Interleukin 13 (IL13), TNF, as well as IFN γ [129]. Moreover, IL18 plays an important role in cytokine activation, including stimulation of reactive oxygen intermediate synthesis, cytokine release and degranulation [130,131]. IL18 alone can induce low levels of IFN γ production in T cells, but when acting in presence of costimulants a synergistic mechanism is activated that yields larger quantities of IFN γ [126]. IL12 upregulates the production of IL18 receptor alpha chain on Th1 cells [132] and its presence is essential to induce IL18 driven IFN γ production in macrophages [133].

Systemic administration of IL18 showed significant antitumor activity in several preclinical animal models including Meth A sarcoma [134], CL8-1 melanoma [135], ARH-77 human multiple myeloma [136], Dunn osteosarcoma [137] and EL4 T cell leukemia [138].

In Phase I clinical trials rhIL18 was administered in 28 patients with solid cancer, at different doses, with a daily two hours intravenous infusion for five consecutive days as a single cycle. Common adverse events were fever, nausea, chills, headache, hypotension, reversible cytopenias, transient transaminase elevation and hypoalbuminemia. IL18 was well tolerated and no MTD was determined. There were two unconfirmed delayed partial responses [139]. A similar study was repeated using the same schedule, but repeating the cycle every 28 days or by administering IL18 once a week during six months. No MTD could be determined

and no objective response could be observed [140]. Finally in a Phase II clinical trial in patients with stage IV melanoma three different doses were tested following the 5-days schedule repeated every 28 days. Out of 63 evaluable subjects, one patient experienced a partial response after 4 cycles and four patients had disease stabilization lasting 6 months or more [141]. IL18 confirmed its safety but also showed limited efficacy as a monotherapy in this setting. Since IL-18 appears to act predominantly as a costimulatory cytokine, its optimal use for cancer therapy may be in combination with other cytokines, vaccines or monoclonal antibodies.

2.9. AIM OF THE THESIS

Many cytokines have shown potent antitumor activities in preclinical experiments and represent promising agents for cancer therapy. However, despite encouraging results in animal models, only a few cytokines, are approved as anticancer drugs. In many cases, impressive preclinical results were obtained with modalities that are rarely applicable in the clinical setting, especially in the case of disseminated disease (e.g. intratumoral application, intratumoral implantation of cytokine producing cells) [10,11,13]. By contrast, complete responses are rarely seen with systemic administration of cytokines [11,14-16]. Serious side effects can be observed in vivo at low doses, which prevent escalation to the concentrations which are needed to achieve curative effects. Since most cytokines do not preferentially localize at the tumor site after intravenous administration, monoclonal antibodies have been used as modular components for the preparation of fusion proteins (“immunocytokines”), which allow the selective localization of the cytokine payload on neoplastic masses. The targeted delivery of these immunostimulatory proteins could lead to an improved therapeutic index and to more potent therapeutic benefit with acceptable toxicities. Antibody-mediated pharmacodelivery strategies have been reported for many cytokines, including Interleukin IL2, IL10, IL12, IL15, GM-CSF, IFN α , IFN γ , TNF (for reviews, see [7,28,142,143]).

Over the last decade, our group has studied the tumor targeting and therapeutic performance of various immunocytokines, based on human monoclonal antibodies specific to splice isoforms of fibronectin and of tenascin-C. This work has led to the investigation of the immunocytokines L19-IL2, L19-TNF and F16-IL2 in Phase I and Phase II clinical trials in patients with cancer, alone or in combination with chemotherapy [45,46]. In this thesis specific emphasis is given on the fusion of cytokines to the scFv(F8), a human antibody fragment specific to the alternatively spliced EDA domain of fibronectin [144]. This antigen has been found

to be virtually undetectable in normal adult tissues (exception made for ovary, placenta and uterus [20]) but to be strongly expressed in vascular and stromal structures of many different tumor types.

We fused four different cytokines to the F8 antibody. Two cytokines, Interleukin 7 and Interleukin 18, showed prominent anti-cancer activity in preclinical models but had never been investigated as immunocytokine components. There has been a long controversy as to whether IL17 has an impact on tumor growth, but the effects of systemic IL17 were never studied, probably due to its potential side effects. We reasoned that an IL17 based immunocytokine could assess whether IL17 may affect tumor growth. Finally IL12 is a very promising cytokine for cancer treatment but clinical investigation had been stopped due to severe side effects [17]. In our lab different IL12 immunocytokines have already been studied, showing impressive preclinical results without worsening of inflammatory processes. However, some important issues about protein yield and quality were raised. Here we propose a new immunocytokine format with increased pharmaceutical quality and comparable therapeutic activity.

Interleukin 7, Interleukin 12, Interleukin 17 and Interleukin 18 were fused to the F8 antibody using different formats and expressed in mammalian cells. The immunocytokines with the best pharmaceutical quality were tested *in vivo* for their targeting and therapeutic potential on syngeneic murine models of cancer. Immunocytokines given as monotherapy rarely exhibit complete cures of cancer in animal models and in patients. However, combination therapies have resulted in complete and long-lasting tumor eradications, which cannot be achieved by conventional chemotherapy. Therefore, the most promising fusion proteins (i.e. F8-mIL7-F8 and mIL12-F8-F8) were administered in combination with chemotherapy and/or F8-IL2.

3. RESULTS

3.1. IMMUNOCYTOKINES BASED ON MURINE INTERLEUKIN 7 [34]

3.1.1. CLONING AND CHARACTERIZATION OF F8-MIL7

3.1.1.1. Cloning and expression

In line with strategies for the construction of immunocytokines previously described by our laboratory [20,33,35,37,39,42,145], we initially prepared a fusion protein consisting of scFv(F8) sequentially fused to murine IL7 (termed “F8-mIL7”). The fusion protein was cloned and expressed in mammalian cells (**Fig. 3.1A**). Within the scFv moiety, a 5-aminoacid linker was used between V_H and V_L, which drives the formation of non-covalent “diabody” structures [25,144] (**Fig. 3.1B**). F8-mIL7 was cloned in pcDNA3.1 and expressed in stably-transfected in CHO-S (Chinese Hamster Ovary) cells. The immunocytokine was purified from the culture medium to homogeneity by protein A chromatography.

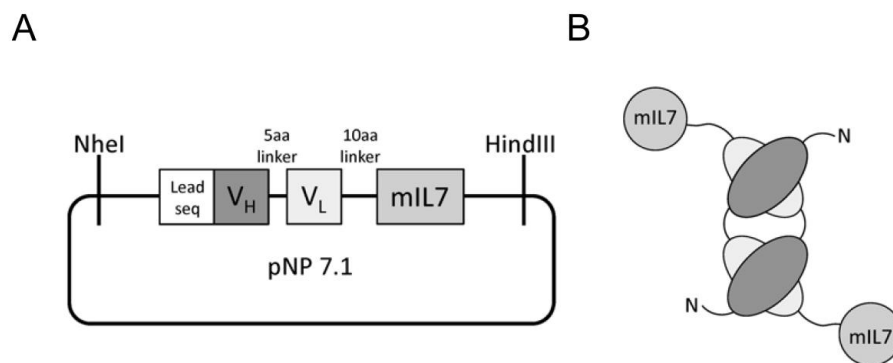


Fig. 3.1 Cloning and expression of F8-mIL7. (A) Schematic representation of the cloning strategy of F8-mIL7 with a 5 amino acid linker between V_H and V_L and 10 amino acid linker between scFv(F8) and mIL7. (B) Domain assembly of F8-mIL7.

3.1.1.2. In vitro characterization

3.1.1.2.1. SDS-PAGE

F8-mIL7 ran as a covalent homodimer in SDS-PAGE (Sodium Dodecyl Sulphate PolyAcrylamide Gel Electrophoresis) analysis in non-reducing conditions and as a monomer in reducing conditions. The broad band visible in the gel could be converted into a sharper and smaller band (approx. 45 kDa) upon treatment with PNGase (Fig 3.2).

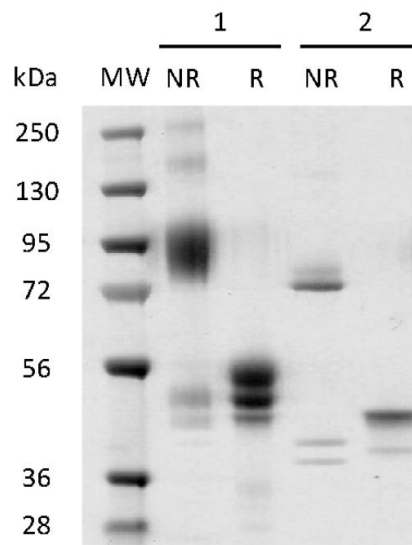


Fig 3.2 SDS-PAGE analysis of F8-mIL7. (1) Purified and (2) PNGase deglycosylated F8-mIL7 showed presence of glycosylated covalent homodimers in non-reducing conditions. MW, molecular weights; NR, non-reducing; R, reducing.

3.1.1.2.2. Size exclusion chromatography

F8-mIL7 exhibited a homogenous profile in size-exclusion chromatography with a retention time corresponding to the expected dimeric structure (**Fig. 3.3**).

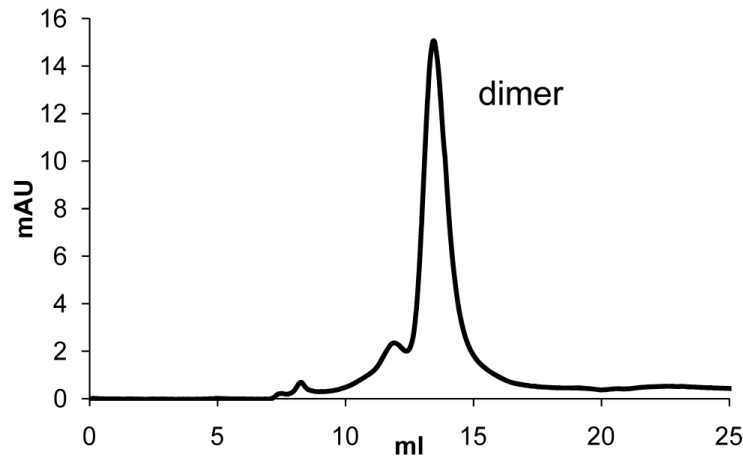


Fig. 3.3 Gel filtration analysis of purified F8-mIL7. The peak corresponds to the homodimeric form of F8-mIL7.

3.1.1.2.3. BIAcore analysis

The BIAcore analysis showed that F8-mIL7 bound to the cognate antigen with high affinity (**Fig. 3.4**).

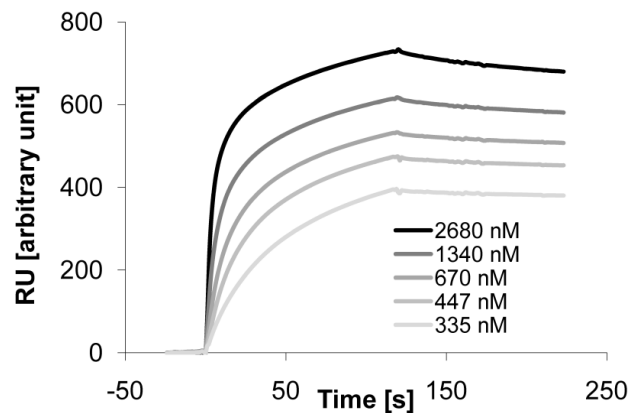


Fig. 3.4 BIAcore analysis of F8-mIL7 on EDA-coated chip. The concentrations of F8-mIL7 for the different sensograms are indicated.

3.1.1.2.4. Immunofluorescence analysis on tumor sections

As expected, F8-mIL7 strongly bound to neo-vascular structures in sections of F9 tumors, as revealed by immunofluorescence analysis (**Fig. 3.5**).

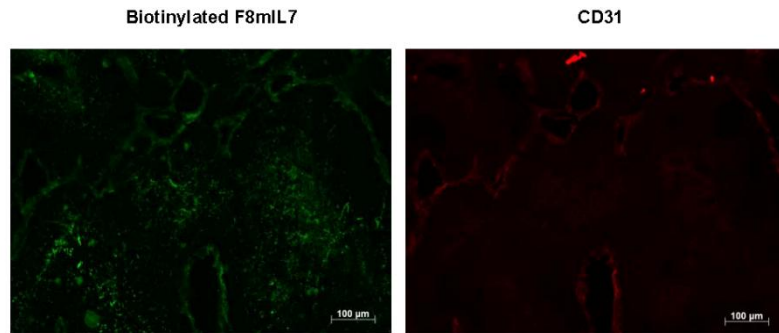


Fig. 3.5 Immunofluorescence analysis of F9 teratocarcinomas. F8-mIL7 was biotinylated and used as staining reagent in an immunofluorescence procedure. Scale bars = 100 µm.

3.1.1.3. In vivo characterization

3.1.1.3.1. Biodistribution studies on F9 teratocarcinoma bearing immunocompetent and athymic mice

A radioiodinated preparation of F8-mIL7 was used for a quantitative biodistribution analysis in both athymic and immunocompetent mice, bearing subcutaneously-grafted murine F9 teratocarcinomas. The results 24 h after i.v. injection were disappointing (**Fig. 3.6**), with approx. 1% injected dose per gram (%ID/g) in the tumor and with elevated levels of radioactivity in liver, spleen and kidney, both in nude mice (**Fig. 3.6A**) and in immunocompetent mice (**Fig. 3.6B**).

The use of larger amounts of radioiodinated protein (110 µg rather than 10 µg) substantially reduced the uptake of F8-mIL7 in normal organs, suggesting that the fusion protein at low doses was trapped by IL7 receptors at locations other than the tumor (**Fig. 3.6B**).

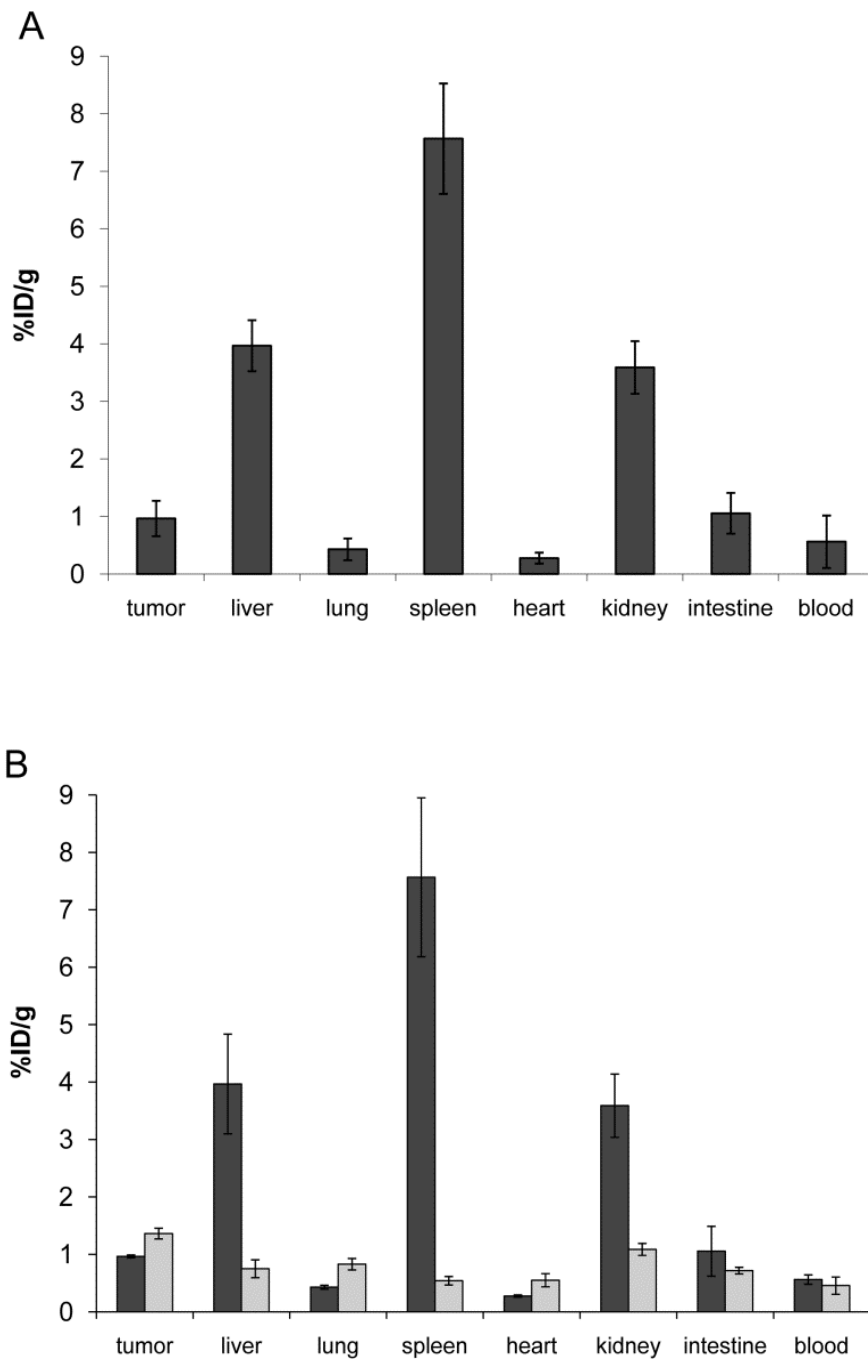


Fig. 3.6 Biodistribution study of radiolabeled F8-mIL7. (A) Athymic Balb/c nude mice and (B) immunocompetent 129/SvEv mice bearing syngenic s.c. F9 teratocarcinoma were injected i.v., respectively, with 15 μ g radiolabeled 125 I-F8-mIL7 (n = 5 athymic mice), with 15 μ g radiolabeled 125 I-F8-mIL7 (■, n = 5 immunocompetent mice) or with 10 μ g radiolabeled 125 I-F8-mIL7 mixed with 100 μ g unlabeled F8-mIL7 (■, n = 4 immunocompetent mice). Mice were sacrificed after 24h. Organs were excised and radioactivity counted, expressing results as percent of injected dose per gram of tissue (%ID/g \pm SE).

3.1.1.3.2. Therapeutic properties on F9 teratocarcinoma bearing immunocompetent and athymic mice

In spite of the disappointing biodistribution results, therapy experiments were performed in immunocompetent and nude mice bearing subcutaneous F9 tumors. While F8-mIL7 displayed no anti-cancer activity in nude mice compared to saline controls (**Fig. 3.7A**), the fusion protein mediated tumor growth retardation in tumor-bearing 129/SvEv mice (**Fig. 3.7B**).

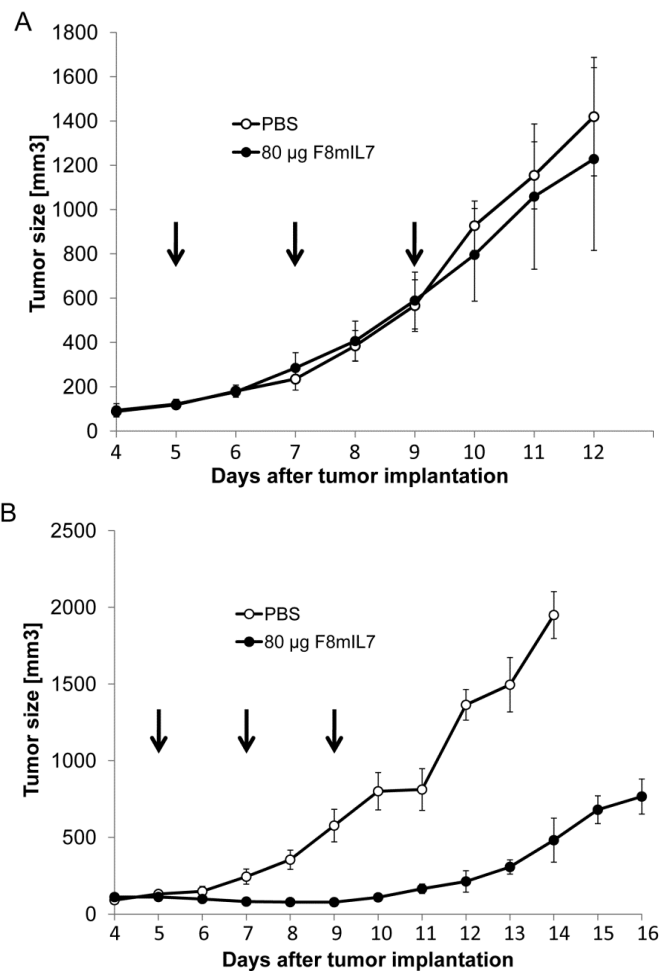


Fig 3.7 Therapeutic activity of F8-mIL7 in murine F9 teratocarcinoma (A) Athymic Balb/c nude ($n = 4$, $n = 3$) and (B) immunocompetent 129/SvEv ($n = 3$, $n = 3$) mice bearing syngenic s.c. F9 teratocarcinomas were treated i.v. with three doses of 80µg F8-mIL7 (●) or PBS (○, Phosphate-Buffered Saline) as control. Treatment was performed on days 5, 7, 9 after tumor implantation (black arrows). Data represent mean tumor volumes \pm SE. Tumor growth curves were stopped when the first tumor per group reached 2000 mm³.

3.1.2. CLONING AND CHARACTERIZATION OF NOVEL FORMATS FOR MIL7-BASED IMMUNOCYTOTOKINES

3.1.2.1. Cloning and expression

With the aim to improve the pharmaceutical properties of fusion proteins composed of scFv(F8) and of mIL7, we investigated the expression and performance of alternative immunocytokine formats.

Using the F8-mIL7 format, we shortened the linker between scFv fragment and mIL7 to 6 amino acids (**Fig. 3.8A,B**), we extended the polypeptide linker between VH and VL to 14 amino acids (**Fig. 3.8C,D**) and we mutated Cys33 and Cys108 to serine(**Fig. 3.8E,F**).

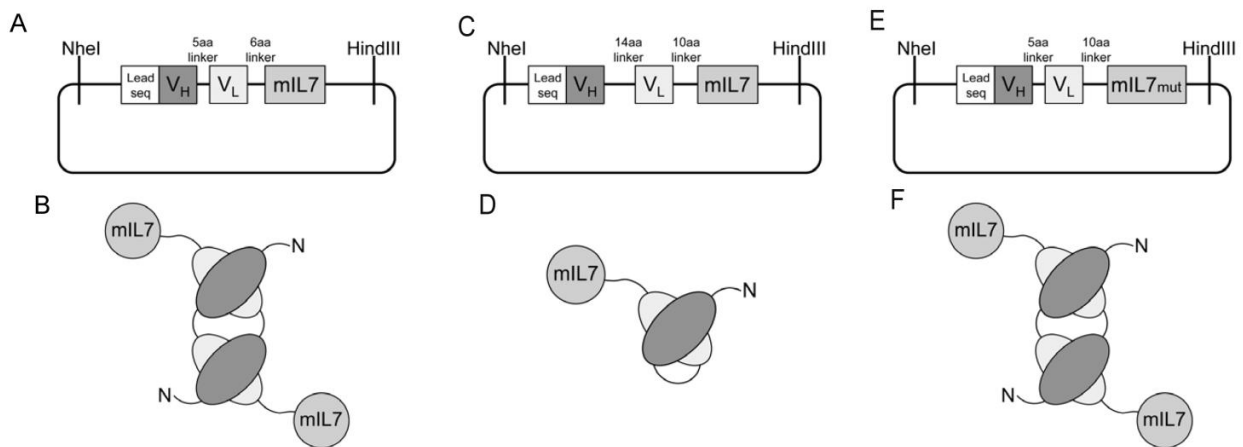


Fig. 3.8 Cloning and expression of different formats of mIL7 fusion proteins. (A, C, E) Schematic representation of the cloning strategy and (B, D, F) domain assembly of (A-B) F8-mIL7 with a 5 amino acid linker between VH and VL and 6 amino acid linker between scFv(F8) and mIL7; (C-D) F8-mIL7 with a 14 amino acid linker between VH and VL and 10 amino acid linker between scFv(F8) and mIL7; (E-F) F8-mIL7 with a 5 amino acid linker between VH and VL and 10 amino acid linker between scFv(F8) and mIL7 bearing two cysteine to serine mutations at positions 33 and 108.

Finally we designed, cloned and expressed a novel immunocytokine format (termed “F8-mIL7-F8”), consisting of a sequential fusion of scFv(F8) with murine IL7 and with a second scFv(F8) moiety.

In order to facilitate comparative biodistribution and therapy studies, the novel immunocytokine format was used also for the production of the KSF-mIL7-KSF fusion protein, which consisted of the antibody fragment KSF specific to hen egg lysozyme [145] and which served as negative control in subsequent experiments (**Fig. 3.9**).

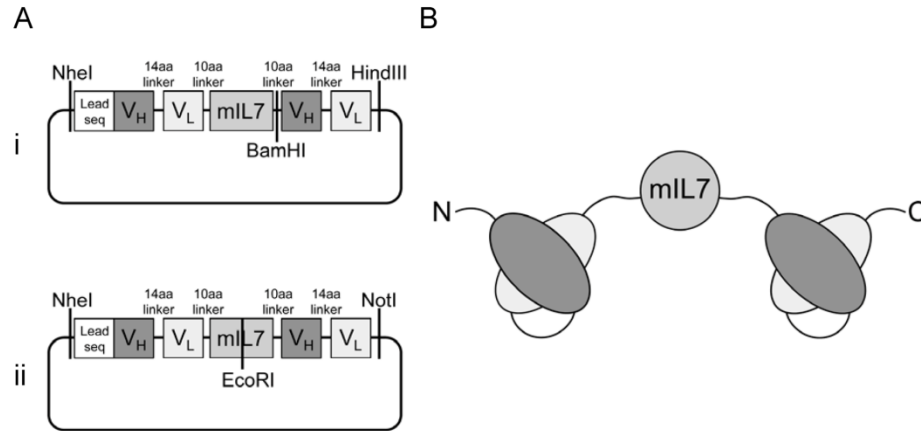


Fig. 3.9. Cloning and expression of F8-mIL7-F8 and KSF-mIL7-KSF. KSF antibody is specific to hen egg lysozyme and used as negative control (A) Schematic representation of the cloning strategy of F8-mIL7-F8 and KSF-mIL7-KSF with a 14 amino acid linker between V_H and V_L and 10 amino acid linker between scFv(F8)/scFv(KSF) and mIL7. (B) Domain assembly of F8-mIL7-F8 and KSF-mIL7-KSF.

3.1.2.2. In vitro characterization

3.1.2.2.1. SDS-PAGE

Shortening the linker between scFv fragment and mIL7 to 6 aminoacids did not reduce the formation of disulfide-linked homodimers in SDS-PAGE analysis (**Fig. 3.10A**). Extending the polypeptide linker between V_H and V_L to 14 aminoacids increased the amount of monomeric proteins in SDS-PAGE analysis run in non-reducing conditions (**Fig. 3.10B**), but a gel-filtration analysis of the resulting fusion protein showed a heterogenous profile, with the majority of the protein present as a monomer and thus smaller than the renal filtration threshold (data not shown). Finally, attempts to mutate Cys33 and Cys108 to serine did not result in improved biochemical quality of the F8-mIL7 fusion protein (**Fig. 3.10C**).

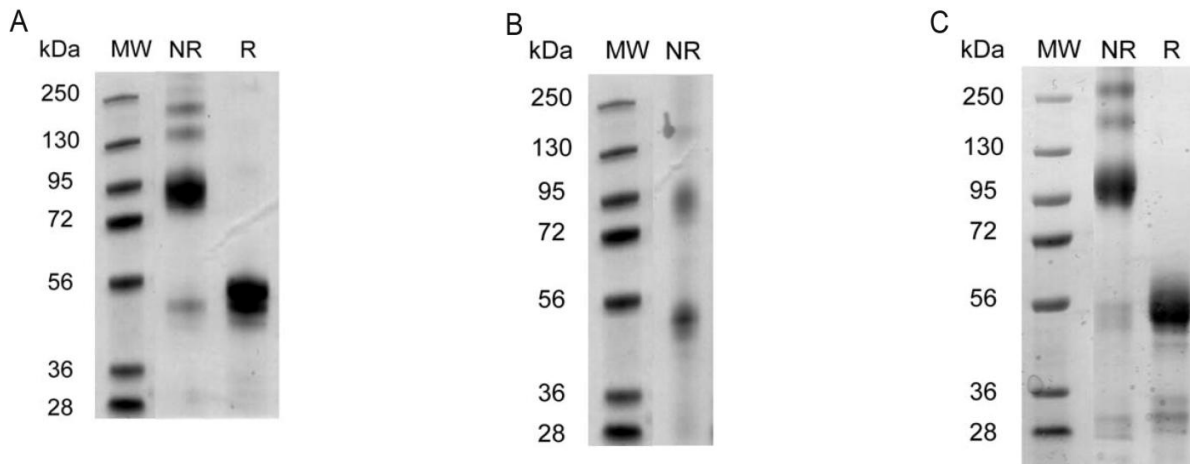


Fig 3.10 SDS-PAGE analysis of different formats of mIL7 fusion proteins. (A) F8-mIL7 with a 5 amino acid linker between VH and VL and 6 amino acid linker between scFv(F8) and mIL7; (B) F8-mIL7 with a 14 amino acid linker between VH and VL and 10 amino acid linker between scFv(F8) and mIL7; (C) F8-mIL7 with a 5 amino acid linker between VH and VL and 10 amino acid linker between scFv(F8) and mIL7 bearing two cysteine to serine mutations at positions 33 and 108 showed presence of covalent homodimers in non-reducing conditions. MW, molecular weights; NR, non-reducing; R, reducing.

The novel immunocytokine F8-mIL7-F8 and its non-targeted counterpart KSF-mIL7-KSF were shown to be homogeneous in SDS-PAGE analysis in reducing and non-reducing conditions. The broad band visible in the gel could be converted into a sharper and smaller band upon treatment with PNGase (Fig. 3.11).

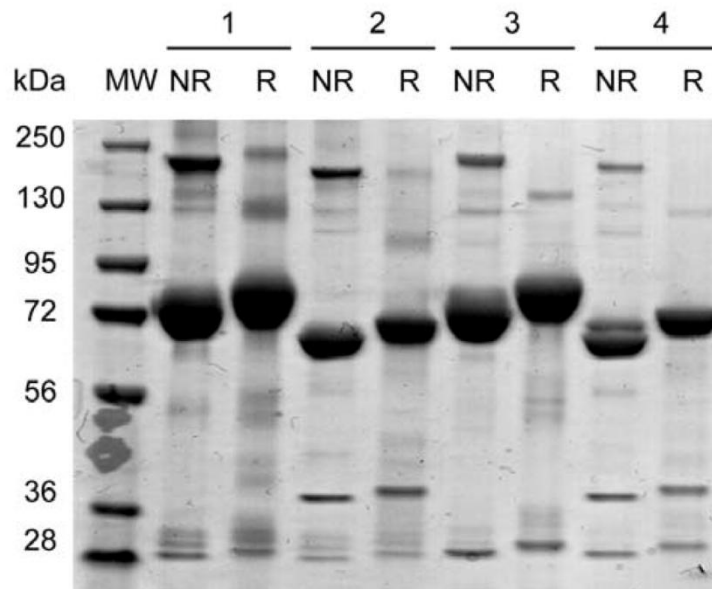


Fig. 3.11 SDS-PAGE analysis of F8-mIL7-F8 and KSF-mIL7-KSF. (1) F8-mIL7-F8, (2) PNGase deglycosylated F8-mIL7-F8, (3) KSF-mIL7-KSF and (4) PNGase deglycosylated KSF-mIL7-KSF showed a predominant presence of glycosylated monomers even under non-reducing conditions. MW, molecular weights; NR, non-reducing; R, reducing.

3.1.2.2.2. Size exclusion chromatography of F8-mIL7-F8 and KSF-mIL7-KSF

Both fusion proteins, were shown a homogeneous profile in gel-filtration analysis with a retention time corresponding to the expected monomeric structure (Fig. 3.12).

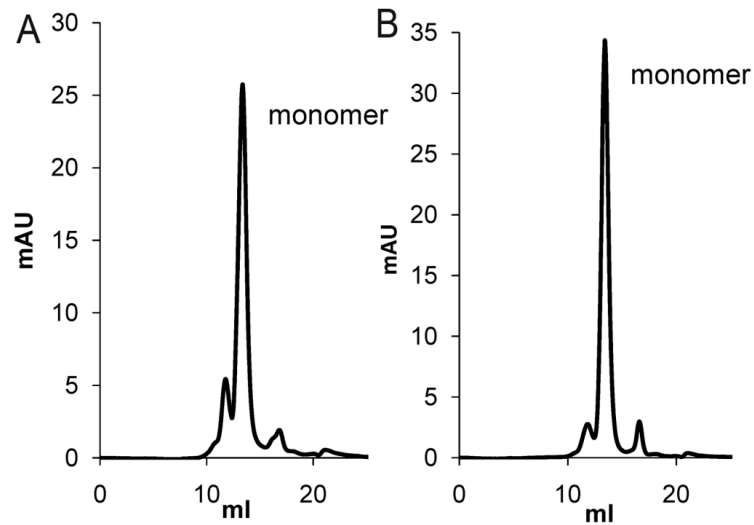


Fig. 3.12 Gel filtration analysis of purified (A) F8-mIL7-F8 and (B) KSF-mIL7-KSF. The peaks elute at a similar retention volume and correspond to the monomeric form of the fusion proteins.

3.1.2.2.3. BIAcore analysis of F8-mIL7-F8

The BIAcore analysis showed that F8-mIL7-F8 bound avidly to the cognate antigen (Fig. 3.13).

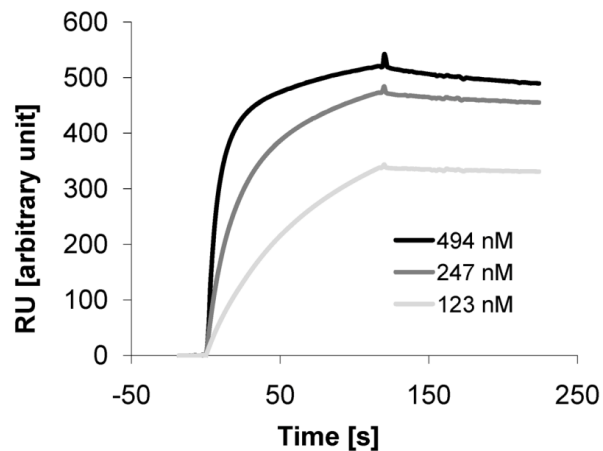


Fig. 3.13 BIAcore analysis of F8-mIL7-F8 on EDA coated chip. The concentrations of F8-mIL7-F8 for the different sensograms are indicated

3.1.2.2.4. F8-mIL7-F8 and KSF-mIL7-KSF immunofluorescence analysis on tumor Sections

As expected, F8-mIL7-F8 strongly bound to neo-vascular structures in sections of F9 tumors, whereas KSF-mIL7-KSF does not, as revealed by immunofluorescence analysis (**Fig. 3.14**).

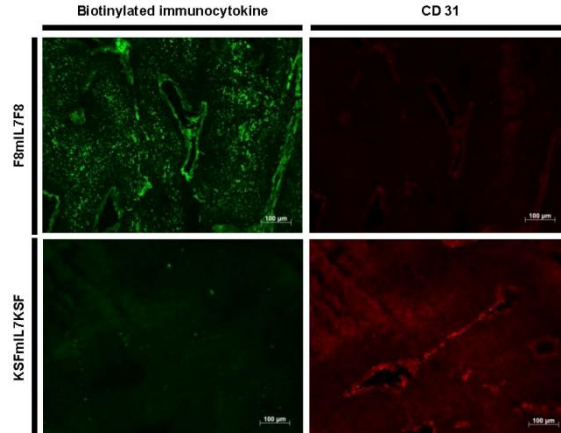


Fig. 3.14 Immunofluorescence analysis of F9 teratocarcinomas. F8-mIL7-F8 and KSF-mIL7-KSF were biotinylated and used as staining reagents in an immunofluorescence procedure. Scale bars = 100 µm.

3.1.2.2.5. F8-mIL7-F8 and KSF-mIL7-KSF stability

Both fusion proteins were found to be stable upon incubation at 37°C for several days (**Fig. 3.15**).

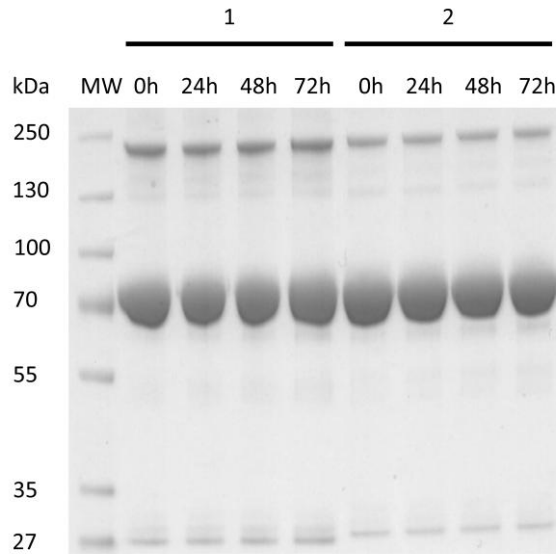


Fig. 3.15. Stability of F8-mIL7-F8 and KSF-mIL7-KSF at 37 °C. SDS-PAGE analysis of purified (1) F8mIL7F8 and (2) KSFmIL7KSF stored in PBS at 37°C for 0, 24, 48 or 72 hours.

3.1.2.2.6. F8-mIL7-F8 and KSF-mIL7-KSF bioactivity assay

Both immunocytokines were found to be active in an *in vitro* cell proliferation assay (Fig. 3.16).

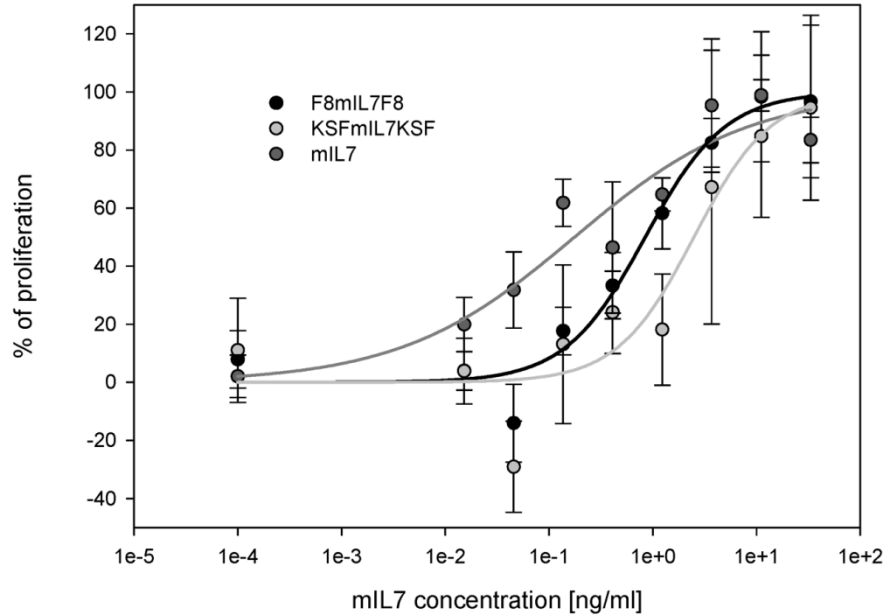


Fig. 3.16 Proliferation bioactivity assay on human peripheral blood mononuclear cells. F8-mIL7-F8 and KSF-mIL7-KSF displayed an *in vitro* biological activity comparable to the one of recombinant mIL7 (mean of 3 replicates \pm SD).

3.1.2.3. In vivo characterization of F8-mIL7-F8 and KSF-mIL7-KSF

3.1.2.3.1. Biodistribution studies on F9 teratocarcinoma bearing immunocompetent mice

Radioiodinated preparations of F8-mIL7-F8 and KSF-mIL7-KSF were administered by intravenous injection to tumor-bearing mice and studied by quantitative biodistribution analysis (Fig. 3.17). The novel format exhibited an improved tumor targeting performance, with tumor-to-blood ratios of 16:1 at 24 hours, while KSF-mIL7-KSF did not exhibit a preferential tumor accumulation at the same time point.

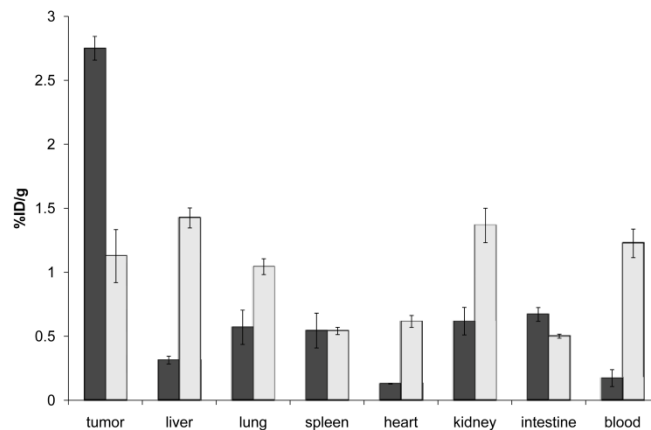


Fig. 3.17 Comparative biodistribution study of radioiodinated, F8-mIL7-F8 and KSF-mIL7-KSF.

Immunocompetent 129/SvEv mice bearing syngenic s.c. F9 teratocarcinomas were injected with 10 μ g radiolabeled 125 I-F8-mIL7-F8 mixed with 100 μ g unlabeled F8-mIL7-F8 (■, n = 3) or with 10 μ g radiolabeled 125 I-KSF-mIL7-KSF mixed with 100 μ g unlabeled KSF-mIL7-KSF (▒, n = 4). Mice were sacrificed after 24h. Organs were excised and radioactivity counted, expressing results as percent of injected dose per gram of tissue (%ID/g) \pm SE.

3.1.2.3.2. Therapeutic properties on F9 teratocarcinoma bearing immunocompetent mice

The therapeutic performance of F8-mIL7-F8 and KSF-mIL7-KSF, used alone or in combination with paclitaxel, was tested in immunocompetent mice bearing subcutaneous F9 tumors (**Fig. 3.18**). F8-mIL7-F8 could induce a tumor growth retardation, but not to the extent which had previously been documented for other immunocytokines targeting oncofetal fibronectin (e.g., those based on IL2, TNF or IL12 [24,37-40]). Similar to IL2-based immunocytokines previously studied by our group [37,38], the combination of F8-mIL7-F8 with paclitaxel exhibited an additive effect, which resulted into greater tumor growth retardation and longer survival (**Fig. 3.18B**).

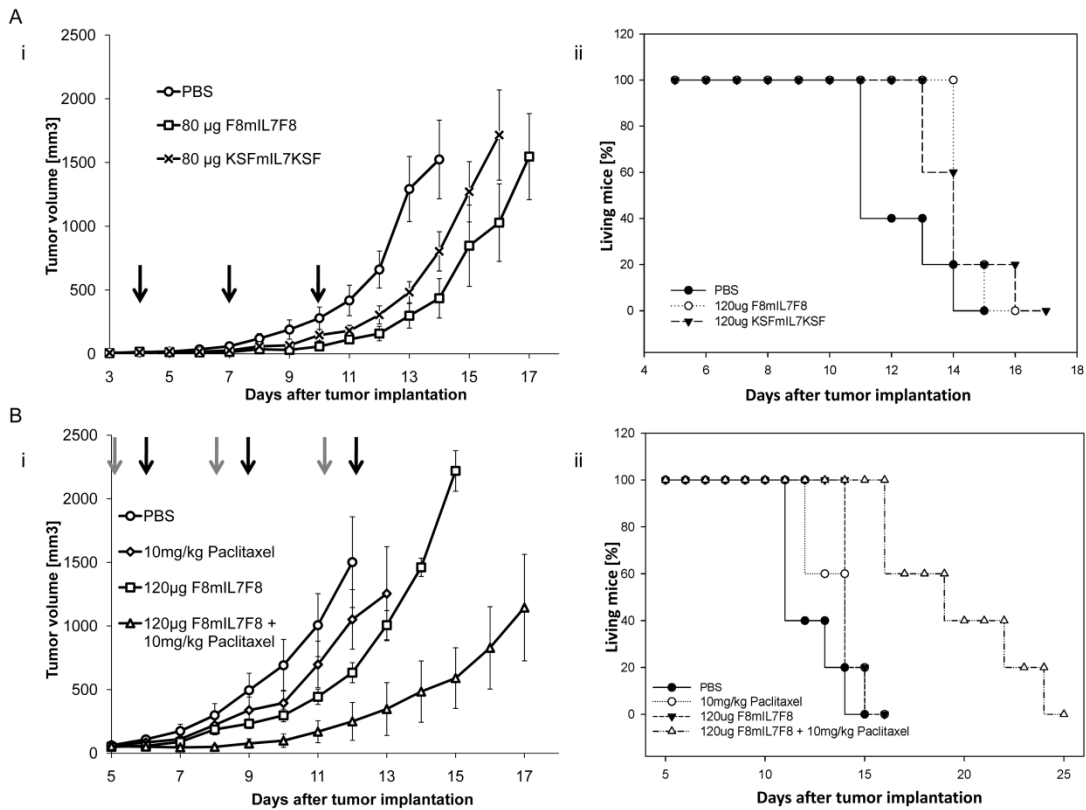


Fig. 3.18 Therapeutic activity of F8-mIL7-F8 alone or in combination with paclitaxel in immunocompetent 129/SvEv mice bearing syngenic s.c. F9 teratocarcinoma. (A) Tumor-bearing mice were treated i.v. with 80µg F8-mIL7-F8 (n = 4) or 80µg KSF-mIL7-KSF (n = 5) or PBS as control (n = 5). Treatment was performed on days 4, 7, 10 after tumor implantation (black arrows). (i) Data represent mean tumor volumes ± SE. Tumor growth curves were stopped when the first tumor per group reached 2000 mm³. (ii) Survival plot. Data represent percent of animals still alive. (B) Mice were treated i.v. with 120µg F8-mIL7-F8 (n = 5) or 10mg/kg paclitaxel (n = 5) or 120µg F8-mIL7-F8 in combination with 10mg/kg paclitaxel (n = 5) or PBS as control (n = 5). Treatment was performed with paclitaxel on days 5, 8, 11 after tumor implantation (grey arrows) and with F8-mIL7-F8 on days 6, 9, 12 after tumor implantation (black arrows). (i) Tumor growth curves. (ii) Survival plot.

3.2. IMMUNOCYTOKINE BASED ON MURINE INTERLEUKIN 17^[146]

3.2.1. CLONING AND CHARACTERIZATION OF F8-mIL17

3.2.1.1. Cloning and expression

We cloned and expressed in mammalian cells a fusion protein consisting of scFv(F8) sequentially fused to a murine IL17 monomer (**Fig. 3.19A**). In order to obtain a fully functional scFv monomer, a 14-amino acid linker was used between V_H and V_L. The two mIL17 monomers drive the disulfide-linked covalent homodimerization of the fusion protein, forming a stable immunocytokine termed “F8-mIL17” (**Fig. 3.19B**). F8-mIL17 was cloned in pcDNA3.1 and expressed in stably-transfected in CHO-S cells. The immunocytokine was purified from the culture medium to homogeneity by protein A chromatography.

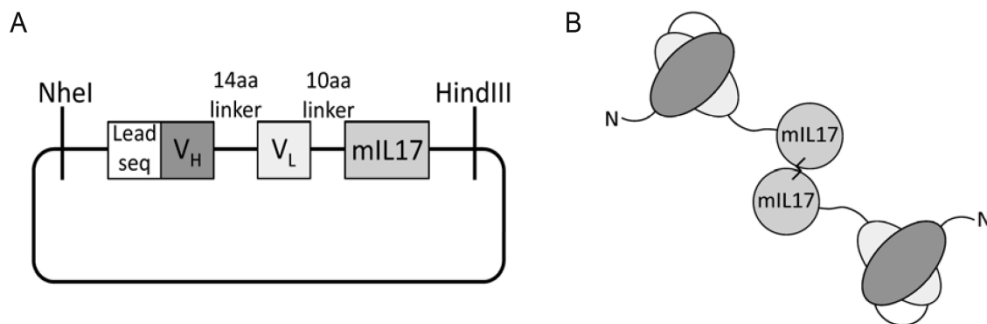


Fig. 3.19 Cloning and expression of F8-mIL17. (A) Schematic representation of the cloning strategy of F8-mIL17 with a 14-amino acid linker between variable heavy (V_H) and light (V_L) chain. (B) Schematic representation of the domain assembly of F8-mIL17.

3.2.1.2. In vitro characterization

3.2.1.2.1. SDS-PAGE

The immunocytokine ran as a covalent homodimer in SDS-PAGE in non-reducing conditions and as a monomer in reducing conditions. The broad band visible in the gel in non-reducing conditions and the two bands visible in reducing conditions could be converted into single, sharper and smaller bands upon treatment with PNGase (Fig. 3.20).

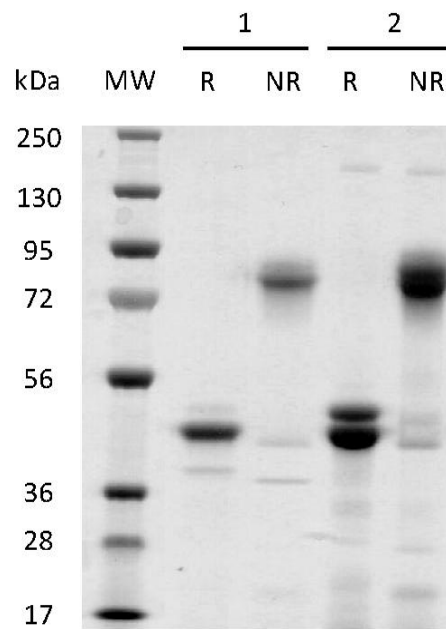


Fig. 3.20 SDS-PAGE analysis of purified F8-mIL17: (1) PNGase deglycosylated and (2) non-PNGase deglycosylated F8-mIL17. The fusion protein is present in different glycosylation forms. MW, molecular weights; NR, non-reducing; R, reducing.

3.2.1.2.2. Size exclusion chromatography

F8-mIL17, exhibited a homogeneous profile in size-exclusion chromatography with a retention time corresponding to the expected dimeric structure (Fig. 3.21).

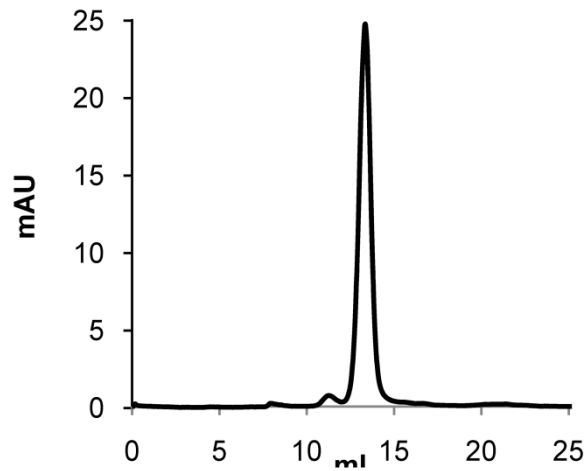


Fig. 3.21 Gel filtration analysis of affinity-purified F8-mIL17. The peak corresponds to the homodimeric form of the fusion protein.

3.2.1.2.3. BIAcore analysis on EDA coated chip

F8-mIL17 was shown to retain the binding affinity of the parental antibody in a BIAcore assay (Fig. 3.22).

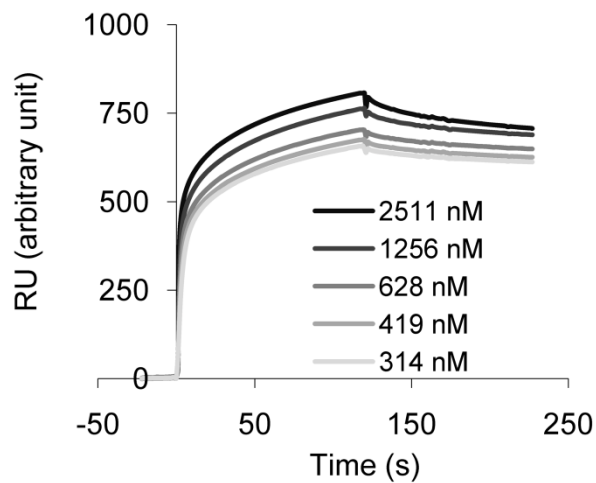


Fig. 3.22 BIAcore analysis of F8-mIL17 on EDA-coated chip. The concentrations of F8-mIL17 for the different sensograms are indicated.

3.2.1.2.4. Bioactivity assay

The immunocytokine was found to be fully active in an *in vitro* cytokine production assay (Fig. 3.23).

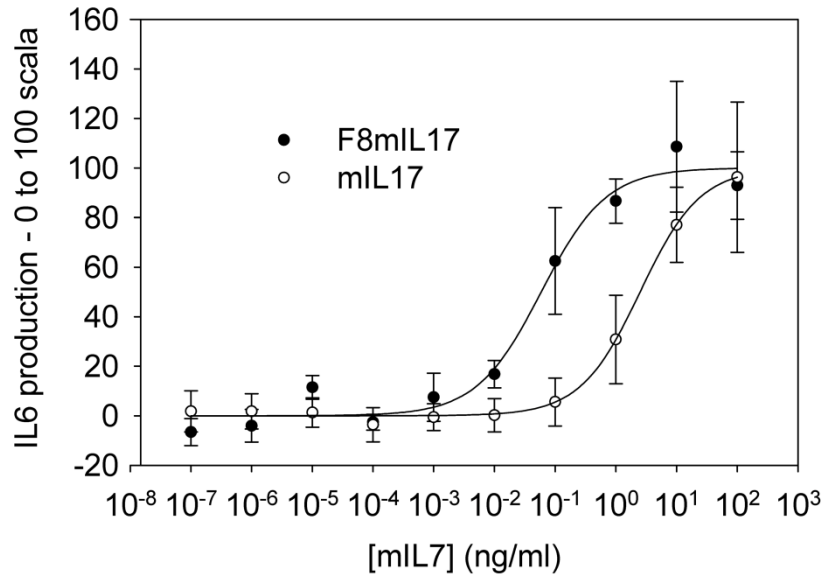


Fig. 3.23 IL6 production bioactivity assay on NIH 3T3 fibroblasts. F8-mIL17 displayed biological activity comparable with the one of recombinant murine IL17 (mean of 3 replicates \pm SD).

3.2.1.2.5. Immunofluorescence analysis on tumor sections

As expected and in line with previous experiments based on the F8 antibody[144], the F8-mIL17 immunocytokine localized around tumor blood vessels (Fig. 3.24).

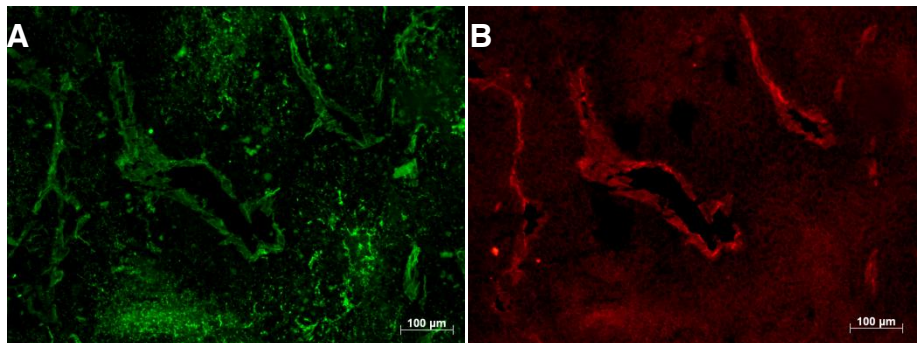


Fig. 3.24 Immunofluorescent staining of F8-mIL17 on F9 tumors. (A) F8-mIL17 was biotinylated and used as staining reagent in an immunofluorescence procedure. (B) CD31 staining. F8-mIL17 shows a vascular staining pattern. Scale bars = 100 μ m.

3.2.2. IN VIVO CHARACTERIZATION

3.2.2.1. Biodistribution studies in F9 teratocarcinoma bearing immunocompetent and athymic mice

A radioiodinated preparation of F8-mIL17 was analyzed in a quantitative biodistribution study in immunocompetent mice bearing subcutaneous F9 tumors, confirming a preferential accumulation in the tumor mass [4.3% %ID/g at 24 h], compared to normal organs [tumor-to-blood ratio of 14:1 (**Fig. 3.25**)]. Similar results were obtained in athymic mice (**Fig. 3.25**). Moreover the use of larger amounts of radioiodinated protein did not affect the targeting performance (**Fig. 3.25**).

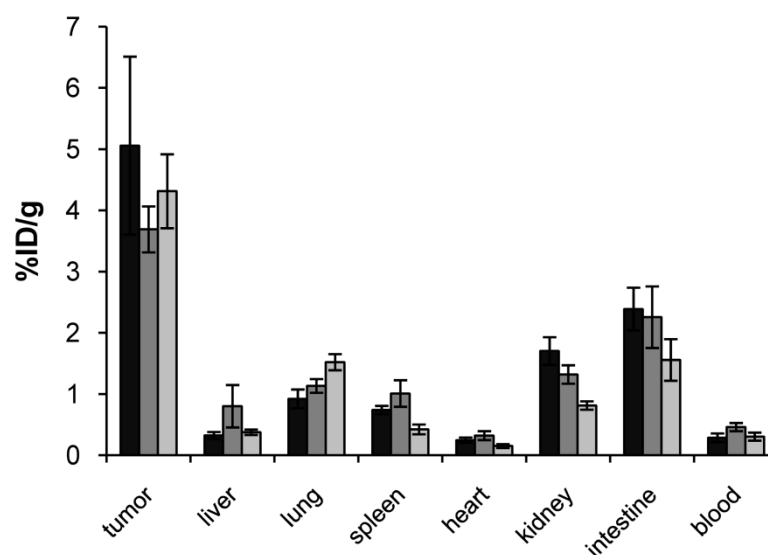


Fig. 3.25 Tumor targeting properties of F8-mIL17 in biodistribution studies. Balb/c nude and 129/SvPas mice (n = 5) bearing subcutaneous F9 tumors. 14.5 μg radiolabeled ^{125}I -F8-mIL17 were injected i.v. in Balb/c nude (■) and 129/SvPas mice (■), 7.5 μg radiolabeled ^{125}I -F8-mIL17 and 60 μg unlabeled F8-mIL17 were mixed and injected i.v. in 129/SvPas mice (□), which were sacrificed after 24 h. Organs were excised and radioactivity counted, expressing results as percent injected dose per gram of tissue (%ID/g) ±SE. A selective accumulation of F8-mIL17 in F9 tumors could be observed over time.

3.2.2.2. Therapeutic properties in F9 teratocarcinoma bearing immunocompetent and athymic mice

When administered intravenously at doses of 100 μ g (day 5, 7, 9), F8-mIL17 displayed no anti-cancer activity in immunocompetent (Fig. 3.26A) and athymic mice (Fig. 3.26B) bearing subcutaneous F9 tumors, compared to the saline control group.

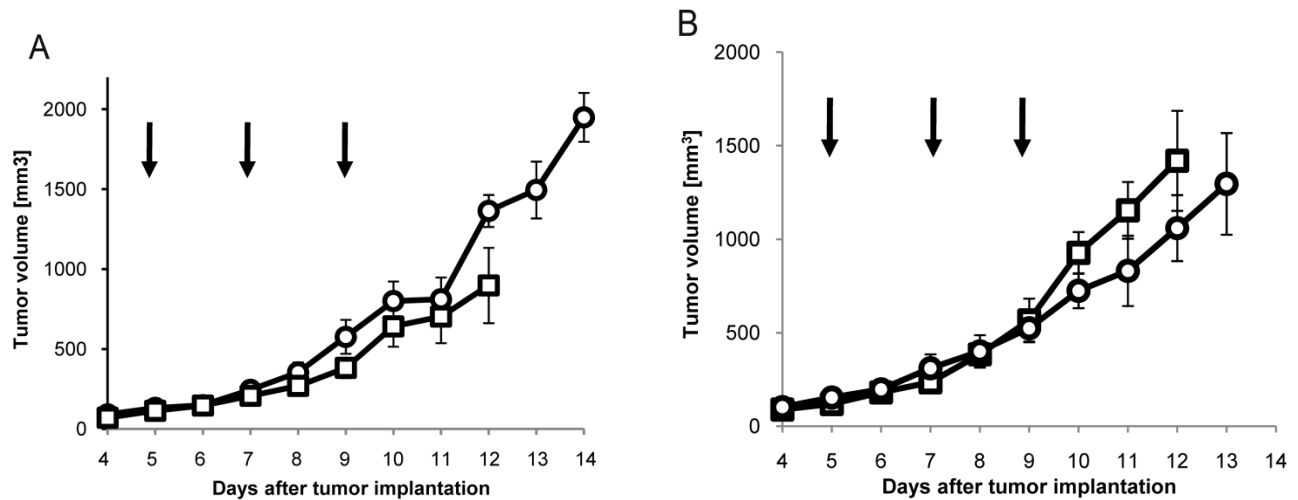


Fig 3.26 Therapeutic activity of F8-mIL17 in murine F9 teratocarcinoma Tumor growth curves of (A) immunocompetent 129/SvPas or (B) athymic Balb/c nude mice bearing F9 tumors after i.v. treatment with three injections of 100 μ g F8-mIL17 (◻; n = 5, n = 5) and saline (O; n = 3, n = 4). Days of treatment (day 5, 7, 9 after tumor implantation) are indicated by arrows. Data represent mean tumor volumes \pm SE.

There was no weight loss in immunocompetent mice (Fig. 3.27A), but up to 15% weight loss in nude mice (Fig. 3.27B).

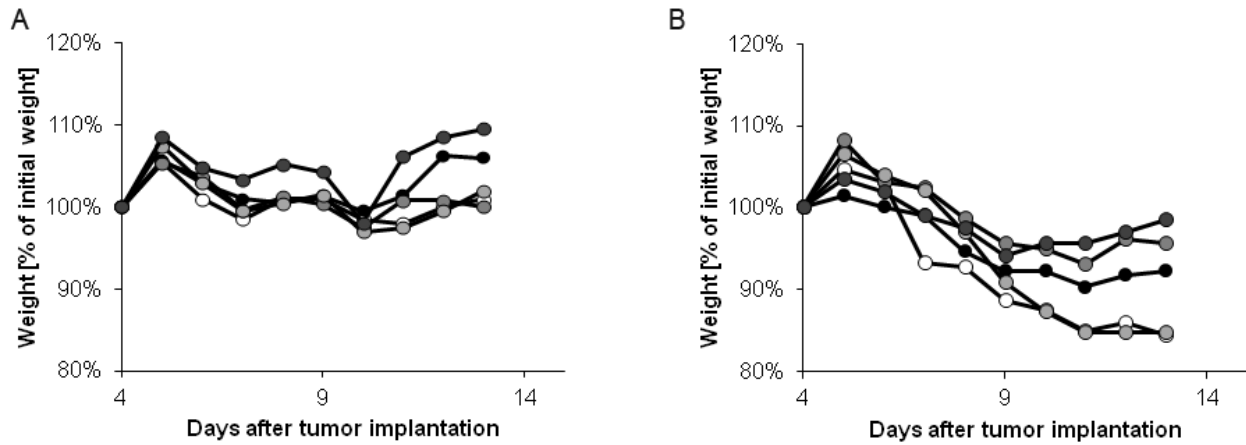


Fig. 3.27 Body weight monitoring during therapy. (A) Balb/c nude and (B) 129/SvPas mice

3.2.2.3. Infiltration studies in F9 teratocarcinoma bearing immunocompetent mice

Fig. 3.28 shows a representative immunofluorescence analysis of the tumor masses at the end of the therapy. Staining of the tumors with an anti-CD45 antibody (**Fig. 3.28i,vi**), F4/80 antibody (**Fig. 3.28ii,vii**), Asialo-GM1 antibody (**Fig. 3.28iii,viii**) and CD4 antibody (**Fig. 3.28iv, ix**) revealed a higher leukocytes, macrophages, NK cells and CD4 T cells (**Fig. 3.28iv,ix**) infiltration in the tumors treated with F8-mIL17 (**Fig. 3.28i-iv**), compared to the saline control group (**Fig. 3.28vi-ix**). By contrast, CD8 T cells were found to be low in both treatment groups (**Fig. 3.28vii,x**).

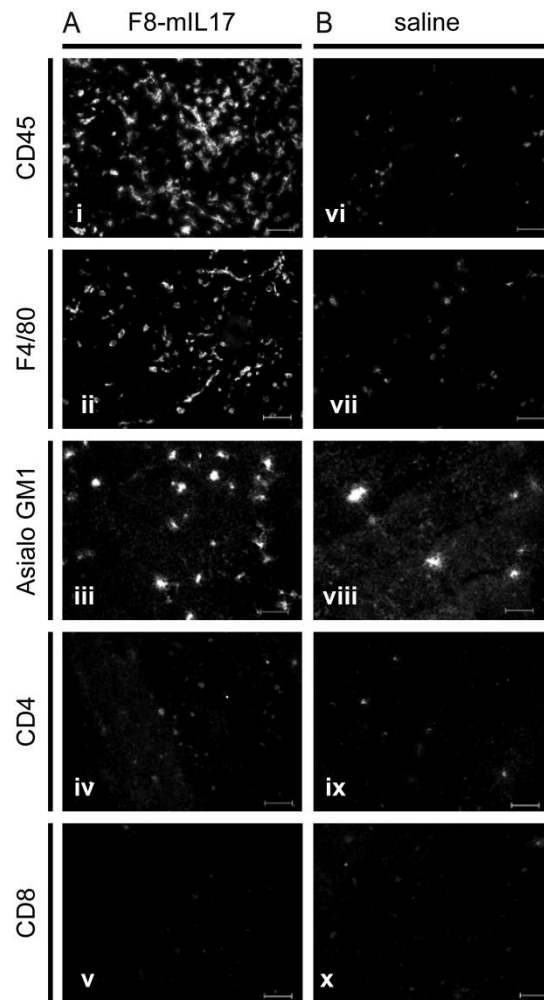


Fig. 3.28 Immunofluorescence analysis of tumor-infiltrating immune cells. Tumor sections of therapy mice treated with (A) F8-mIL17 or (B) saline, were stained for leukocytes (CD45), macrophages (F4/80), NK cells (Asialo/GM1), CD4 T cells and CD8 T cells. Scale bars = 100μm. Representative images of leukocytes (i, vi), macrophages (ii, vii), NK cells (iii, viii), CD4 T cells (iv, ix) and CD8 T cells (v,x) staining in F8mIL17 (A i-v) and saline (B vi-x) treated tumors.

3.2.2.4. Blood vessels density studies in F9 teratocarcinoma bearing immunocompetent mice

Fig. 3.29A,B shows representative images (the experiment was repeated twice) of tumor blood vessels three days after the last injection, from mice treated with F8-mIL17 (**Fig. 3.29A i-vi**) or with saline (**Fig. 3.29B vii-xii**). F8-mIL17 treatment resulted in a significant ($p < 0.01$) increase in blood vessel density (**Fig. 3.29C**).

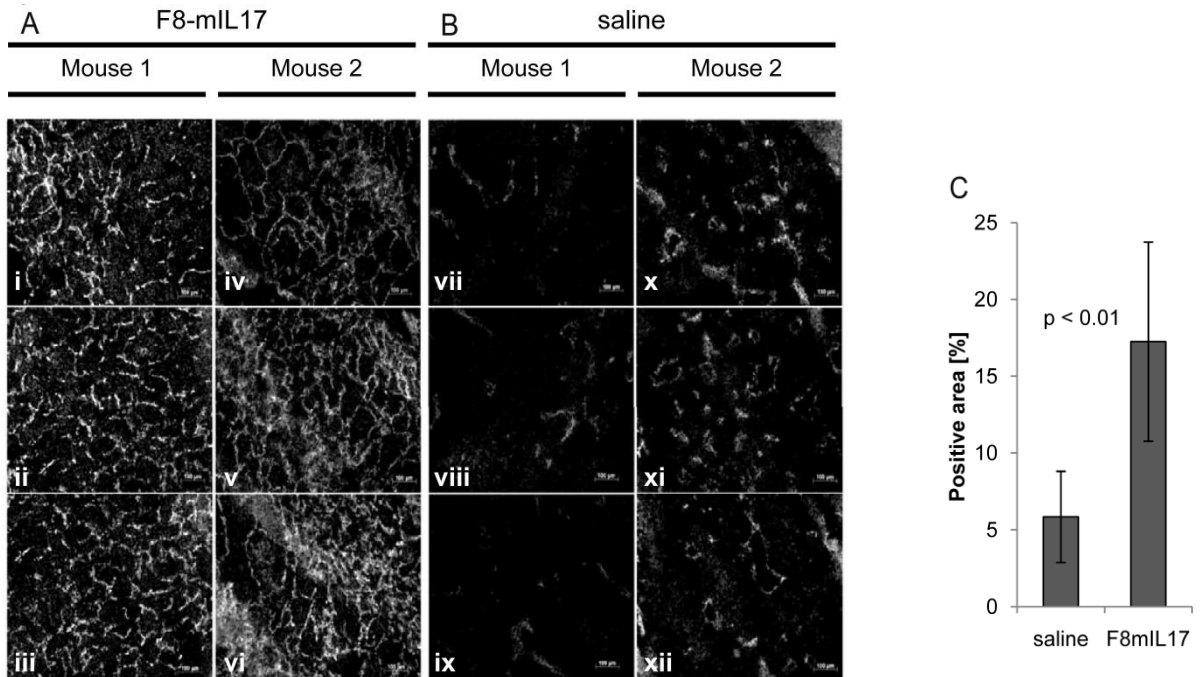


Fig. 3.29 Immunofluorescence analysis of vasculature (CD31 staining). Immunocompetent F9 tumor-bearing mice were injected i.v. three times every 48h with (A) 100 μ g F8-mIL17 or (B) saline. Mice were sacrificed three days after last injection. Tumor sections were stained for endothelial cells. Representative images of 2 mice treated with F8-mIL17 (i-iii,iv-vi) or 2 mice treated with saline (vii-ix,x-xii). (C) F9 tumor sections were evaluated for area percentage positive staining using ImageJ ($p < 0.01$, Student t-test).

3.3. IMMUNOCYTOKINES BASED ON MURINE INTERLEUKIN 18

3.3.1. CLONING AND CHARACTERIZATION OF F8-mIL18

3.3.1.1. Cloning and expression

We initially prepared a fusion protein consisting of scFv(F8) sequentially fused to murine IL18 (termed “F8-mIL18”). The fusion protein was cloned and expressed in mammalian cells (**Fig. 3.30A**). Within the scFv moiety, a 5-aminoacid linker was used between V_H and V_L, which drives the formation of non-covalent “diabody” structures [25,144] (**Fig. 3.30B**).

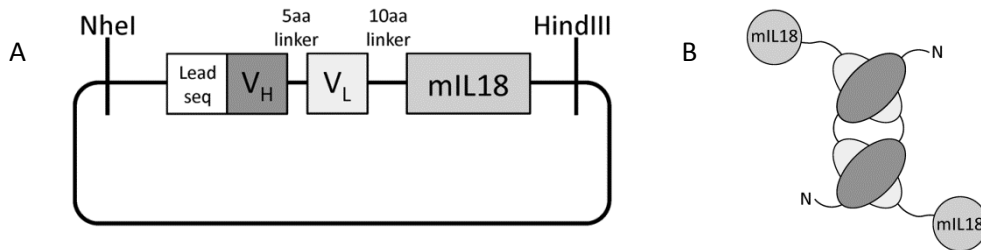


Fig. 3.30 Cloning and expression of F8-mIL18. (A) Schematic representation of the cloning strategy of F8-mIL18 with a 5 amino acid linker between V_H and V_L and 10 amino acid linker between scFv(F8) and mIL18. (B) Domain assembly of F8-mIL18.

F8-mIL18 was cloned in pcDNA3.1 and expressed in stably-transfected in CHO-S cells. The immunocytokine was purified from the culture medium to homogeneity by protein A chromatography followed by preparative size exclusion chromatography.

3.3.1.2. In vitro characterization

3.3.1.2.1. SDS-PAGE

F8-mIL18 ran as a covalent homodimer in SDS-PAGE analysis in non-reducing conditions and as a monomer in reducing conditions. Diabodies are non covalent homodimeric forms of scFv fragments and IL18 is described in the literature as a monomeric protein. For these reasons, one would expect F8-mIL18 to run as

a monomer in SDS-PAGE analysis both in reducing and in non-reducing conditions. The observation of disulfide-linked multimers strongly suggests that undesired disulfide bonds drive the formation of misfolded or partially misfolded aggregates (**Fig. 3.31**).

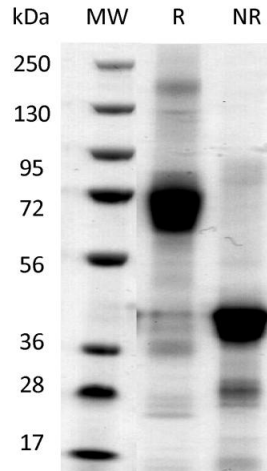


Fig. 3.31 SDS-PAGE analysis of F8-mIL18. Purified F8-mIL18 showed presence of covalent homodimers in non-reducing conditions. MW, molecular weights; NR, non-reducing; R, reducing.

3.3.1.2.2. Size exclusion chromatography

F8-mIL18 exhibited a homogenous profile in size-exclusion chromatography with a retention volume corresponding to the expected dimeric structure (**Fig. 3.32**).

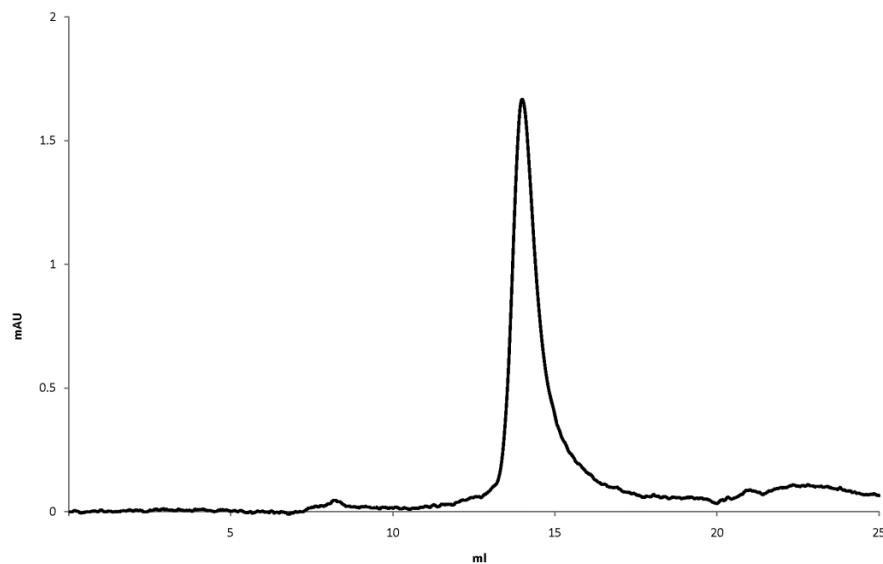


Fig. 3.32 Gel filtration analysis of purified F8-mIL18. The peak corresponds to the homodimeric form of F8-mIL18.

3.3.1.2.3. BIAcore analysis on EDA coated chip

In order to assess the immunoreactivity and the binding properties of F8-mIL18, the protein was analyzed by surface plasmon resonance analysis on a BIAcore microsensor chip, coated with recombinant EDA domain of fibronectin (i.e., with the 11-EDA-12 repeats of fibronectin). The BIAcore analysis showed that F8-mIL18 bound to the cognate antigen with high affinity (**Fig. 3.33**). It was not possible to quantitatively determine the K_D of the immunocytokine due to the avidity effect caused by the two scFv moieties.

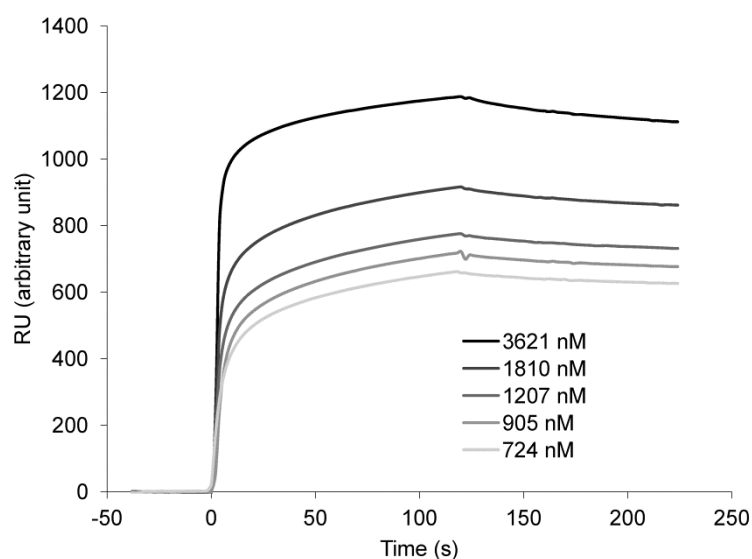


Fig. 3.33 BIAcore analysis of F8-mIL18 on EDA-coated chip. The concentrations of F8-mIL18 for the different sensograms are indicated.

3.3.1.2.4. Immunofluorescence analysis on tumor sections

In order to assess the ability of F8-mIL18 to recognize the cognate antigen in a more natural environment, I performed immunofluorescence studies on freshly frozen tumor sections. As expected, a biotinylated derivative of F8-mIL18 strongly bound to neo-vascular structures in sections of F9 tumors, as revealed by streptavidin-based immunofluorescence detection (**Fig. 3.34**).

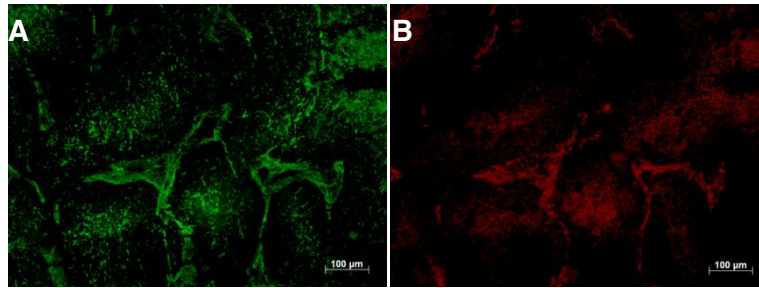


Fig. 3.34 Immunofluorescence analysis of F9 teratocarcinomas. (A) F8-mIL18 was biotinylated and used as staining reagent in an immunofluorescence procedure. (B) CD31 staining. Scale bars = 100 μm .

3.3.1.3. In vivo characterization

3.3.1.3.1. Biodistribution studies on F9 teratocarcinoma bearing immunocompetent and athymic mice

A radioiodinated preparation of F8-mIL18 was used for a quantitative biodistribution analysis in both athymic and immunocompetent mice, bearing subcutaneously-grafted murine F9 teratocarcinomas. After 24h an accumulation in the tumor mass could be observed for both mouse models, with 2.7% %ID/g (athymic mice) and 7.5%ID/g (immunocompetent mice) in the tumor. Unfortunately, elevated levels of radioactivity in spleen and kidney were observed (**Fig. 3.35**).

The use of larger amounts of radioiodinated protein (67.5 μg rather than 15 μg) enhanced the targeting performance (14.5% ID/g at 24h) and substantially reduced the uptake of F8-mIL18 in normal organs (tumor-to-blood ratio 1:17), suggesting that the fusion protein at low doses was trapped by IL18 receptors at locations other than the tumor (**Fig. 3.35**).

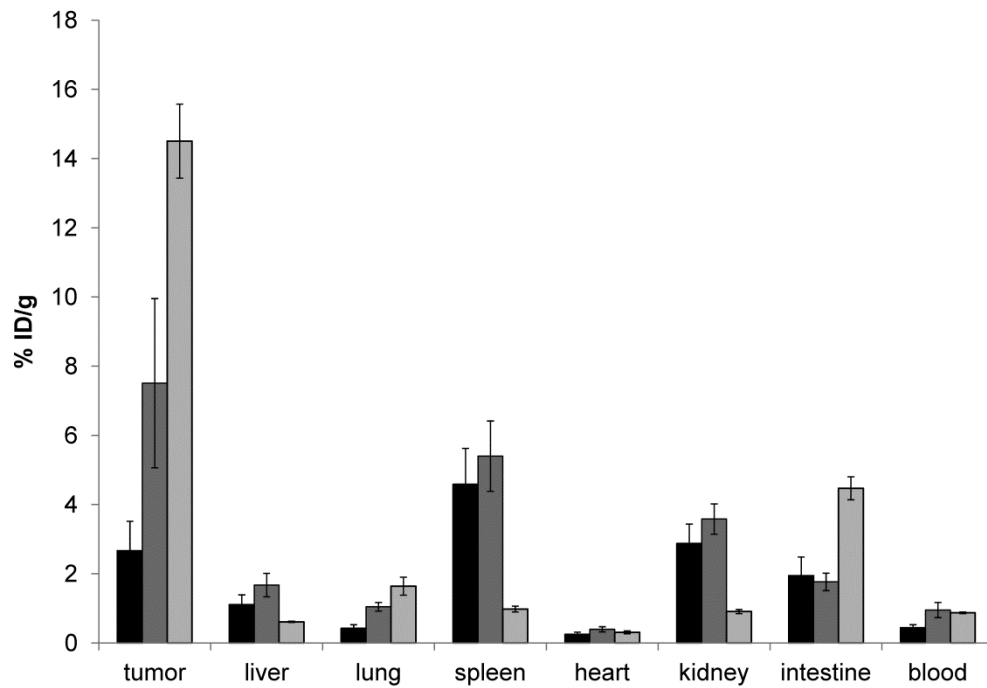


Fig. 3.35 Biodistribution study of radioiodinated F8-mIL18. Athymic Balb/c nude mice and immunocompetent 129/SvEv mice bearing syngenic s.c. F9 teratocarcinoma were injected i.v., respectively, with 15µg radiolabeled ¹²⁵I-F8-mIL18 (■, n = 7 athymic mice), with 15µg radiolabeled ¹²⁵I-F8-mIL18 (■, n = 7 immunocompetent mice) or with 7.5µg radiolabeled ¹²⁵I-F8-mIL18 mixed with 60µg unlabeled F8-mIL18 (■, n = 4 immunocompetent mice). Mice were sacrificed after 24h. Organs were excised and radioactivity counted, expressing results as percent of injected dose per gram of tissue (%ID/g ± SE).

3.3.1.3.2. Therapeutic properties on F9 teratocarcinoma bearing immunocompetent and athymic mice

Therapy experiments were performed in immunocompetent and nude mice bearing subcutaneous F9 tumors. While F8-mIL18 displayed no anti-cancer activity in nude mice compared to saline controls (**Fig. 3.36A**), the fusion protein displayed a slight tumor growth retardation (which was not statistically significant) in tumor-bearing 129/SvEv mice (**Fig. 3.36B**).

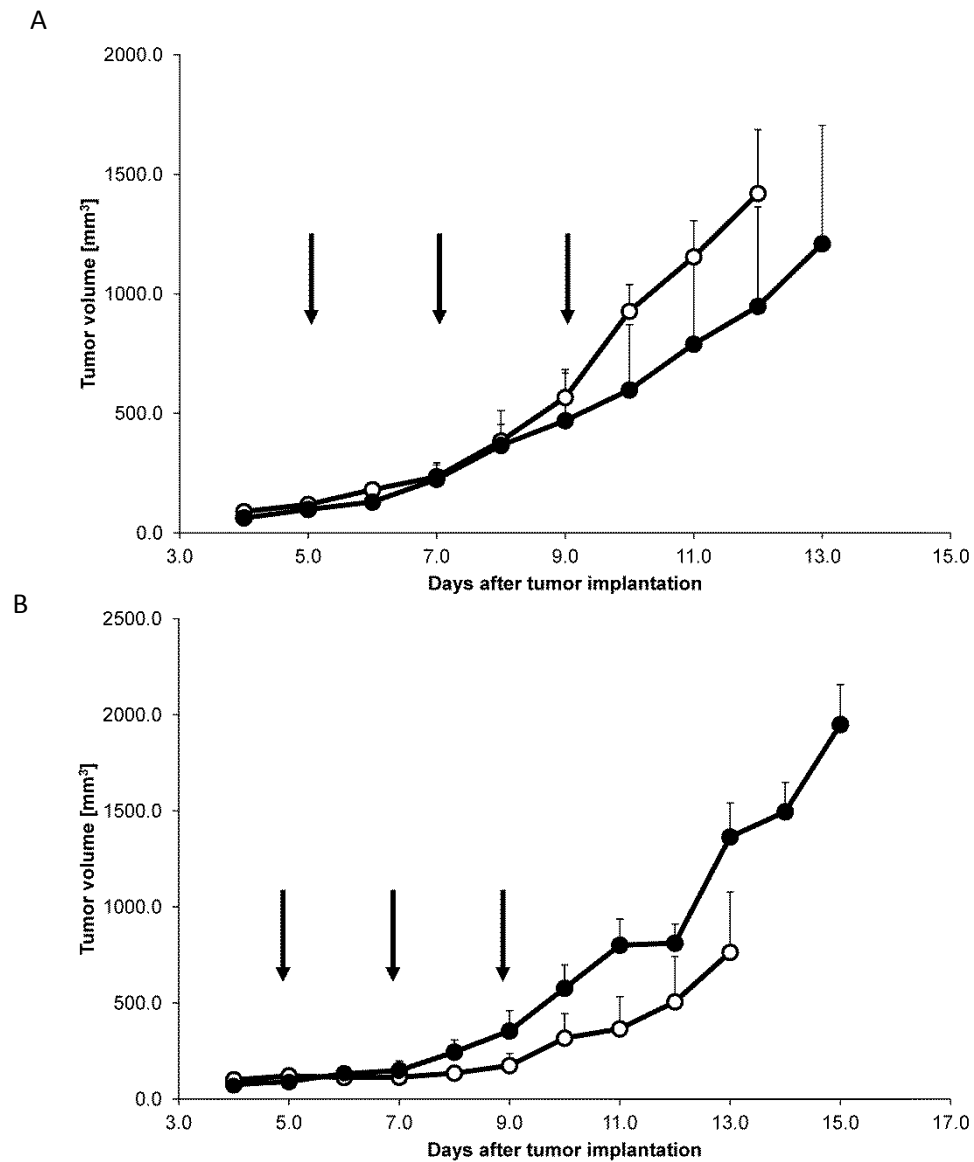


Fig 3.36 Therapeutic activity of F8-mIL7 in murine F9 teratocarcinoma (A) Athymic Balb/c nude (n = 4, n = 3) and (B) immunocompetent 129/SvEv (n = 3, n = 3) mice bearing syngenic s.c. F9 teratocarcinomas were treated i.v. with three doses of 50µg F8-mIL18 (○) or PBS (●) as control. Treatment was performed on days 5, 7, 9 after tumor implantation (black arrows). Data represent mean tumor volumes ± SE. Tumor growth curves were stopped when the first tumor per group reached 2000 mm³.

3.3.2. CLONING AND CHARACTERIZATION OF MIL18

In order to validate literature data, in which murine IL18 is described as a monomeric protein, the cytokine was cloned and expressed in CHO-S cells using transient gene expression. The supernatant was analyzed with western blot using an anti-mIL18 antibody. The cytokine ran as a monomer in non-reducing conditions (Fig. 3.38).

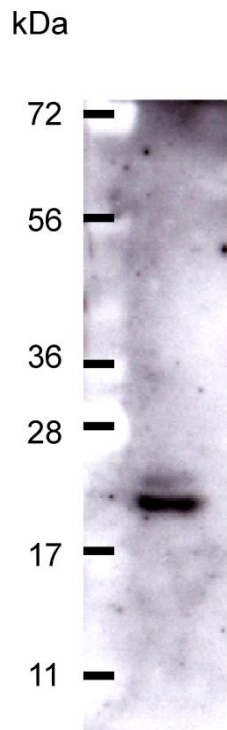


Fig. 3.38 Western blot analysis of the supernatant of CHO-S cells expressing mIL18. mIL18 runs as a monomer with a molecular weight of about 20kDa.

3.3.3. CLONING AND CHARACTERIZATION OF CYSTEINE TO SERINE MUTANTS OF F8-MIL18

Additional strategies were investigated in order to produce mIL18-based immunocytokines, which would result in fusion proteins with correct disulfide bond formation. Our group has previously observed that the substitution of cysteine residues with serine residues can improve the folding of the protein. In a first approach, the three cysteine residues of mIL18 were substituted by serines either individually or simultaneously. The resulting seven mIL18 mutants were fused to scFv(F8). The wild-type F8-mIL18 as well

as the seven mutants were expressed in CHO-S cells using transient gene expression. The corresponding supernatants were analyzed with western blot analysis using an anti-mIL18 antibody (Fig. 3.37).

The mutation of one or two cysteines did not improve the folding of the immunocytokines. All the single and double mutants ran as homodimers in non-reducing conditions (Fig. 3.37A). The removal of the three cysteines resulted in a fusion protein running as a monomer in non-reducing conditions (Fig. 3.37B), but at very low expression yields.

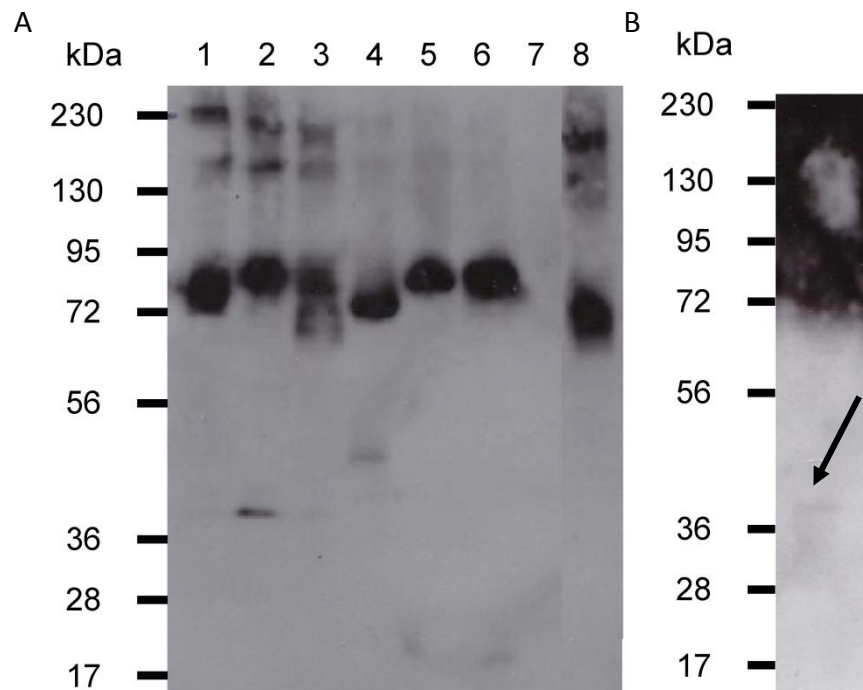
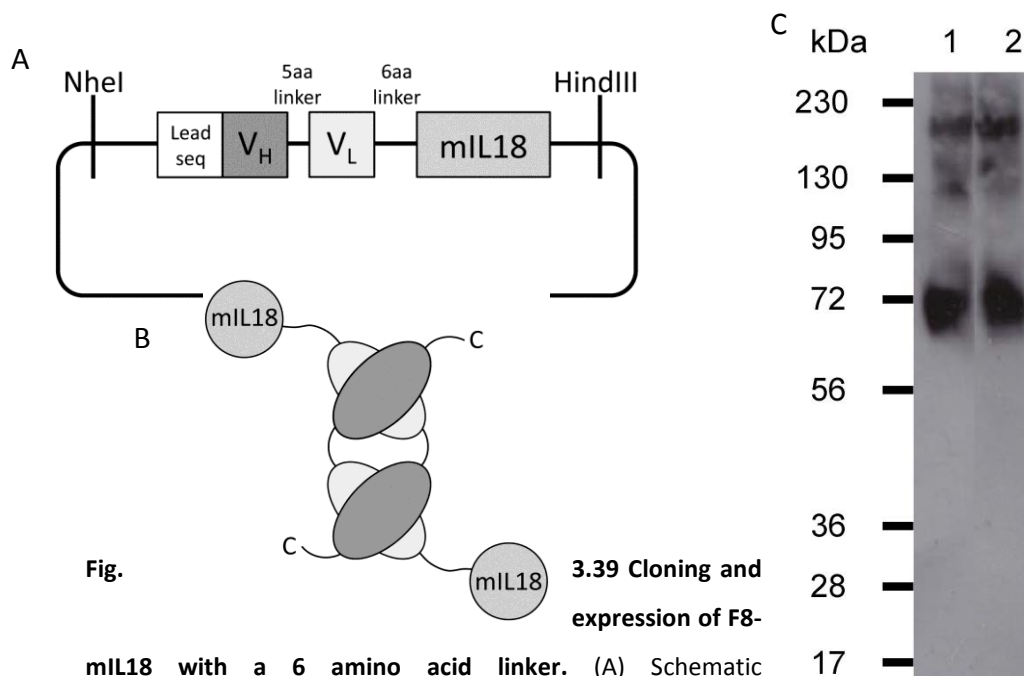


Fig. 3.37 Western blot analysis of the supernatant of CHO-S cells expressing F8-mIL18 mutants. Anti mIL18 antibody was used as a primary antibody. (A) (1) Cys7, (2) Cys75, (3) Cys125, (4) Cys7 and Cys75, (5) Cys7 and Cys125, (6) Cys75 and Cys125, (7) all three cysteines were mutated into serines, (8) wild-type protein. In all mutants the homodimeric form of F8-mIL18 is present; the triple mutant was not visible. (B) Triple mutant runs as a monomer, but band is very faint.

3.3.4. CLONING AND CHARACTERIZATION OF NOVEL FORMATS FOR MIL18-BASED IMMUNOCYTOTOKINES

3.3.4.1. Cloning and expression of F8-mIL18 with 6 amino acids linker

Similarly to mIL7, we investigated the expression and performance of alternative immunocytokine formats. Using the F8-mIL18 format, we shortened the linker between scFv fragment and mIL18 from 10 to 6 amino acids. We cloned and expressed the fusion protein using transient gene expression (Fig. 3.39A,B). The supernatant was analyzed with western blot analysis using an anti-mIL18 antibody. Unfortunately, also in this case, the formation of a disulfide-linked homodimer could not be avoided (Fig. 3.39C).



3.3.4.2. Cloning, expression and in vitro characterization of F8-mIL18-F8

3.3.4.2.1. Cloning and expression

In order to search for mIL18-based immunocytokine formats of improved pharmaceutical properties, we cloned and expressed, using transient gene expression, a novel immunocytokine format (termed “F8-mIL18-F8”) consisting of a sequential fusion of scFv(F8) with single murine IL18 monomer and with a second scFv(F8) moiety (**Fig. 3.40**).

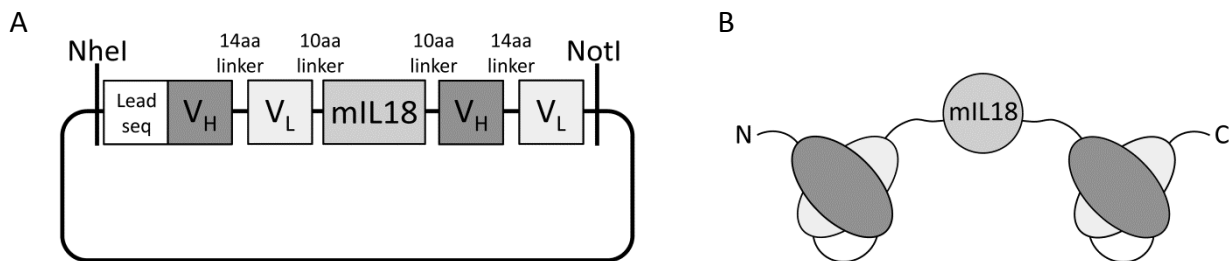


Figure 3.40. Cloning and expression of F8-mIL18-F8. (A) Schematic representation of the cloning strategy of F8-mIL18-F8 with a 14 amino acid linker between VH and VL and 10 amino acid linker between scFv(F8) and mIL18. (B) Domain assembly of F8-mIL18-F8.

F8-mIL18-F8 was purified from the culture medium by protein A chromatography. More than 60% of the immunocytokine was lost during filtration after dialysis, suggesting high protein aggregation.

3.3.4.2.2. SDS-PAGE

F8-mIL18-F8 ran as a monomer in SDS-PAGE analysis in non-reducing and reducing conditions. Bands of lower and higher molecular weight are also visible, indicating protein aggregation and degradation (**Fig. 3.42**).

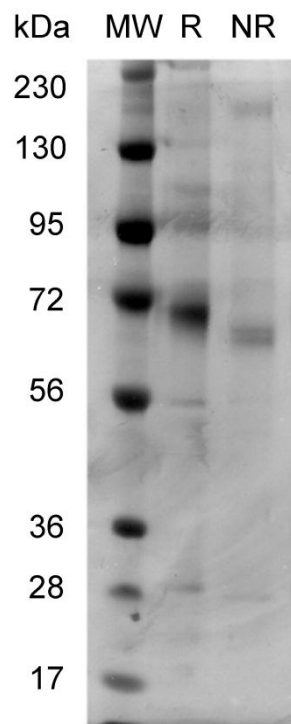


Fig. 3.42 SDS-PAGE analysis of purified F8-mIL18-F8: The fusion protein is present mostly as a monomer. MW, molecular weights; NR, non-reducing; R, reducing.

3.3.4.2.3. Size exclusion chromatography

The immunocytokine did not elute as a single peak, confirming the presence of protein aggregates, as well as protein degradation (Fig. 3.43).

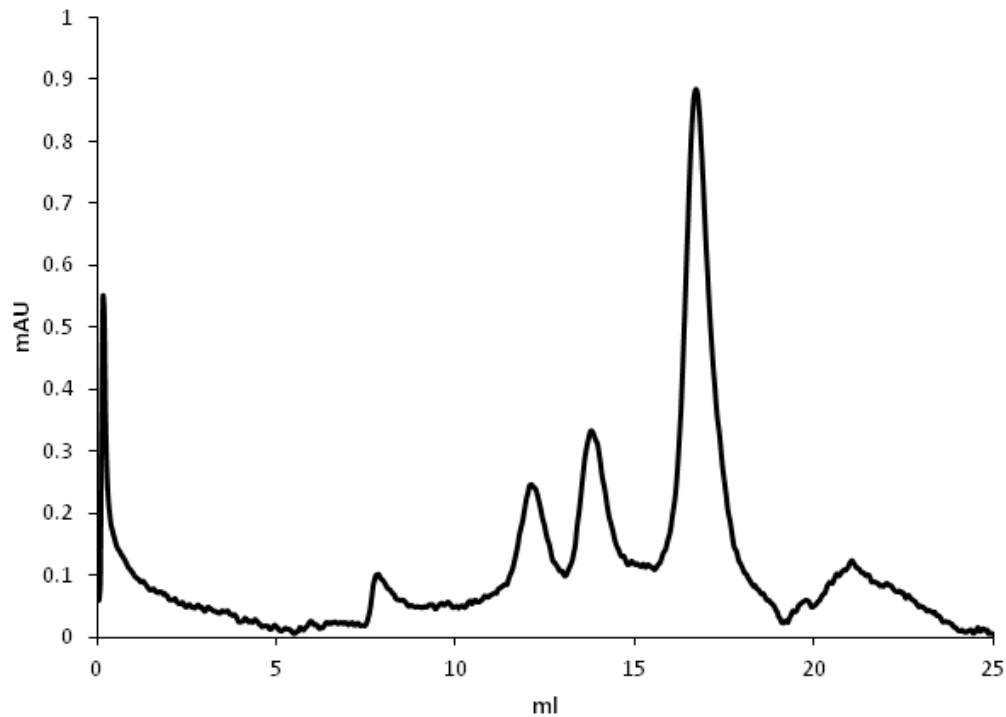


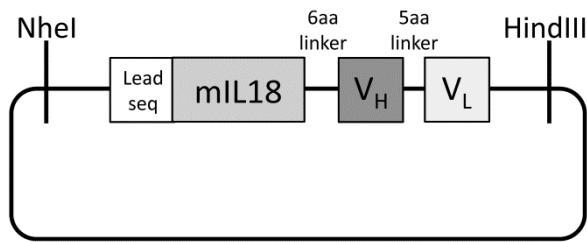
Fig. 3.43 Gel filtration analysis of purified F8-mIL18-F8. The protein did not elute as a single peak.

3.3.4.3. Cloning, expression and in vitro characterization of mIL18 – F8

3.3.4.3.1. Cloning and expression

Finally, we fused the cytokine moiety to the N-terminus of the scFv(F8) (“mIL18-F8”), using a 6 amino acid linker. This format results in the positioning of two mIL18 monomeric units at distal locations within the non-covalent diabody structure, with the potential to avoid undesired disulfide-linked covalent bond formation. The immunocytokine was cloned in pcDNA3.1 and expressed in stably-transfected in CHO-S cells (Fig. 3.41).

A



B

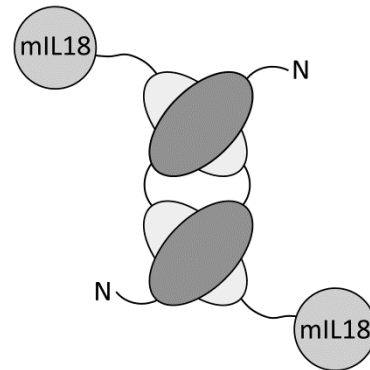


Figure 3.41. Cloning and expression mIL18-F8. (A)

Schematic representation of the cloning strategy of mIL18-F8 with a 6 amino acid linker between mIL18 and F8 and a 5 amino acid linker between V_H and V_L. (B) Domain assembly of mIL18-F8.

The immunocytokine was purified from the culture medium to homogeneity by protein A chromatography and submitted to analytical controls.

3.3.4.3.2. SDS-PAGE

In SDS-PAGE analysis, mIL18-F8 ran as a monomer in reducing conditions, whereas in non-reducing conditions the fusion protein ran as a monomer as well as a covalent homodimer. Bands of lower and higher molecular weight are also visible, indicating protein aggregation and degradation. With addition of 0.01% Tween to the protein preparation, only the monomer band and the lower band were visible (**Fig. 3.44**). Even though the immunocytokine ran as a monomeric protein in non reducing and reducing conditions, the pharmaceutical quality was not acceptable, since products of proteolysis were observed after affinity purification.

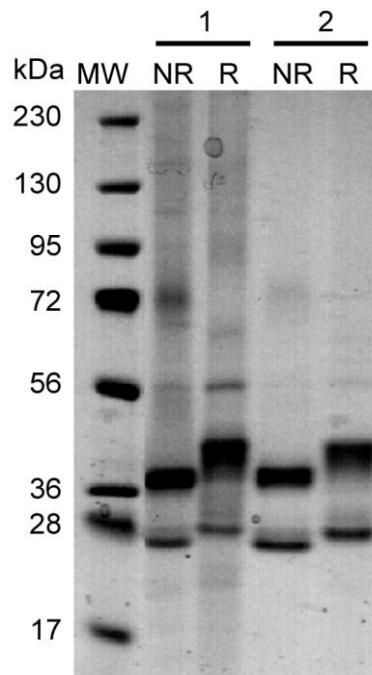


Fig. 3.44 SDS-PAGE analysis of purified mIL18-F8. (1) mIL18-F8 in PBS pH 7.4 and (2) mIL18-F8 in PBS-Tween 0.01% pH 7.4. The fusion protein is present mostly as a monomer in both buffers and there are no covalent aggregates with Tween 0.01%, unfortunately protein degradation is visible. MW, molecular weights; NR, non-reducing; R, reducing.

3.3.4.3.3. Size exclusion chromatography

The immunocytokine mIL18-F8 eluted at a retention volume corresponding to the void volume of the column, confirming the presence of protein aggregates (**Fig. 3.45A**). The addition of Tween 0.01% did not improve the elution profile (**Fig. 3.45B**). It was not possible to isolate the fraction corresponding to the non covalent homodimeric immunocytokine, since no peak was visible at the expected retention volume.

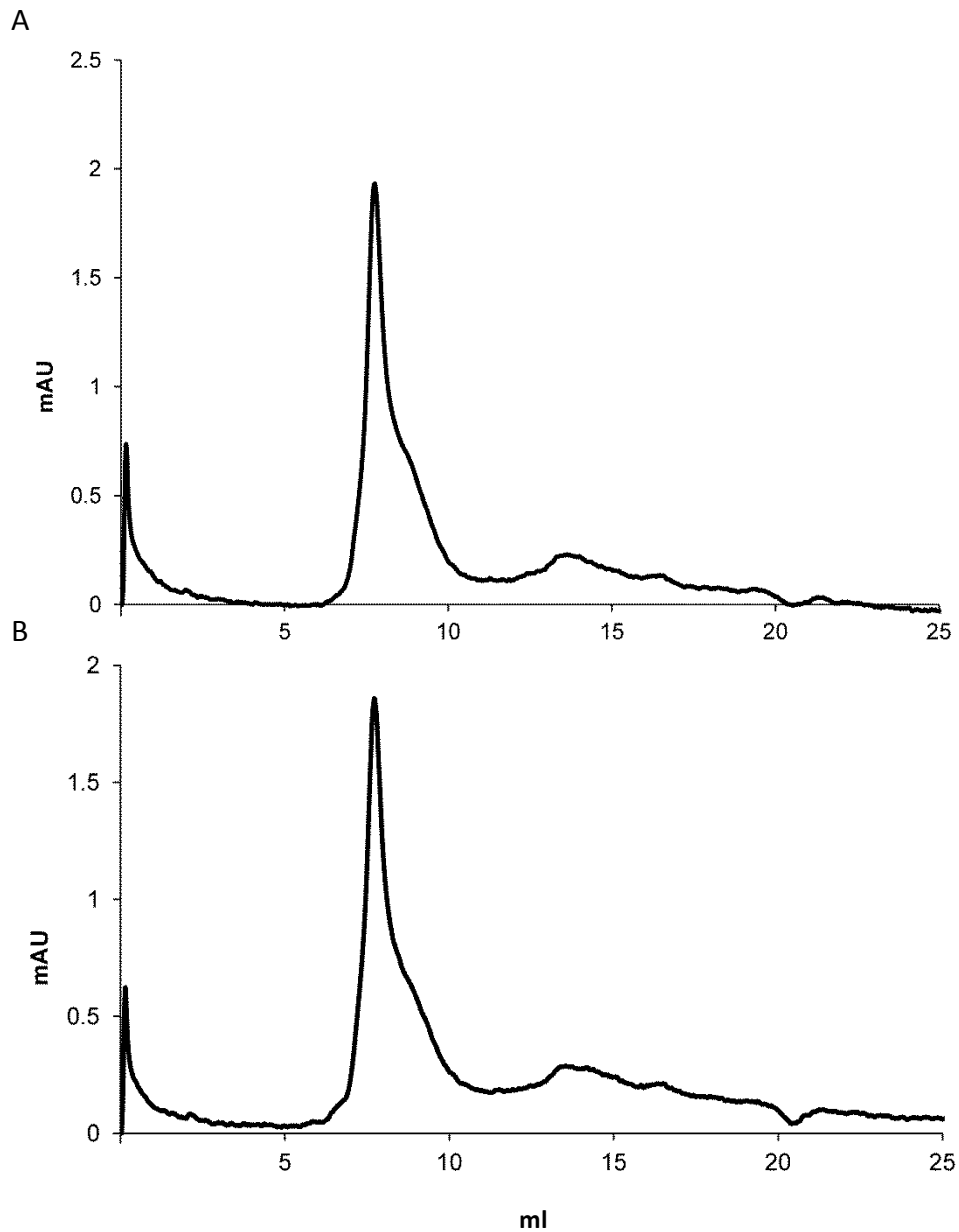


Fig. 3.45 Gel filtration analysis of purified mL18-F8. (A) mL18-F8 in PBS pH 7.4 and (B) mL18-F8 in PBS-Tween 0.01% pH 7.4. Protein is completely aggregated, Tween 0.01% did not prevent the formation of non-covalent aggregates.

In conclusion, in spite of numerous attempts, we were not able to generate an immunocytokine based on scFv(F8) and mL18 of satisfactory pharmaceutical quality.

3.4. IMMUNOCYTOKINES BASED ON MURINE INTERLEUKIN 12 ^[147]

3.4.1. CLONING AND EXPRESSION OF MIL12-F8-F8 AND MIL12-KSF-KSF

The chimeric immunocytokine mIL12-F8-F8, containing the single-chain murine IL12 moiety sequentially fused to two units of the human scFv(F8), was expressed in CHO-S cells and purified to homogeneity. In addition, we produced the fusion protein mIL12-KSF-KSF (based on an antibody specific to hen egg lysozyme and thus not reactive with any mouse protein; [145]) as negative control for *in vivo* studies (Fig, 3.46).

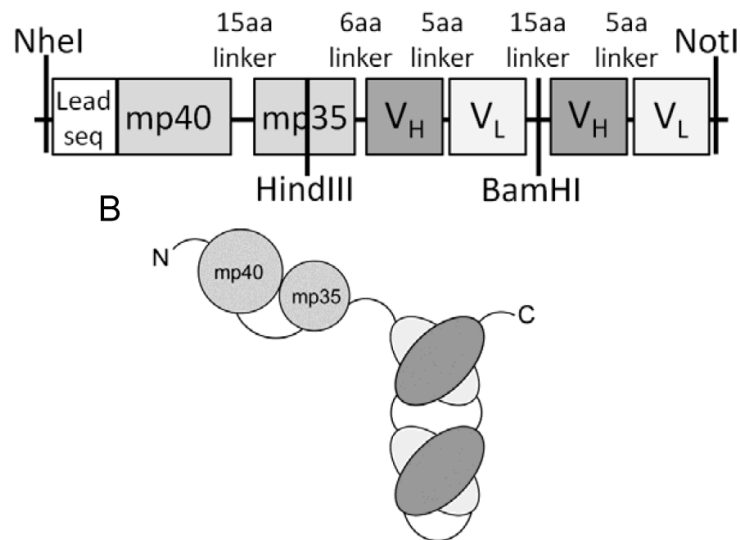


Fig. 3.46 Cloning and expression of mIL12-F8-F8 and mIL12-KSF-KSF. (A) Schematic representation of the cloning strategy of mIL12-F8-F8 and mIL12-KSF-KSF as a single-chain fusion protein. (B) Domain assembly of mIL12-F8-F8 and mIL12-KSF-KSF.

3.4.2. IN VITRO CHARACTERIZATION OF mL12 FUSION PROTEINS

3.4.2.1. SDS-PAGE

Both immunocytokines exhibited a favorable performance in SDS-PAGE running as monomers in non-reducing and reducing conditions (Fig. 3.47).

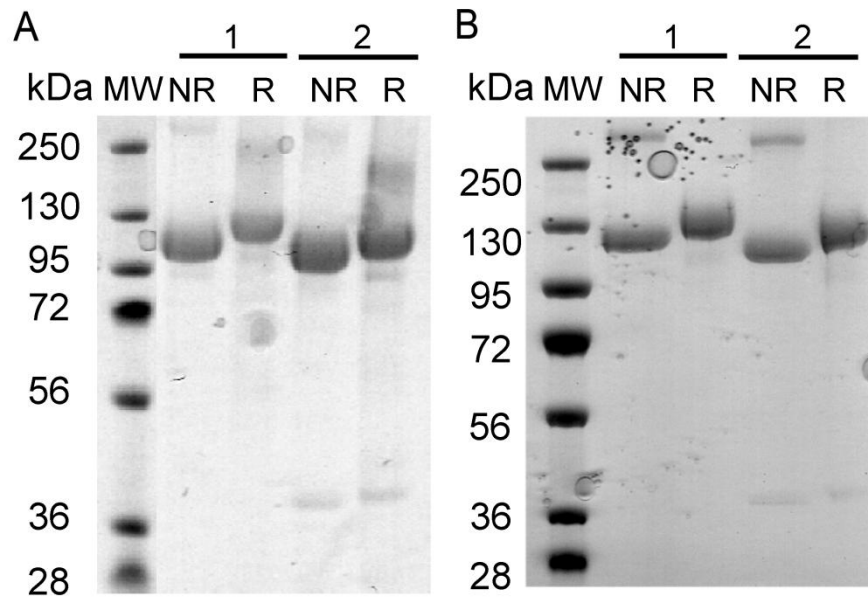


Fig 3.47 SDS-PAGE analysis of (A) mL12-F8-F8 and (B) mL12-KSF-KSF. (1) Purified and (2) PNGase deglycosylated mL12-F8-F8 and mL12-KSF-KSF were running as monomers in reducing and non-reducing conditions. MW, molecular weights; NR, non-reducing; R, reducing.

3.4.2.2. Size exclusion chromatography

Both immunocytokines eluted at the expected retention volume in a gel filtration analysis (**Fig. 3.48**).

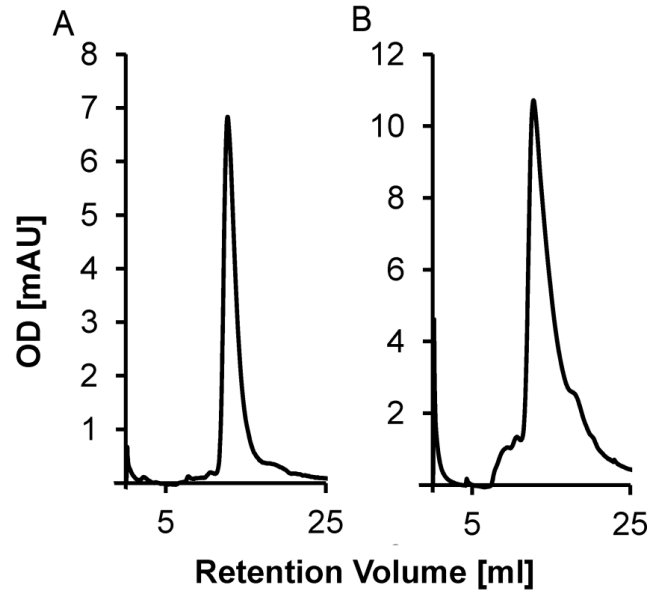


Fig. 3.48 Gel filtration analysis of (A) mIL12-F8-F8 and (B) mIL12-KSF-KSF. The peaks correspond to the monomeric form of mIL12-F8-F8 and mIL12-KSF-KSF.

3.4.2.3. BIAcore analysis on EDA coated chip

A BIAcore analysis revealed that mIL12-F8-F8 bound to the cognate antigen with high functional affinity and slow dissociation kinetics (**Fig. 3.49**).

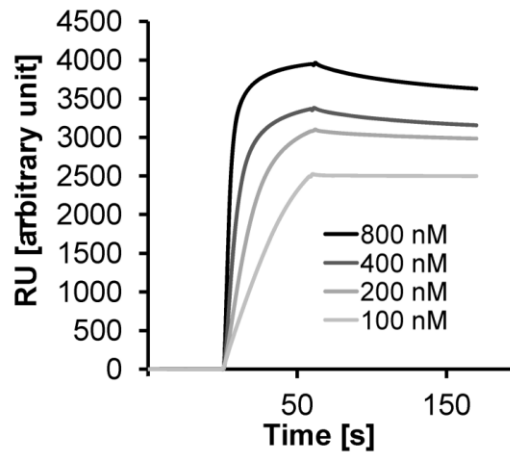


Fig. 3.49 BIAcore analysis of mIL12-F8-F8 on EDA-coated chip. The concentrations of F8-mIL18 for the different sensograms are indicated.

3.4.2.4. Immunofluorescence analysis on tumor sections

An immunofluorescence analysis revealed that mL12-F8-F8 strongly reacted with neo-vascular structures in sections of F9 teratocarcinoma and CT26 colon carcinoma, whereas mL12-KSF-KSF did not stain the tissue sections (Fig. 3.50).

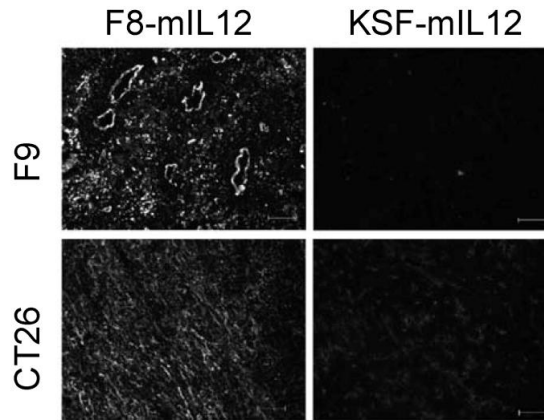


Fig. 3.50 Immunofluorescence analysis of F9 teratocarcinoma and CT26 colon carcinoma. The immunocytokines mL12-F8-F8 and mL12-KSF-KSF were used as staining reagents in an immunofluorescence procedure. Scale bars = 100 μ m.

3.4.2.5. Stability

Both immunocytokines were found to be stable upon incubation at 37 °C for up to four days (Fig. 3.51).

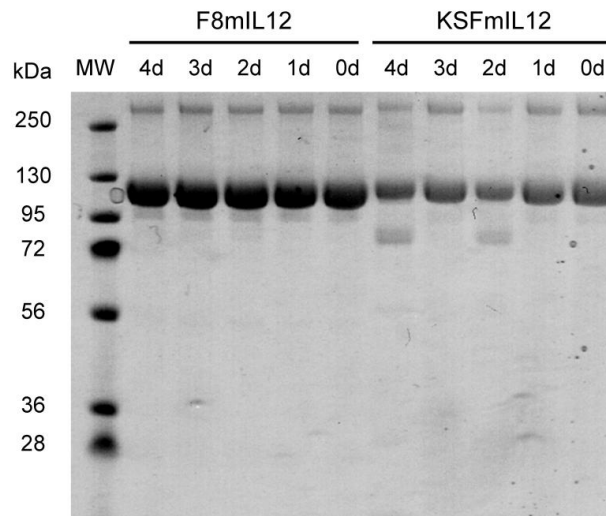


Fig. 3.51 Stability of mL12-F8-F8 and mL12-KSF-KSF SDS-PAGE analysis of purified mL12-F8-F8 and mL12-KSF-KSF stored in PBS at 37°C for 0, 24, 48, 72 or 96 hours.

3.4.2.6. Blood binding assay

A radioiodinated preparation of mL12-F8-F8 was incubated *in vitro* at a concentration of 0.035 $\mu\text{g/ml}$ (i.e., the same concentration used for therapy experiments) with blood freshly obtained from Balb/c mice. After ten minutes and following centrifugation, >80% of the protein could be found in plasma, confirming that the majority of the immunocytokine was not associated with cellular components and was thus available for *in vivo* targeting of the antigen, located in the sub-endothelial extracellular matrix of tumor blood vessels.

3.4.3. IN VIVO CHARACTERIZATION

3.4.3.1. Biodistribution studies on F9 teratocarcinoma bearing immunocompetent mice

The tumor targeting performance of mL12-F8-F8 (black) was comparable to the one of the fully human immunocytokine, with 4.3%ID/g in the tumor at 24 h and a tumor-to-blood ratio of 8:1. As expected, mL12-KSF-KSF (grey) did not exhibit a preferential accumulation in the tumor at the same time point (**Fig. 3.52**).

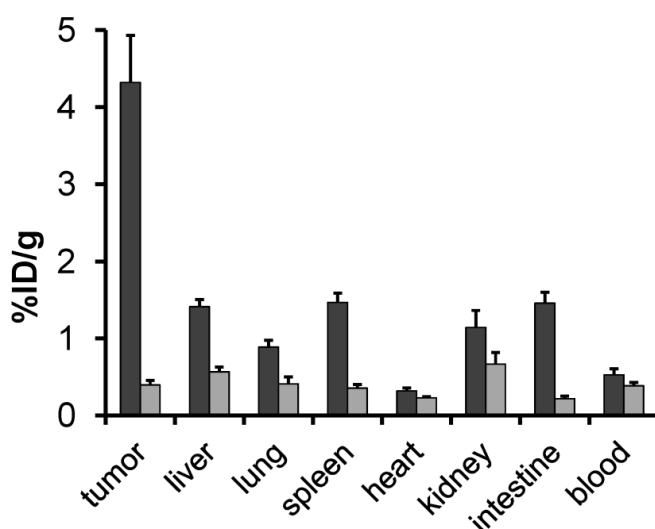


Fig. 3.52 Biodistribution study of radioiodinated mL12-F8-F8 and mL12-KSF-KSF. Immunocompetent 129/SvEv mice bearing syngenic s.c. F9 teratocarcinomas were injected with 7 μg radiolabeled ^{125}I - mL12-F8-F8 (■, n = 5) or with 7 μg radiolabeled ^{125}I -mL12-F8-F8 (■, n = 5). Mice were sacrificed after 24h. Organs were excised and radioactivity counted, expressing results as percent of injected dose per gram of tissue (%ID/g) \pm SE.

3.4.3.2. Therapeutic properties

3.4.3.2.1. F9 teratocarcinoma bearing immunocompetent mice

3.4.3.2.1.1. mIL12-F8-F8 as monotherapy

The therapeutic performance of mIL12-F8-F8 and mIL12-KSF-KSF was tested in immunocompetent mice bearing subcutaneous F9 tumors. With a low dose i.v. injection (1.75 μ g immunocytokine corresponding to 1 μ g mIL12 equivalents) to mice carrying small tumors (around 50 mm³), both immunocytokines induced a tumor growth retardation compared to mice which received PBS (Phosphate-Buffered Saline) treatment ($p < 0.05$ from day 7, $p < 0.01$ from day 11) (**Fig. 3.53**).

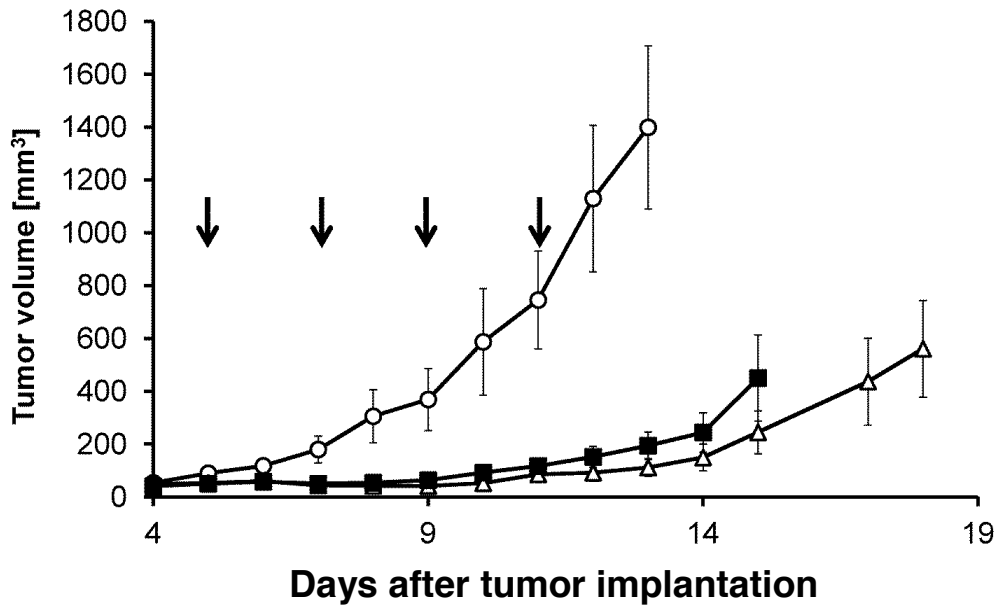


Fig. 3.53 Therapeutic activity of 1.75 μ g mIL12-F8-F8 or mIL12-KSF-KSF (corresponding to 1 μ g mIL12 equivalents) in immunocompetent 129/SvEv mice bearing syngeneic s.c. F9 teratocarcinoma. Tumor-bearing mice were treated i.v. with mIL12-F8-F8 (1.75 μ g, $n = 5$, \triangle), mIL12-KSF-KSF (1.75 μ g, $n = 5$, \blacksquare) or PBS ($n = 5$, \circ). Treatment was performed on day 5, 7, 9, 11 after tumor implantation (black arrows). Data represent mean tumor volumes \pm SE. Tumor growth curves were stopped when the first tumor per group reached 2000 mm³.

When a higher dose of immunocytokine was administered (6 μg , corresponding to 3.75 μg mL12 equivalents) to mice carrying larger tumors (150-250 mm^3), only mL12-F8-F8 mediated a significant tumor growth retardation (vs PBS: $p < 0.05$ from day 10; vs mL12-KSF-KSF $p < 0.05$ from day 9, $p < 0.01$ from day 10, $p < 0.001$ from day 12, $p < 0.0001$ from day 14) (Fig. 3.54).

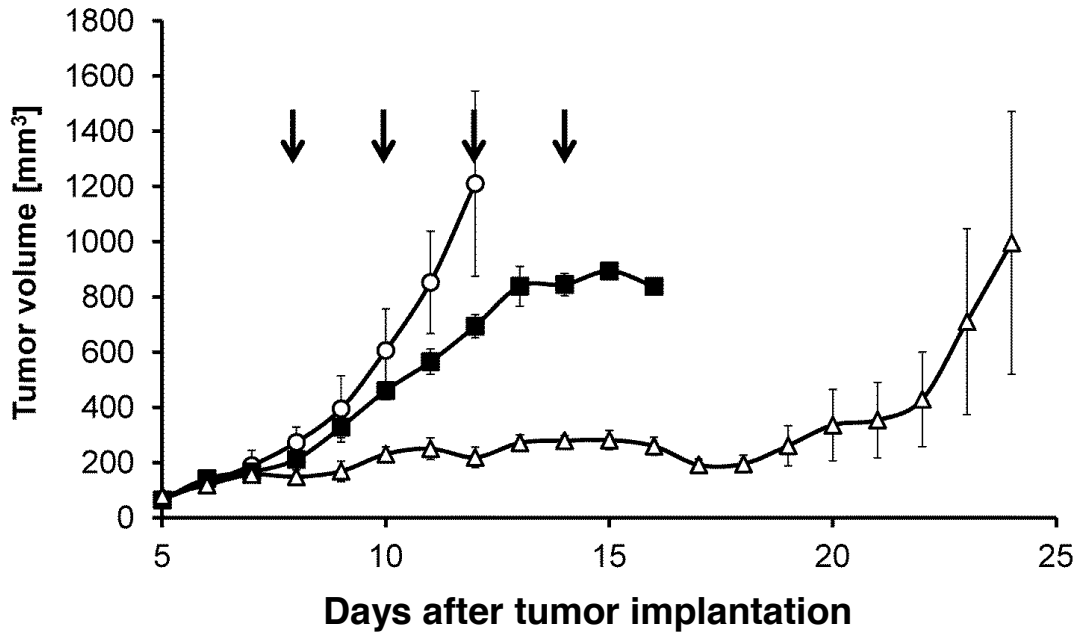


Fig. 3.54 Therapeutic activity of 6 μg mL12-F8-F8 or mL12-KSF-KSF (corresponding to 3.4 μg mL12 equivalents) in immunocompetent 129/SvEv mice bearing syngeneic s.c. F9 teratocarcinoma. Tumor-bearing mice were treated i.v. with mL12-F8-F8 (6 μg , $n = 4$, \triangle), mL12-KSF-KSF (6 μg , $n = 3$, \blacksquare) or PBS ($n = 4$, \circ). Treatment was performed on day 8, 10, 12, 14 after tumor implantation (black arrows). Data represent mean tumor volumes \pm SE. Tumor growth curves were stopped when the first tumor per group reached 2000 mm^3 .

3.4.3.2.1.2. mL12-F8-F8 intratumoral injections

No significant difference in tumor growth retardation was observed when comparing intravenous and intratumoral injections of mL12-F8-F8 (8.75 μg , corresponding to 5 μg mL12 equivalents), even though two out of three mice were cured as a result of the intratumoral administration of the immunocytokine (Fig. 3.55).

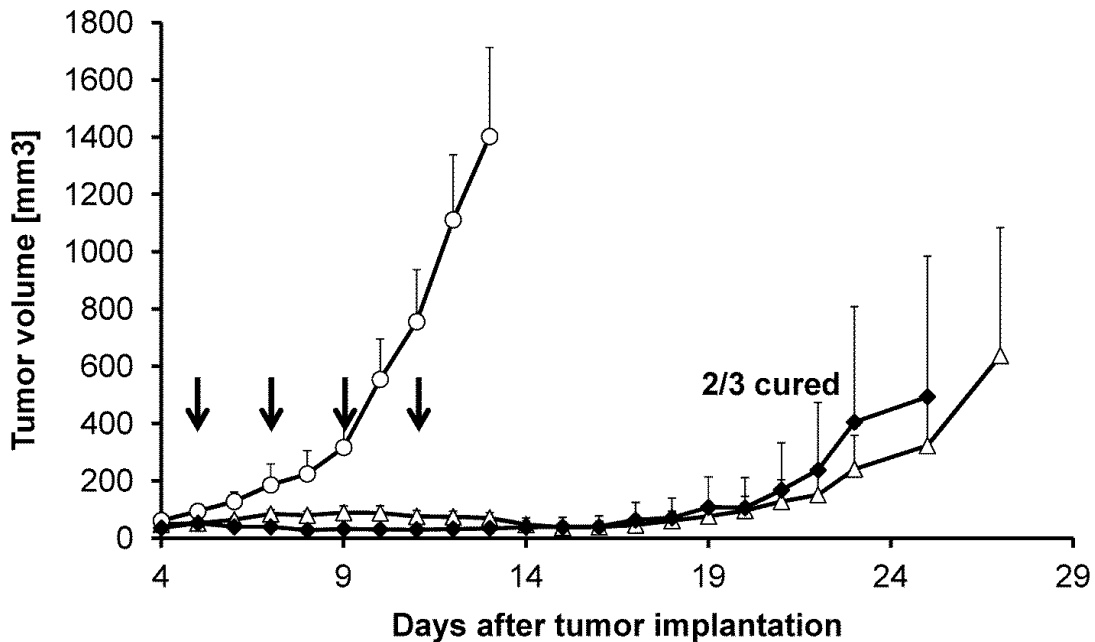


Fig. 3.55 Therapeutic activity of 8.75 μ g mIL12-F8-F8 (corresponding to 5 μ g mIL12 equivalents) injected i.v. or i.t. in immunocompetent 129/SvEv mice bearing syngeneic s.c. F9 teratocarcinoma. Tumor-bearing mice were treated with mIL12-F8-F8 (8.75 μ g, n = 5, Δ) i.v., mIL12-F8-F8 (8.75 μ g, n = 3, \blacklozenge) i.t. or PBS (n = 4, \circ). Treatment was performed on day 5, 7, 9, 11 after tumor implantation (black arrows). Two mice out of three treated with i.t. injections were cured. Data represent mean tumor volumes \pm SE. Tumor growth curves were stopped when the first tumor per group reached 2000 mm³.

3.4.3.2.1.3. Combination therapies

3.4.3.2.1.3.1. mIL12-F8-F8 and F8-IL2

As combinations of different immunocytokines have previously demonstrated the ability to completely eradicate tumors in rodents [32,40], we tested the therapeutic activity of mIL12-F8-F8 (6 μ g) in combination with F8-IL2 (20 μ g; [37]) (**Fig. 3.56**). F9 tumor-bearing mice were injected twice (day 5 and day 8). Substantial toxicity was observed after the second injection in the combination group (lethargy, ruffled fur, body weight loss around 10%), indicating an additive toxicity of the two immunocytokines. Both immunocytokines (alone or in combination) significantly reduced tumor growth rate compared to the PBS group (mIL12-F8-F8: $p < 0.05$ day 11; F8-IL2: $p < 0.05$ day 8 and from day 10; combination: $p < 0.05$ from day 6, $p < 0.01$ day 8 and from day 10), but the difference between the therapeutic performance of F8-IL2 alone and the same product in combination with mIL12-F8-F8 was not statistically significant.

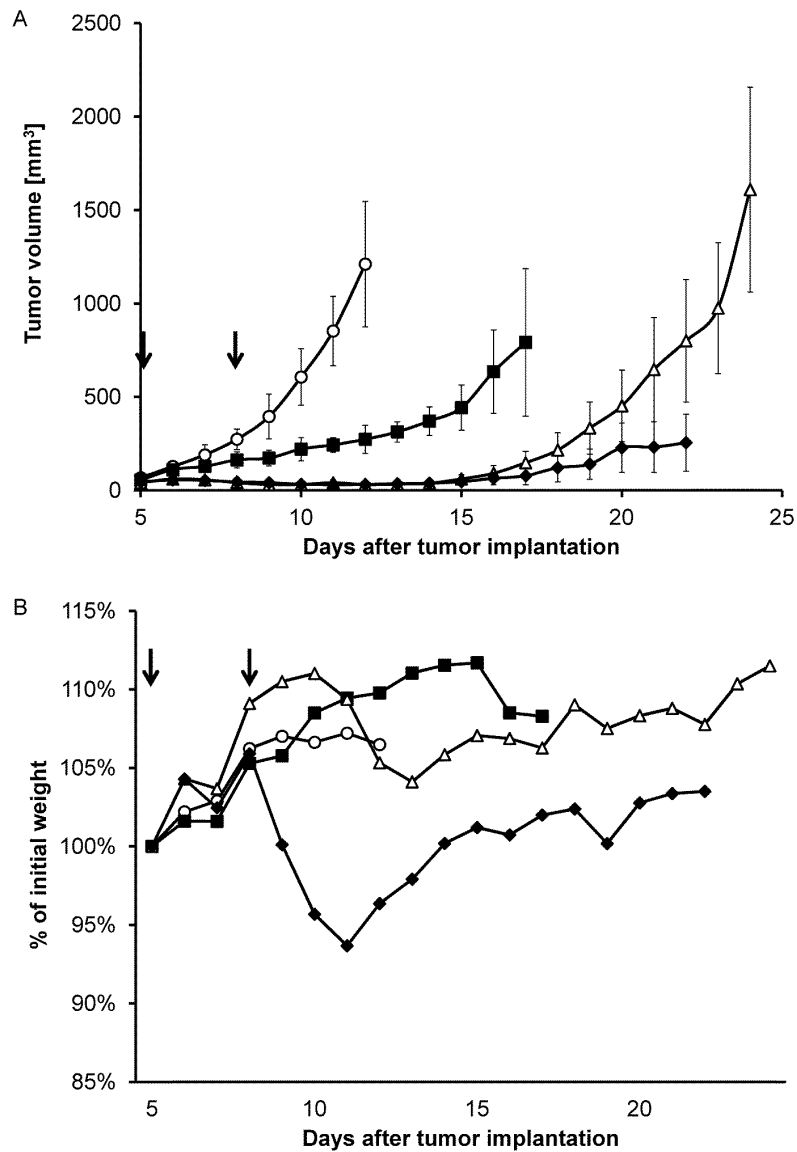


Figure 3.56. Therapeutic activity of mIL12-F8-F8 in combination with F8-IL2 in immunocompetent 129/SvEv mice bearing syngenic s.c. F9 teratocarcinoma. (A) Tumor-bearing mice were treated i.v. with mIL12-F8-F8 (6 μ g, corresponding to 3.4 μ g of mIL12 equivalents, n = 3, ■), F8-IL2 (20 μ g, corresponding to 6.6 μ g of IL2 equivalents, n = 3, △), mIL12-F8-F8 (6 μ g) in combination with F8IL2 (20 μ g) (n = 4, ◆) or PBS (n = 4, ○). Treatment was performed on day 5 and 8 after tumor implantation (black arrows), then the treatment was stopped due to toxicity issues. Data represent mean tumor volumes \pm SE. Tumor growth curves were stopped when the first tumor per group reached 2000 mm³. **(B)** Weight monitoring depicted as percentage of the initial weight. The combination group showed a transient weight reduction and signs of toxicity from day 9 to day 11.

3.4.3.2.1.3.2. mL12-F8-F8 and Paclitaxel

The therapeutic performance of mL12-F8-F8 was also tested in combination with paclitaxel, since we have frequently observed that this cytotoxic agent strongly potentiates the action of other immunocytokines [34,37,148]. Both mL12-F8-F8 used as a single agent and the combination of mL12-F8-F8 and paclitaxel exhibited an additive therapeutic effect in mice bearing F9 tumors (**Fig. 3.57A**). While paclitaxel had only a small tumor growth retardation effect, in spite of being used at high dose (10mg/kg), the use of mL12-F8-F8 at a dose of 8.75 μ g (four injections) led to a long-lasting tumor growth control (PBS vs mL12-F8-F8: $p < 0.05$ from day 9, $p < 0.01$ from day 10; PBS vs combination: $p < 0.05$ from day 9, $p < 0.01$ from day 11; mL12-F8-F8 vs combination $p < 0.05$ day 14]. While eventually tumors grew in all mice treated with mL12-F8-F8, two out of four mice, which had received the combination treatment, were cured and were later submitted to a re-challenge with 107 F9 tumor cells. Unfortunately, both mice developed tumors after the re-challenge at the new cell injection site, indicating that a protective immunity had not been established. Paclitaxel injections in the combination group caused a transient body weight loss, but mice recovered after administration of mL12-F8-F8 (**Fig. 3.57B**).

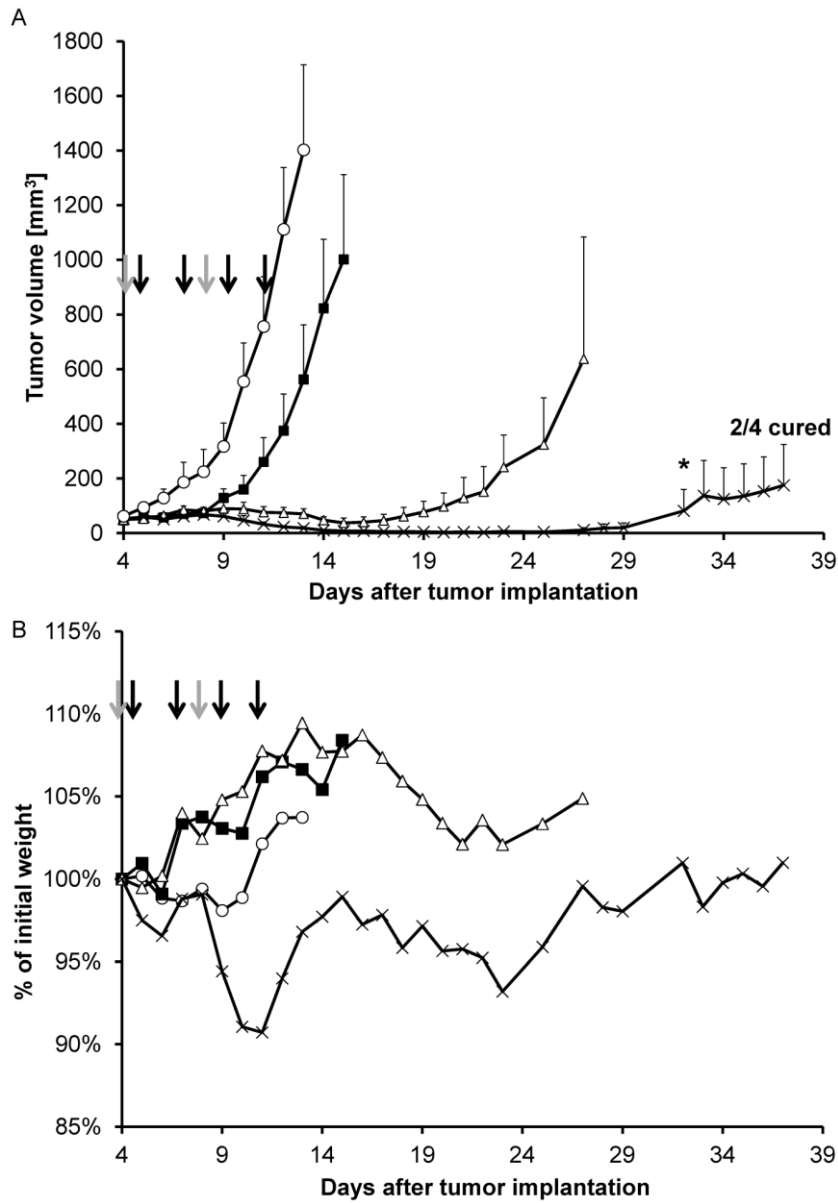


Figure 3.57. Therapeutic activity of mIL12-F8-F8 in combination with paclitaxel in immunocompetent 129/SvEv mice bearing syngenic s.c. F9 teratocarcinoma. (A) Tumor-bearing mice were treated i.v. with mIL12-F8-F8 (8.75 μ g, corresponding to 5 μ g of mIL12 equivalents, n = 5, Δ), paclitaxel (10mg/kg, n = 4, \blacksquare), mIL12-F8-F8 (8.75 μ g) in combination with paclitaxel (10mg/kg) (n = 4, \times) or PBS (n = 4, O). Paclitaxel was administered on days 4 and 8 (grey arrows), mIL12-F8-F8 on days 5, 7, 9 and 11 (black arrows). Two mice out of four of the combination group were cured. Data represent mean tumor volumes \pm SE. Tumor growth curves were stopped when the first tumor per group reached 2000 mm³. **(B)** Weight monitoring depicted as percentage of the initial weight. The combination group showed weight reduction.

3.4.3.2.2. Combination therapy of mIL12-F8-F8 and paclitaxel on CT26 teratocarcinoma bearing immunocompetent mice

A similar tumor therapy experiments was performed in Balb/c mice bearing murine CT26 tumors (**Fig. 3.58**). Two out of five mice in the combination group were cured ($p < 0.05$ from day 7, $p < 0.01$ from day 10, $p < 0.0001$ from day 13), while one mouse was cured in the mIL12-F8-F8 monotherapy group ($p < 0.05$ from day 7, $p < 0.01$ from day 10, $p < 0.001$ from day 13). No significant tumor growth retardation could be observed between the mIL12-F8-F8 and the combination group.

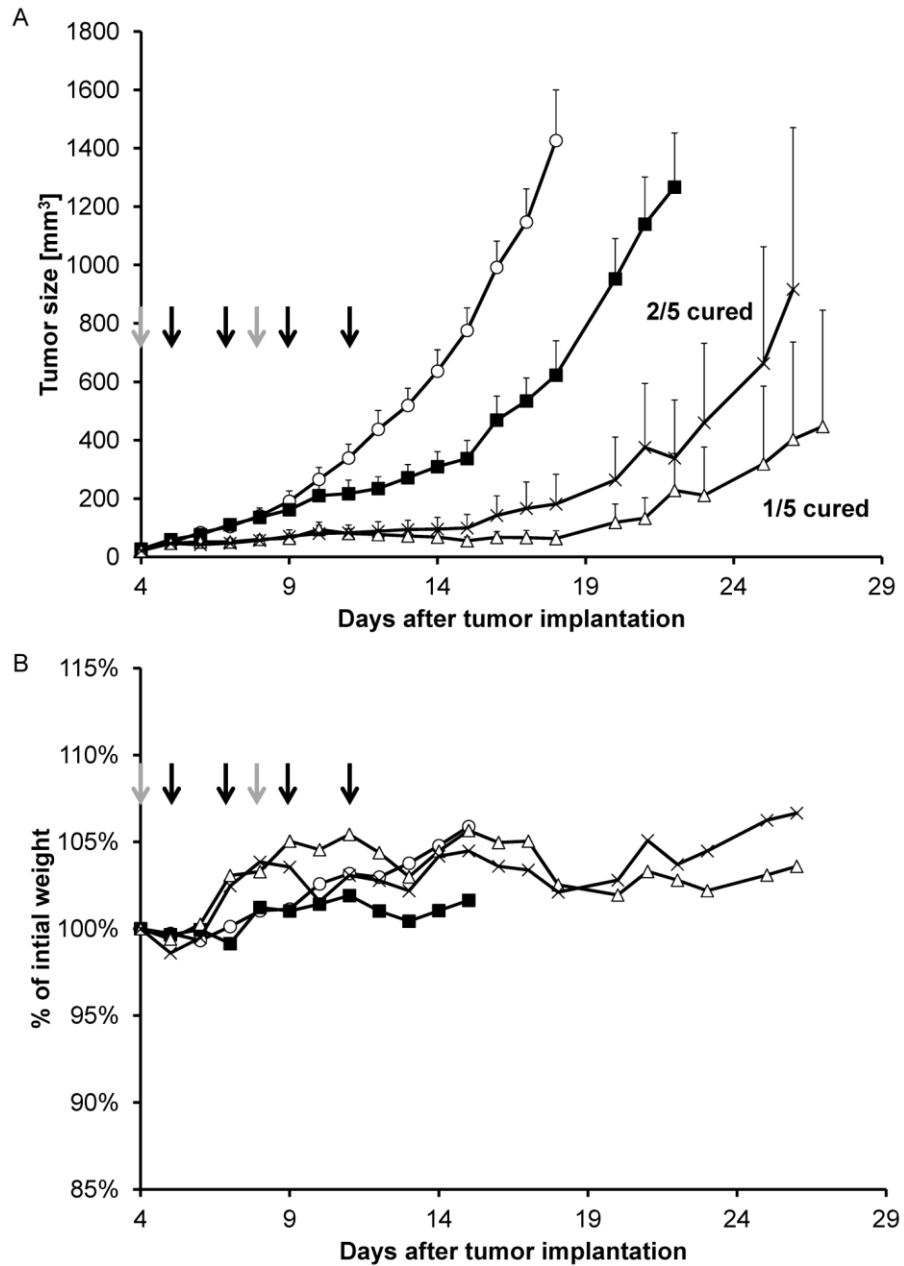


Figure 3.58. Therapeutic activity of mIL12-F8-F8 in combination with paclitaxel in immunocompetent Balb/c mice bearing syngenic s.c. CT26 colon carcinoma. (A) Tumor-bearing mice were treated i.v. with mIL12-F8-F8 (8.75µg, corresponding to 5µg of mIL12 equivalents, n = 5, △), paclitaxel (10mg/kg, n = 5, ■), mIL12-F8-F8 (8.75µg) in combination with paclitaxel (10mg/kg) (n = 5, ×) or PBS (n = 5, ○). Paclitaxel was administered on days 4 and 8 (grey arrows), mIL12-F8-F8 on days 5, 7, 9 and 11 (black arrows). One mouse out of four of the mIL12-F8-F8 group and two mice out of five of the combination group were cured. Data represent mean tumor volumes ± SE. Tumor growth curves were stopped when the first tumor per group reached 2000 mm³. **(B)** Weight monitoring depicted as percentage of the initial weight. No toxicity was observed.

4. MATERIALS AND METHODS

4.1. CELL LINES AND ANIMALS

Adherent CHO-S cells (Invitrogen, Switzerland) were cultured in RPMI 1640 (Gibco, Switzerland) containing 10% FCS (Fetal Calf Serum, Invitrogen), 2mM Ultraglutamine (Lonza, Switzerland). CHO-S cells in suspension were cultivated in shaker incubators in PowerCHO-2CD (Lonza, Switzerland) containing 8mM Ultraglutamine, HT supplement (Lonza, Switzerland). Human peripheral mononuclear blood cells were cultured in RPMI 1640 supplemented with 10% FCS, 2mM Ultraglutamine, 1mM Sodium Pyruvate (Gibco) and 50 μ M β -Mercaptoethanol (Gibco). NIH 3T3 fibroblasts were cultured in RPMI 1640 (Gibco) containing 10% FCS (Invitrogen), 2mM Ultraglutamine (Lonza), 1mM Sodium Pyruvate (Gibco) and 50 μ M β -Mercaptoethanol (Gibco). The tumor cell lines used for therapy studies were the murine teratocarcinoma cell line F9 (CRL-1720, ATCC) and the murine colon carcinoma cell line CT26 (CRL-2638, ATCC). F9 cells were cultured on 0.1% gelatin-coated tissue flasks in DMEM (Gibco) supplemented with 10% FCS, CT26 cell were cultured with DMEM (Gibco) supplemented with 10% FCS. If not otherwise specified cells incubated at 37 °C and 5% CO₂. Female 129/SvPas mice were obtained from Taconic (Denmark). Female 129Sv/Ev, Balb/c and Balb/c nude mice were obtained from Charles River (Germany).

4.2. CLONING OF FUSION PROTEINS

4.2.1. CLONING OF MURINE INTERLEUKIN 7 BASED IMMUNOCYTOKINES

The murine IL7 gene was isolated from a commercial cDNA library (Clontech, USA) by PCR (Polymerase Chain Reaction) using the primer pair NP12 (5'-gagtgccacattaaagacaaagaag-3') and NP10 (5'-tatactgcccttcaaaattttattccaacaag-3'). The gene structures for the F8 antibody in scFv [144] or diabody format [42] have previously been described. The isolation of the KSF antibody, specific to hen egg lysozyme, has previously been described [145]. For the cloning of F8-mIL7, containing a NheI restriction site upstream of the leader sequence, the gene for F8 in diabody format was PCR amplified from the previously describe

clone of F8-IL2 immunocytokine [42] using primers RS9 (5'-ctagctagcgtcgaccatgggctggagcctgat-3') and NP28 (5'-acctccaccgccagaaccacttcgcctgattgattccaccttggtcccttg-3'), which appends a 10-amino acid linker at the C-terminus of the antibody moiety. The murine IL7 gene was PCR amplified using primers NP29 (5'-tcaggcggaaagtgggttctggcgggtggaggtgagtgccacattaaagacaaagaag-3') and NP21 (5'-atagaagctttcattatatactgcccttcaaaattt-3'), that contains two stop codons and a HindIII restriction site at the 3'. In a final step, the F8 diabody and the murine IL7 genes were PCR-assembled using primers RS9 and NP21. The double-digested NheI/HindIII assembly product was cloned into the mammalian cell expression vector pcDNA3.1(+) (Invitrogen).

For the cloning of F8(6aa)-mIL7 the F8 diabody gene was PCR amplified using primers RS9 and NP19 (5'-gcactcacctccatcagcgttcttggattccaccttggtcccttg-3'), that appends a 6-amino acid linker and part of the murine IL7 sequence at the C-terminus of the antibody moiety. The murine IL7 gene was amplified by PCR with primers NP20 (5'-atcaaaggaagcgtgatggaggtgagtgccacattaaagacaaagaag-3') and NP21. Finally, the F8 diabody and the murine IL7 genes were PCR assembled using primers RS9 and NP21. After double digestion, the assembly product was cloned into the pcDNA3.1(+) vector as described for F8mIL7.

For the cloning of scFv(F8)-mIL7, the scFv(F8) and the murine IL7 genes were amplified and PCR-assembled as described for F8-mIL7, using clone F8-SIP [144] for the PCR amplification of the scFv(F8) gene. The gene coding for the resulting fusion protein scFv(F8)-mIL7 was cloned into the pcDNA3.1(+) vector as described for F8-mIL7.

For the cloning of F8-mIL7mut, a fragment of the F8-mIL7 gene was PCR-amplified with primers RS9 and NP40 (5'-tcattattcggggaattactatcag-3'), which inserts a cysteine to serine mutation in the amino acid 33 of the murine IL7 gene. A second fragment of mIL7 was amplified with primers NP39 (5'-ctgatagtaattccccgaataatga-3') and NP42 (5'-ctcttaggaaagatgcatcattct 3'), leading to a change of amino acids 33 and 108 from cysteine into serine. The two fragments were then assembled by PCR. The last fragment of the mutated mIL7 gene was amplified from wildtype murine IL7 using primers NP41 (5'-gaatgatgcatctttcctaaagag-3') and NP21. The two intermediate fragments were eventually PCR-assembled with primers RS9 and NP21 and cloned into the pcDNA3.1(+) vector.

For the cloning of F8-mIL7-F8, the scFv(F8)-mIL7 gene was PCR-amplified with primers RS9 and NP46 (5'-gaaccggatccgctgatatactgcccttcaaaattttattcc-3'), which appends a 10-amino acid linker containing a BamHI restriction site at the 3'. The gene for scFv(F8) was amplified by PCR using primers NP47 (5'-tcaggcggatccggttctggcgggtggaggtgaggtgcagctgttgagctctggg-3', which introduces a BamHI restriction site) and NP45 (5'-tagaagctttcattatttgattccaccttggtcccttg-3'), which contains two stop codons and a HindIII restriction site at the 3'. The scFv(F8)-mIL7 and the scFv(F8) genes were digested with BamHI and then

ligated. The resulting F8mIL7F8 gene was double-digested with NheI/Hind III and cloned into the pcDNA3.1(+) vector.

For the cloning of KSF-mIL7-KSF, the scFv(KSF) gene [145,149] was PCR-amplified with primers RS9 and NP32 (5'-acctccaccgccagaaccacttccgctgagcctaggacggtagcttggtc-3'), that appends a 10 amino acid linker at the C-terminus of the antibody moiety. The gene for murine IL7 was amplified by PCR with primers NP29 and NP46. The scFv(KSF) and the murine IL7 gene fragments were PCR-assembled, double-digested with NheI/EcoRI and cloned into the pcDNA3.1(+) vector. The gene for murine IL7 was amplified by PCR with primers NP12 and NP46. The gene for scFv(KSF) was amplified by PCR with primers NP47 and NP53 (5'-atgcccgcctcattagcctaggacggtagct-3') that contains two stop codons and a NotI restriction site. The murine IL7 and the scFv(KSF) genes were then PCR assembled. Exploiting the fact that both scFv(KSF)-mIL7 and mIL7-scFv(KSF) fragments contained an EcoRI restriction site within the mIL7 moiety, double digestions of PCR assembly product and intermediate vector with EcoRI/NotI, followed by ligation, yielded a pcDNA3.1(+)-based vector driving the expression of KSF-mIL7-KSF.

4.2.2. CLONING OF MURINE INTERLEUKIN 17 BASED IMMUNOCYTOKINE

For the cloning of F8-mIL17, containing a NheI restriction site upstream of the leader sequence, the (scFv)F8 gene was PCR amplified from the previously described clone F8-SIP[144] using primers RS9 and NP28. The mIL17 gene (Source BioScience) was amplified by PCR with primers NP30 (5'-tcaggcggaaagtgggttctggcggtggaggtgcagcgatcatccctcaaagctc-3') and NP24 (5'-tcgataagctttcattaggctgcctggcgacaatcgag-3') introducing two stop codons and a HindIII restriction site. The scFv(F8) and the mIL17 genes were PCR-assembled using primers RS9 and NP24. The double-digested NheI/HindIII assembly product was cloned into pcDNA3.1(+) (Invitrogen) vector.

4.2.3. CLONING OF MURINE INTERLEUKIN 18 BASED IMMUNOCYTOKINES

The murine IL18 gene was isolated from a commercial cDNA library (Clontech, USA) by PCR using the primer pair NP18 (5'-aactttggccgacttactgtac-3') and NP16 (5'-actttgatgtaagttagtgagagtgaaca-3'). For the cloning of F8-mIL18, containing a NheI restriction site upstream of the leader sequence, the gene for F8 in diabody format was PCR amplified from the previously describe clone of F8-IL2 immunocytokine [42] using primers RS9 and NP28. The murine IL18 gene was PCR amplified using primers NP31 (5'-

tcaggcggaagtgggttctggcgggtggaggtaactttggccgacttcactgtac -3') and NP27 (5'-gccatagaagctttcattaactttgatgtaagttagtgagagt -3'), that contains two stop codons and a HindIII restriction site at the 3'. In a final step, the F8 diabody and the murine IL18 genes were PCR-assembled using primers RS9 and NP27. The double-digested NheI/HindIII assembly product was cloned into the mammalian cell expression vector pcDNA3.1(+) (Invitrogen).

For the cloning of F8(6aa)-mIL18 the F8 diabody gene was PCR amplified using primers RS9 and NP25 (5'-aaagttacctccatcagcggcttcttgattccaccttggtcccttg -3'), that appends a 6-amino acid linker and part of the murine IL18 sequence at the C-terminus of the antibody moiety. The murine IL18 gene was amplified by PCR with primers NP26 (5'-atcaaaggaagcgtgatggaggtaactttggccgacttcactgtaca -3') and NP25. Finally, the F8 diabody and the murine IL18 genes were PCR assembled using primers RS9 and NP27. After NheI/HindIII double digestion, the assembly product was cloned into the pcDNA3.1(+) vector as described for F8-mIL18.

For the cloning of F8-mIL18 (Ser7), a fragment of the F8-mIL18 gene was PCR-amplified with primers RS9 and NP34 (5'-ctgcggttagagtggaagtcggc -3'), which inserts a cysteine to serine mutation in the amino acid 7 of the murine IL18 gene. The final fragment of mIL18 was amplified with primers NP33 (5'-gccgacttcactctacaaccgcag -3') and NP27, leading to a change of amino acid 7 from cysteine into serine. The two fragments were then assembled by PCR using primers RS9 and NP27. The double-digested NheI/HindIII product was cloned into the pcDNA3.1(+) vector. F8-mIL18 (Ser75) and F8-mIL18 (Ser125) were cloned following the same schema but using primer pairs RS9/NP36 (5'-atctgttcttagaggagaggtag -3') and RS9/NP38 (5'-ttccttttgggaagcaagaaagt -3') instead of RS9/NP34 for the first fragment, NP35 (5'-ctaccctctctctaagaacaagat -3')/NP27 and NP37 (5'-actttctgcttccaaaggaa -3')/NP27 instead of NP33/NP27 for the second fragment, which led to a change of amino acid 75 or 125 from cysteine into serine. For the PCR assembly primers RS9 and NP27 were used.

For the cloning of F8-mIL18 (Ser7, Ser75), a fragment of the F8-mIL18 (Ser7) gene was PCR-amplified with primers RS9 and NP36, then the final part of mIL18 was PCR-amplified with primers NP35 and NP27. The two fragments were PCR assembled using primers RS9 and NP27. The double-digested NheI/HindIII product was cloned into the pcDNA3.1(+) vector.

For the cloning of F8-mIL18 (Ser7, Ser125), a fragment of the F8-mIL18 (Ser7) gene was PCR-amplified with primers RS9 and NP38, then the final part of mIL18 was PCR-amplified with primers NP37 and NP27. The two fragments were PCR assembled using primers RS9 and NP27. The double-digested NheI/HindIII product was cloned into the pcDNA3.1(+) vector.

For the cloning of F8-mIL18 (Ser75, Ser125), a fragment of the F8-mIL18 (Ser75) gene was PCR-amplified with primers RS9 and NP38, then the final part of mIL18 was PCR-amplified with primers NP37 and NP27. The two fragments were PCR assembled using primers RS9 and NP27. The double-digested NheI/HindIII product was cloned into the pcDNA3.1(+) vector.

For the cloning of F8-mIL18 (Ser7, Ser75, Ser125), a fragment of the F8-mIL18 (Ser7, Ser75) gene was PCR-amplified with primers RS9 and NP38, then the final part of mIL18 was PCR-amplified with primers NP37 and NP27. The two fragments were PCR assembled using primers RS9 and NP27. The double-digested NheI/HindIII product was cloned into the pcDNA3.1(+) vector.

For the cloning of mIL18-F8, the mIL18 gene was PCR amplified using primers NP56 (5'-tcctgttctctcgtcgtgtggctacaggtgtgcactcgaactttggccgacttcactgtaca-3') that inserts the final part of the secretion sequence and primer NP57 (5'-acctccaccaccgcttccactttgatgtaagttagtgagagt-3'), containing a 6 amino acid linker at the 3'. The gene for F8 in diabody format was PCR amplified from F8-mIL18 using primers NP58 (5'-ggaagcgggtggagggtgaggtgcagctgttgagctctggg-3') and NP27. The two fragments were PCR-assembled using primers SW2 and NP27. The double-digested NheI/HindIII product was cloned into pcDNA3.1(+) vector.

For the cloning of F8-mIL18-F8, the scFv(F8) and the murine IL18 genes were amplified and PCR-assembled as described for F8-mIL18, using clone F8-SIP [144] for the PCR amplification of the scFv(F8) gene. The gene coding for the resulting fusion protein scFv(F8)-mIL18 was cloned into the pcDNA3.1(+) vector as described for F8-mIL18. The mIL18 gene was PCR-amplified with primers NP31 and NP50 (5'-ctccggaaccacttccgcctgaactttgatgtaagttagtgagagt-3'), which appends a 10-amino acid linker at the 3'. The gene for scFv(F8) was amplified by PCR using primers NP51 (5'-gttccggaggtggagggtgaggtgcagctgttgagctctg-3') and SW1. The two fragments were PCR-assembled using primers NP31 and SW1. Exploiting the fact that both scFv(F8)-mIL18 and mIL18-scFv(F8) fragments contained a BamHI restriction site within the mIL18 moiety, double digestions of PCR assembly product and intermediate vector with BamHI/NotI, followed by ligation, yielded a pcDNA3.1(+)-based vector driving the expression of F8-mIL18-F8.

For the cloning of murine IL18, mIL18 gene was PCR amplified using from the mIL18-F8 clone using primers SW2 and NP69 (3'-atagaagctttcattagtgatggtgatggtgatgactttgatgtaagttagtgagagt-5'), which inserts a His-Tag, two stop codons and a HindIII restriction site downstream of the mIL18 gene. The double-digested NheI/HindIII product was cloned into the pcDNA3.1(+) vector.

4.2.4. CLONING OF MURINE INTERLEUKIN 12 BASED IMMUNOCYTOKINES

For the cloning of mL12-F8-F8 the gene for F8 in diabody format was PCR-amplified from the previously described clone of F8-mIL7 immunocytokine [34] using primers NP68 (5'-ctcatccggaagtagctcttcgggatcctcgtccagcggcgagggtgcagctgttgagctgg-3') which appends a 15 amino acid linker containing a BamHI restriction site at the N-terminus of the antibody moiety and SW1 that contains two stop codons and a NotI restriction site at the 3'. The double-digested BamHI/NotI PCR product was cloned into the mammalian cell expression vector pcDNA3.1(+) (Invitrogen). The gene for mp40 was PCR amplified from the previously described L19-IL12 clone [24] using primers NP59 (5'-tcctgttctcgtcgtctgtggctacaggtgtgcactcgcgatgtggagctggagaaagacgtt-3') containing the C-terminus of the leader sequence and NP60 (5'-tgtgttcctgcagggtccgatccggtggaggcggttcaggcggaggtggctct-3'), which appends a 15 amino acid linker at the C-terminus of the mp40 subunit. The gene for mp35 was PCR amplified from the previously described L19-IL12 clone [24] using primers NP61 (5'-ggtggaggcggttcaggcggaggtggctctggcgggtggcgatcgagggtcattccagtctctggacct-3'), which inserts a 15 amino acid linker at the N-terminus of the mp35 subunit and NP62 (5'-ccagagaaaagcttaaacattatt-3'), which inserts a HindIII restriction site in the mp35 gene. The mp40 and mp35 genes were PCR-assembled using primers SW2, containing a NheI restriction site upstream of the leader sequence and NP62. The double-digested NheI/HindIII PCR product was cloned into the mammalian cell expression vector pcDNA3.1(+) (Invitrogen). The gene for mp35 was PCR amplified from the previously described L19-IL12 clone [24] using primers NP63 (5'-ccagagaaaagcttaaacattatt-3') and NP64 (5'-gtgatgggctatctgagctccgccgtagcgtgatggaggt-3'), which appends a 6 amino acid linker at the C-terminus of the mp35 subunit. The gene for F8 diabody was PCR amplified from the previously described clone of F8-mIL7 immunocytokine [146] using primers NP65 (5'-ggtagcgtgatggaggtgaggtgcagctgttgagctggg-3'), which inserts a 6 amino acid linker at the N terminus of the diabody and NP66 (5'-caagggaccaaggtggaaatcaaattcttctcatccggaagtagctcttcgggatcctcgt-3'), which inserts a 15 amino acid linker containing a BamHI restriction site at the C terminus of the antibody moiety. The mp35 and F8 diabody genes were PCR-assembled using primers NP63 and NP66. The double-digested HindIII/BamHI PCR product was cloned into the previously constructed pcDNA3.1(+) vector containing the F8 diabody gene.

Finally, the mp40-mp35 gene was obtained by NheI/HindIII double-digestion of the pcDNA3.1(+) vector containing the right sequence and inserted into the previously constructed pcDNA3.1(+) vector containing the mp35-F8 diabody – F8 diabody gene.

For the cloning of mIL12-KSF-KSF, the KSF diabody gene [145,149] was PCR-amplified with primers NP65 and NP71 (5'-aatcggctctggaatgcctgagggc-3') which removes the BamHI restriction site present in the KSF sequence and with primers NP70 (5'-gccctcaggcattccagaccgatt-3') and NP67 (5'-gaccaagctgaccgtcctaggctcttctcatccggaagtagctcttcgggatcctcgt-3'), which inserts a 15 amino acid linker containing a BamHI restriction site. The genes encoding for KSF were then PCR assembled. The gene for mp35 was PCR-amplified using primers NP63 and NP64, it was then PCR-assembled with the KSF diabody gene using primers NP63 and NP67. The double-digested HindIII/BamHI PCR product was cloned into the previously constructed pcDNA3.1(+) vector containing the mp40-mp35 gene.

The KSF gene was PCR-amplified from the new vector using primers NP68 and NP53 (3'-atcggccgctcattagcctaggacggctcagct-5'), which appends two stop codons and a NotI restriction site at the 3' end. The double-digested BamHI/NotI PCR product was cloned into a pcDNA3.1(+) vector. Finally the mp40-mp35-KSF gene was obtained by NheI/BamHI double-digestion of the pcDNA3.1(+) vector containing the right sequence and inserted into the previously constructed pcDNA3.1(+) vector containing the KSF diabody gene.

4.3. EXPRESSION, PURIFICATION AND CHARACTERIZATION OF IMMUNOCYTOTOKINES

Adherent CHO-S cells were stably transfected by electroporation with the plasmid driving F8-mIL7, F8-mIL17 or F8-mIL18 expression. Selection was carried out in the presence of G418 (0.5 g/L) (Calbiochem, Germany). Clones of G418 resistant cells were screened for the expression of the fusion protein by ELISA using recombinant EDA of human fibronectin and protein A – HRP (Horseradish Peroxidase) for detection (GE Healthcare). The best expressing clone was adapted to grow in suspension in PowerCHO-2CD protein free medium for large-scale production of F8-mIL7.

All the other fusion proteins were expressed using transient gene expression. For 1 ml of production 1×10^6 CHO-S cells in suspension were centrifuged and resuspended in 0.5ml ProCHO4 (Lonza). 1.25 μ g of plasmid DNA were mixed with 150mM NaCl to reach a final volume of 25 μ L, 5 μ L of 25 kDa linear polyethylene imine (PEI) (1 mg/mL solution in water at pH 7.0) (Polysciences, Germany) were mixed with 20 μ L of 150 mM NaCl. The PEI/NaCl solution was added to the DNA/NaCl solution and allowed to stand at room temperature for

10 min. The solution containing the PEI–DNA complexes was then added to the cells and gently mixed. The transfected cultures were incubated in a shaker incubator at 37 °C [150]. At 4 h post-transfection, the transfected culture was diluted with 0.5 mL of PowerCHO-2CD and then incubated at 31 °C in a shaker incubator for 6 days. The procedure was scaled up to reach the desired production volume.

The fusion proteins, either produced with stable or transient gene expression, were purified from the cell culture medium by protein A affinity chromatography. The size of the fusion proteins was analyzed under reducing and non reducing conditions by SDS-PAGE and under native conditions by FPLC (Fast Protein Liquid Chromatography) gel filtration on a Superdex200 10/300 GL size exclusion column (GE Healthcare). The binding affinity of the immunocytokines was qualitatively determined by BIAcore on an EDA antigen coated sensor chip.

4.4. WESTERN BLOT ANALYSIS

For mIL18 fusion proteins Western blotting was performed on CHO-S supernatants 6 days post-transfection. SDS PAGE was performed using 4-12% BisTris Gel and MOPS as a running buffer. Blotting was performed using MOPS buffer 20% Methanol. Proteins were blotted on a nitrocellulose membrane (Protran BA 85, Whatman, Germany) during 2 hours, with 165mA and 20V. The blotted membrane was blocked in Milk-PBS 2% (MPBS) for 2 hours, then washed three times with PBS. 10ml of primary antibody (goat-a-mIL18, Santa Cruz Biotechnology, USA) were added. After 1 hour incubation the membrane was washed three times with Tween 0.1% PBS and three times with PBS. Then 10ml of secondary antibody (anti-goat-IgG – HRP, Dako, Denmark) were added and after 1 hour incubation the membrane was washed as described over.

Amersham ECL Plus Western Blotting detection system (Solution A and solution B, GE Healthcare, UK) was used. Solution A (2 ml) was mixed to solution B (50µl) and the mixture was poured on the membrane that was kept in dark. After 5 minutes incubation a high performance chemiluminescence film (GE Healthcare, UK) was exposed to the membrane. After different time points the films were developed.

4.5. DEGLYCOSILATION

To deglycosylate purified immunocytokines, 40µg protein were incubated with 2500 units PNGase F (NEB, UK) for 20h at 37 °C.

4.6. STABILITY

Immunocytokines were stored at 37 °C for 24h, 48h, 72h or 96h. The stability of fusion proteins was analyzed by SDS PAGE under non-reducing conditions.

4.7. BIOACTIVITY ASSAYS

4.7.1. MURINE INTERLEUKIN 7 BIOACTIVITY ASSAY

The biological activity of F8-mIL7-F8 and KSF-mIL7-KSF was determined by a T cell proliferation assay. Freshly isolated human peripheral blood mononuclear cells were cultured immediately after isolation with 25µg/ml mitogen phytohemagglutinin-M (Roche Diagnostics, Germany) for 3 days. 200µl cells were seeded in 96-well plates at a density of 4×10^5 cells/ml in a medium containing serial dilutions of either F8-mIL7-F8 or KSF-mIL7-KSF or commercially available, recombinant, murine IL7 (Chemie Brunschwig, Switzerland) as a standard or culture medium as a negative control. After 48h, 40µl Cell Titer 96 Aqueous One Solution (Promega, USA) were added to each well. The plate was incubated for 3h and absorbance was read at 490nm. The experiment was performed in triplicates.

(Adapted from: E-Bioscience, Best Protocols, Functional Activity Protocols, Cytokines Bioassays Protocol)

4.7.2. MURINE INTERLEUKIN 17 BIOACTIVITY ASSAY

The biological activity of F8-mIL17 was determined by its ability to induce IL6 production in NIH 3T3 fibroblasts. 4×10^4 cells were seeded in 96-well plates in medium containing serial dilutions of F8-mIL17 or recombinant mIL17 (standard, Chemie Brunschwig) or culture medium (negative control). After 48h, cytokine expression in supernatants was determined with Mouse IL6 ELISA Ready-SET-Go! (BD Biosciences). The experiment was performed in triplicates.

(Adapted from: E-Bioscience, Best Protocols, Functional Activity Protocols, Cytokines Bioassays Protocol)

4.8. IMMUNOFLUORESCENCE ANALYSIS ON TUMOR SECTIONS

Cryostat sections (10µm) of frozen syngeneic F9 teratocarcinoma specimens were fixed in ice cold acetone, rehydrated with PBS and blocked with FCS. As primary antibodies biotinylated immunocytokines (F8-mIL7, F8-mIL7-F8, KSF-mIL7-KSF, F8mIL17, F8mIL18), mIL12-F8-F8, rat-a-mouse-CD31 (BD Biosciences, Germany), rat anti F4/80 (macrophages, Abcam), rat anti CD45 (leukocytes, BD Biosciences), rat anti CD31 (endothelial cells, BD Biosciences), rat anti CD4 (CD4 T cells), rat anti CD8 (CD8 T cells) and rabbit anti Asialo/GM1 (NK cells, Wako Pure Chemical Industries) antibodies were used. Rat-a-IL12/IL23 mp40 (eBiosciences) was used as secondary antibody. Anti rat IgG-AlexaFluor488, anti rat IgG-AlexaFluor594, anti rabbit IgG-AlexaFluor488, as well as streptavidin-AlexaFluor488, were used as secondary/tertiary reagents for microscopic detection. Slides were mounted with fluorescent mounting medium (Dako, Denmark) and analyzed with an Axioskop2 mot plus microscope (Zeiss, Switzerland).

Images were obtained with an Axioskop2 mot plus microscope (Zeiss), the staining areas were analyzed using ImageJ software and expressed as percentage of measurement area.

4.9. QUANTITATIVE BIODISTRIBUTION STUDIES

The in vivo targeting performance of the immunocytokines was evaluated by quantitative biodistribution analysis. Briefly, the fusion proteins were radioiodinated with ¹²⁵I and Chloramine T hydrate (0.25 µg/µg protein, Sigma, Switzerland) and purified on a PD10 column (GE Healthcare). Radiolabeled proteins were injected into the lateral tail vein of immunocompetent 129/SvEv mice or athymic Balb/c nude mice bearing s.c. implanted F9 murine teratocarcinoma. Mice were sacrificed 24h after injection. Organs were weighed and radioactivity was counted using a Packard Cobra gamma counter. Radioactivity content of representative organs was expressed as the percentage of the injected dose per gram of tissue (%ID/g ± standard error).

4.9.1. MURINE INTERLEUKIN 7 BASED IMMUNOCYTOTOKINES

Radiolabeled F8-mIL7 was injected in both mouse models bearing F9 murine teratocarcinoma at low dose (15µg, 3µCi) and in 129/SvEv mice at high dose (10µg radiolabeled protein and 100µg unlabeled protein,

5 μ Ci). Radiolabeled F8-mIL7-F8 and KSF-mIL7-KSF were injected in 129Sv/Ev mice at high dose (10 μ g radiolabeled protein and 100 μ g unlabeled protein, 5 μ Ci resp. 9 μ Ci).

4.9.2. MURINE INTERLEUKIN 17 BASED IMMUNOCYTOKINE

F8-mIL17 was radioiodinated and injected into 129/SvPas (14.5 μ g radiolabeled protein or 7.5 μ g radiolabeled plus 60 μ g unlabeled protein) or Balb/c nude mice (Charles Rivers) (14.5 μ g radiolabeled protein) bearing s.c. implanted F9 tumors.

4.9.3. MURINE INTERLEUKIN 18 BASED IMMUNOCYTOKINES

F8-mIL18 was radioiodinated and injected into 129/SvPas (15 μ g radiolabeled protein or 7.5 μ g radiolabeled plus 60 μ g unlabeled protein) or Balb/c nude mice (Charles Rivers) (15 μ g radiolabeled protein) bearing s.c. implanted F9 tumors.

4.9.4. MURINE INTERLEUKIN 12 BASED IMMUNOCYTOKINES

The immunocytokines mIL12-F8-F8 and mIL12-KSF-KSF were radioiodinated and injected into 129/SvEv (7 μ g) bearing s.c. implanted F9 tumors.

4.10. SYNGENEIC TUMOR MOUSE MODELS IN IMMUNOCOMPETENT AND ATHYMIC MICE

Tumor bearing mice were obtained by s.c. injection of F9 teratocarcinoma cells (10⁷) in the flank of 12 weeks old female 129/SvEv, 129/SvPas or Balb/c nude mice or by s.c. injection of CT26 colon carcinoma cells (2x10⁶) in the flank of 12 weeks old female Balb/c mice. Normally, 4 to 5 days after tumor implantation, when tumors were clearly palpable, mice were grouped (n \geq 3) and injected i.v. into the lateral tail.

Mice were monitored daily, tumor volumes were measured daily with a digital caliper and calculated using the formula: volume = length x width² x 0.5. Animals were sacrificed when tumor volumes reached

2000mm³. Experiments were performed under a project license granted by the Veterinäramt des Kantons Zürich, Switzerland (169/2008).

4.10.1. MURINE INTERLEUKIN 7 BASED IMMUNOCYTOTOKINES

129SvEv and Balb/c nude mice were injected three times every 48h with F8-mIL7 (80µg) or saline.

129SvEv mice were injected three times every 72h with F8-mIL7-F8 (80µg) or KSF-mIL7-KSF (80µg) or saline.

129SvEv mice were injected three times every 72h with paclitaxel (10mg/kg) or F8-mIL7-F8 (120µg) or paclitaxel (10mg/kg) in combination with F8-mIL7-F8 (120µg) or saline. Paclitaxel was injected first, followed after 24h by the immunocytokine.

4.10.2. MURINE INTERLEUKIN 17 BASED IMMUNOCYTOTOKINE

Four days after tumor implantation, mice were grouped and injected into the lateral tail vein three times every 48h with F8-mIL17 (100µg) or saline. The experiment was repeated in immunocompetent mice, which were sacrificed three days after last injection. Tumors were excised, embedded in cryoembedding medium (ThermoScientific) and stored at -80 °C.

4.10.3. MURINE INTERLEUKIN 18 BASED IMMUNOCYTOTOKINES

Five days after tumor implantation, mice were grouped and injected into the lateral tail vein three times every 48h with F8-mIL18 (50µg) or saline.

4.10.4. MURINE INTERLEUKIN 12 BASED IMMUNOCYTOTOKINES

129SvEv mice were injected four times, every 48h, starting 5 days after tumor implantation, with mIL12-F8-F8 (1.75µg, corresponding to 1µg of mIL12 equivalents, n = 5), mIL12-KSF-KSF (1.75µg, corresponding to 1µg of mIL12 equivalents, n = 5) or PBS (n = 5).

129SvEv mice were injected four times, every 48h, starting 8 days after tumor implantation, with mIL12-F8-F8 (6µg, corresponding to 3.4µg of mIL12 equivalents, n = 4), mIL12-KSF-KSF (6µg, corresponding to 3.4µg of mIL12 equivalents, n = 3) or PBS (n = 4).

129SvEv mice were injected four times, every 48h, starting 5 days after tumor implantation, with mIL12-F8-F8 (8.75 μ g, corresponding to 5 μ g of mIL12 equivalents, n = 5) i.v., with mIL12-F8-F8 (8.75 μ g, corresponding to 5 μ g of mIL12 equivalents, n = 3) i.t. or PBS i.v. (n = 4).

129SvEv mice were injected two times, every 72h, starting 5 days after tumor implantation, with mIL12-F8-F8 (6 μ g, n = 3), F8-IL2 (20 μ g, corresponding to 6.6 μ g of IL2 equivalents, n = 3), mIL12-F8-F8 (6 μ g) in combination with F8-IL2 (20 μ g) (n = 4) or PBS (n = 4).

129SvEv mice bearing F9 teratocarcinoma and Balb/c mice bearing CT26 Colon carcinoma were injected two times, every 96h, starting 4 days after tumor implantation with paclitaxel (10mg/kg; n = 4, n = 5) or four times, every 48h, starting 5 days after tumor implantation with mIL12-F8-F8 (8.75 μ g; n = 5, n = 5) or with a combination of paclitaxel (10mg/kg, starting on day 4, every 96h, twice) and mIL12-F8-F8 (8.75 μ g, starting on day 5, every 48h, four times; n = 4, n = 5) or PBS (n = 4, n = 5).

The mice bearing F9 teratocarcinoma that were cured were re-challenged by injecting 10^7 F9 cells into the opposite flank.

5. DISCUSSION

There is a growing interest in the use of immunocytokines as a promising type of “armed” antibodies. Compared to other forms of antibody derivatives (e.g., antibody-drug conjugates or radiolabeled antibodies; [151-153]), immunocytokines are easier to develop in clinical trials when the corresponding cytokine has already been studied and may represent “biosuperior” versions of previously used biopharmaceuticals [28,154]. Importantly, unlike antibody-drug conjugates or radiolabeled antibodies, immunocytokines typically spare the organs which mediate the clearance of the product from circulation. The limiting toxicities associated with pro-inflammatory cytokines are hypotension and flu-like symptoms, which can be manageable and which orthogonal to the side effects of most cytotoxic drugs, thus favoring combination studies in which both agents are used at the recommended dose [46].

We have described the cloning, expression and characterization of novel immunocytokines, consisting of the F8 antibody and of murine IL7 as modular building blocks for the assembly of fusion proteins in various formats. The study was stimulated by the fact that recombinant IL7 is currently being investigated as an anti-cancer therapeutic agent in patients with metastatic melanoma, renal cell carcinoma and refractory solid tumors [100,155].

The study of various formats for the production of fusion proteins based on F8 and mIL7 has revealed novel features, which we had rarely encountered with other fusion proteins.

- (i) For many immunocytokines, a sequential fusion of scFv and cytokine moieties leads to the production of proteins of good pharmaceutical properties and capable of selective localization at

the tumor site [33,39]. By contrast, the sequential fusion of scFv(F8) with mIL7 led to the production of a fusion protein (“F8-mIL7”) which formed covalent aggregates, as revealed by SDS-PAGE analysis in non-reducing conditions. This feature is indicative of wrong disulfide bond formation, involving cysteine residues of the antibody or the cytokine moiety. Not surprisingly, the poor pharmaceutical quality of the F8-mIL7 fusion protein was paralleled by inadequate

tumor targeting performance in biodistribution studies. Curiously, however, F8-mIL7 displayed a full retention of immunoreactivity *in vitro* and a potent therapeutic activity *in vivo*.

- (ii) While normalized biodistribution results (expressed as %ID/g) for antibodies specific to splice-isoforms of fibronectin are typically independent of the concentration of antibody used in the assay over a broad range [156], the tumor targeting properties of F8-mIL7 exhibited a concentration dependence, with more favorable tumor-to-organ ratios observed at high doses of immunocytokine (i.e., > 100 µg/mouse). Interestingly, there was no significant difference in biodistribution data between the use of nude or immunocompetent mice bearing the same type of murine subcutaneous tumor, in spite of the fact that the IL7 receptor is mainly expressed in B cells, T cells, NK cells, mast cells and neutrophils.

- (iii) A novel immunocytokine format, in which the mIL7 moiety was flanked by two scFv moieties ("F8-mIL7-F8"), yielded proteins of excellent pharmaceutical quality and characterized by improved biodistribution data in tumor-bearing mice.

Both F8-mIL7 and F8-mIL7-F8 mediated a statistically-significant retardation of F9 tumor growth, but only in immunocompetent mice. However, unlike other immunocytokines [24,33,37] for which the antibody-mediated targeting leads to a dramatic potentiation of therapeutic activity, only a subtle superiority could be observed when a tumor targeting antibody moiety (F8-mIL7-F8) was used instead of an antibody of irrelevant specificity in the mouse (KSF-mIL7-KSF). Similar to what has previously been reported for IL2-based immunocytokines [37,148], the therapeutic activity of F8-mIL7-F8 could be boosted by the combination with paclitaxel.

When comparing the therapeutic properties of mIL7-based immunocytokines with the ones previously reported by us and others with immunocytokines based on other immunomodulatory proteins (e.g., IL2, IL12, IL15, TNF, IFN γ , GM-CSF [24,33,35,37-40,42]), it appears that mIL7 may not be the first choice for future clinical development activities. The main limitations encountered in this study were both in terms of absolute protein delivery to the tumor (2-3% ID/g at 24h, compared to approx. 20% ID/g observed with the F8 alone or with other F8-based fusion proteins [40,99,144]) and in term of insufficient tumor growth retardation.

Similar to IL7, also IL18 was already studied in clinical trials. When we tried to fuse this cytokine to scFv(F8) in diabody format, protein quality problems (covalent homodimerization) and dose-dependent biodistribution were observed for F8-mIL18. The favorable targeting properties of the immunocytokine and the successful reformatting adopted for IL7-base immunocytokines stimulated the development of F8-mIL18 mutants and alternative fusion protein formats, as well as formulation studies. Unfortunately, no improvement could be achieved in terms of pharmaceutical quality of IL18-based immunocytokines.

Exploiting the fact that IL17 is an homodimeric protein, we cloned a fusion protein consisting of a fully functional scFv(F8) sequentially fused to mIL17 and self-assembling in a homodimeric immunocytokine. F8-mIL17 showed impressive pharmaceutical quality associated with concentration independent, good targeting properties. We observed that the antibody-based targeted delivery of mIL17 to the tumor blood vessels enhances tumor angiogenesis and leukocyte infiltration into the tumor mass, but this does not lead to a measurable anti-cancer activity in immunocompetent or in nude mice. Our findings are consistent with previous publications, in which no difference in tumor growth rate was observed in IL17^{-/-} mice compared to wild-type mice [125], or in which tumor cells transfected with mIL17 displayed no anti-cancer activity[119,120,122]. It remains to be seen whether the activity of IL17 could be different in an orthotopic setting. In spite of these considerations, it would be conceivable to use IL17-based immunocytokines to stimulate therapeutic angiogenesis at sites of disease [157].

As observed with IL7 fusion proteins, the ability of immunocytokines to selectively localize at the tumor site is crucial for displaying superiority compared to the non-targeted version of the cytokine. Indeed, in mouse models of cancer, the antibody-mediated targeted delivery of anti-cancer cytokines allows to achieve comparable therapeutic effects by administering 20-fold lower concentrations (or more) of the immunocytokine, compared to the parental recombinant cytokine [23,24,32]. In the case of IL12-based immunocytokines, the best tumor targeting results were so far obtained with a heterodimeric format [98,99], which however complicated GMP manufacture procedures and pharmaceutical analytics. We designed a novel format, which combines good pharmaceutical quality, easy manufacturability, efficient *in vivo* tumor targeting and potent anti-cancer activity. It is thus ideally suited for pharmaceutical development.

Our laboratory has tested a large variety of different immunocytokines for cancer treatment [28] and IL12 stands up as one of the most promising candidates for product development, also thanks to the promising

preclinical data obtained in murine tumor models of cancer which cannot be cured by conventional chemotherapy [23,24,32,37,40,98].

IL12 not only directly enhances cytotoxic cell activity, but also stimulates IFN γ production through several pathways. IFN γ was shown to be crucial for the eradication of tumors by CD4 T cells, with a mechanism which may involve a direct cytotoxic activity on tumor cells and an enhanced expression of MHC class II molecules [158]. Moreover, the production of the anti-angiogenic chemokine IP-10 (IFN- γ inducible protein 10, CXCL10), capable of inducing tumor growth-retardation, [159] is also stimulated by IL12.

While immunocytokines based on IL2 or TNF transiently worsened inflammatory conditions in animal models of psoriasis [160], arthritis [161] and endometriosis [162] (but, importantly, not in animal models of atherosclerosis [163]), the targeted delivery of IL12 does not seem to have a negative impact on inflammation in mouse models [160].

The combination of IL2- and TNF-based immunocytokines has previously been reported to eradicate tumors, which cannot be cured by the action of IL2 or TNF alone [32]. We have also previously reported on the synergistic action of IL12- and TNF-based immunocytokines. In this study, we have observed that the combination of F8-IL2 and mIL12-F8-F8 led to potent therapeutic activities, but only at the expense of severe toxicities. By contrast, as already observed with F8-mIL7-F8, promising therapeutic results have been observed combining mIL12-F8-F8 with paclitaxel [34,37,148].

The only two IL12-based immunocytokines in clinical development featured a fusion of IL12 to an antibody in full IgG format [56]. In principle, the Fc portion of this multifunctional molecule can contribute to a long circulatory half-life (22h) [56] and may cross-link IL12 to leukocytes carrying Fc γ receptors on their surface. The use of antibody fragments in scFv format may favor shorter half-lives in blood (thus reducing side effects) [45], promote an efficient tumor targeting and avoid IL12 delivery to non-target cells.

6. CONCLUSIONS AND OUTLOOK

Immunocytokines are able to localize at sites of disease, thus increasing the therapeutic index of the corresponding cytokine. When used alone, they rarely exhibit complete cures of cancer in animal models and in patients. However, combination therapies have resulted in complete and long-lasting tumor eradications, which cannot be achieved by conventional chemotherapy. It is still largely unknown why some patients respond to therapy and other patients do not. Similarly, different therapeutic outcomes are sometimes observed in different mouse models of cancer, using the same immunocytokine.

The main value of the three studies on Interleukin 7, Interleukin 17 and Interleukin 18 consists in having expanded the set of immunocytokines studied by our group, thus increasing our knowledge in the field. The availability of multiple immunocytokines differing in format and/or biological payload allows a comparative evaluation of different fusion proteins.

Our study, which involved the cloning, expression and characterization of 20 immunocytokines, revealed that favorable disease-homing properties and acceptable pharmaceutical quality represent indispensable prerequisites for the development of immunocytokines suitable for clinical study programs.

In our early studies, we showed that protein quality and preclinical performance can be improved by designing innovative antibody-cytokine fusion formats. We also demonstrated that the length of linkers joining antibody and cytokine domains may have an impact on the pharmaceutical quality of the corresponding immunocytokine. For example, the fusion protein IL12-F8-F8 combines good pharmaceutical quality, easy manufacturability, efficient *in vivo* tumor targeting properties and potent anti-cancer activity.

The IL12-F8-F8 product could potentially be used for the treatment of a variety of different cancer types, since the F8 antibody recognizes neo-vascular and stromal structures in the majority of human tumors tested [164,165], while reacting only with placenta and the endometrium in the proliferative phase in a panel of freshly-frozen 36 human normal tissues [20]. The first clinical development programs should probably be designed for the treatment of non-Hodgkin lymphomas, since recombinant hIL12 has exhibited

a potent therapeutic effect for this indication [96] and since the alternatively-spliced EDA domain of fibronectin is strongly expressed in the majority of different lymphoma types [165].

Immunocytokines will find an increasing use in the clinical setting. Progress in this field will crucially rely on the identification of accessible good-quality markers of pathology. The EDA domain of fibronectin, used as tumor-associated antigen in the targeting strategies described in this thesis, represents a biomarker which is over-expressed in the majority of aggressive human malignancies [164,165]. However, since it is expressed at sites of active tissue remodeling, it is also found in chronic inflammatory conditions such as arthritis, atherosclerosis and endometriosis [20,162,166,167]. For the future, we will have to learn how strict the target expression has to be for a given tumor type, in comparison to normal organs in healthy and in polymorbid conditions.

Protein engineering will play a fundamental role for the development of clinical-grade immunocytokines. The choice of antibody format affects the pharmaceutical quality of fusion proteins and has a significant impact on their disease-targeting performance. The IgG format has often been used for immunocytokines development, despite its long circulatory half-life. The sequential fusion of cytokines and antibody fragments using suitable linkers allows the generation of novel tumor-targeting pro-inflammatory proteins exhibiting favorable tumor-to-organ ratios at early time points after intravenous administration and advantageous pharmacokinetic profiles.

Last but not least, the judicious choice of suitable cytokines and combination partners will determine the success of the immunocytokine in clinical development programs. Until now, highly potent cytokines have been the preferred partners for immunocytokine development and for pharmaco delivery approaches. However, the performance of strong proinflammatory cytokines in the context of polymorbid patients deserves a closer analysis and will have to be studied in the future. In a mouse model of psoriasis and arthritis, the antibody-mediated targeted delivery of IL2 and TNF worsened the inflammatory conditions, while IL12-based immunocytokines did not [160,161]. These results, combined with the observation that IL12-based immunocytokines display a potent therapeutic activity in mouse models of cancer, suggest that IL12 may be a particularly suitable payload for the treatment of cancer patients, who have additional angiogenesis-related diseases.

Synergistic effects have often been observed combining immunocytokines and chemotherapy. The mechanism underlying this effect should be further investigated in order to rationally design combination

studies in the clinical setting. When designing combination strategies, not only the choice of the combination partner is important, but also the dose injected (i.e. doses with manageable toxicities vs high dose in intensive care units), as well as the duration of the infusion. Of major relevance is also the schedule used, including the sequence of administration. In fact, in a mouse model it was shown that injecting paclitaxel prior to immunocytokine administration resulted in an impressive improvement of the therapeutic effect [148].

7. REFERENCES

- 1 Kohler, G. and Milstein, C. (1975) Continuous cultures of fused cells secreting antibody of predefined specificity. *Nature* 256 (5517), 495-497
- 2 Liu, A.Y. et al. (1987) Chimeric mouse-human IgG1 antibody that can mediate lysis of cancer cells. *Proc Natl Acad Sci U S A* 84 (10), 3439-3443
- 3 Riechmann, L. et al. (1988) Reshaping human antibodies for therapy. *Nature* 332 (6162), 323-327
- 4 Grillo-Lopez, A.J. et al. (2002) Rituximab: ongoing and future clinical development. *Semin Oncol* 29 (1 Suppl 2), 105-112
- 5 Walsh, G. Biopharmaceutical benchmarks 2010. *Nat Biotechnol* 28 (9), 917-924
- 6 Tuma, R.S. (2011) Strides in melanoma announced: maximizing value comes next. *J Natl Cancer Inst* 103 (13), 997-999
- 7 Schrama, D. et al. (2006) Antibody targeted drugs as cancer therapeutics. *Nat Rev Drug Discov* 5 (2), 147-159
- 8 Younes, A. et al. (2012) Brentuximab vedotin. *Nat Rev Drug Discov* 11 (1), 19-20
- 9 Aoki, T. et al. (1992) Expression of murine interleukin 7 in a murine glioma cell line results in reduced tumorigenicity in vivo. *Proc Natl Acad Sci U S A* 89 (9), 3850-3854
- 10 Barker, S.E. et al. (2007) Immunotherapy for neuroblastoma using syngeneic fibroblasts transfected with IL-2 and IL-12. *Br J Cancer* 97 (2), 210-217
- 11 Jackaman, C. et al. (2003) IL-2 intratumoral immunotherapy enhances CD8+ T cells that mediate destruction of tumor cells and tumor-associated vasculature: a novel mechanism for IL-2. *J Immunol* 171 (10), 5051-5063
- 12 Koshita, Y. et al. (1995) Efficacy of TNF-alpha gene-transduced tumor cells in treatment of established in vivo tumor. *Int J Cancer* 63 (1), 130-135
- 13 Miller, P.W. et al. (2000) Intratumoral administration of adenoviral interleukin 7 gene-modified dendritic cells augments specific antitumor immunity and achieves tumor eradication. *Hum Gene Ther* 11 (1), 53-65
- 14 Becker, J.C. et al. (1996) T cell-mediated eradication of murine metastatic melanoma induced by targeted interleukin 2 therapy. *J Exp Med* 183 (5), 2361-2366

- 15 Becker, J.C. et al. (1996) Eradication of human hepatic and pulmonary melanoma metastases in SCID mice by antibody-interleukin 2 fusion proteins. *Proc Natl Acad Sci U S A* 93 (7), 2702-2707
- 16 Xiang, R. et al. (1997) Elimination of established murine colon carcinoma metastases by antibody-interleukin 2 fusion protein therapy. *Cancer Res* 57 (21), 4948-4955
- 17 Leonard, J.P. et al. (1997) Effects of single-dose interleukin-12 exposure on interleukin-12-associated toxicity and interferon-gamma production. *Blood* 90 (7), 2541-2548
- 18 Neri, D. and Bicknell, R. (2005) Tumour vascular targeting. *Nat Rev Cancer* 5 (6), 436-446
- 19 Neri, D. and Supuran, C.T. (2011) Interfering with pH regulation in tumours as a therapeutic strategy. *Nat Rev Drug Discov* 10 (10), 767-777
- 20 Schwager, K. et al. (2009) Preclinical characterization of DEKAVIL (F8-IL10), a novel clinical-stage immunocytokine which inhibits the progression of collagen-induced arthritis. *Arthritis Res Ther* 11 (5), R142
- 21 Borgia, B. et al. A proteomic approach for the identification of vascular markers of liver metastasis. *Cancer Res* 70 (1), 309-318
- 22 Schliemann, C. et al. In vivo biotinylation of the vasculature in B-cell lymphoma identifies BST-2 as a target for antibody-based therapy. *Blood* 115 (3), 736-744
- 23 Carnemolla, B. et al. (2002) Enhancement of the antitumor properties of interleukin-2 by its targeted delivery to the tumor blood vessel extracellular matrix. *Blood* 99 (5), 1659-1665
- 24 Halin, C. et al. (2002) Enhancement of the antitumor activity of interleukin-12 by targeted delivery to neovasculature. *Nat Biotechnol* 20 (3), 264-269
- 25 Holliger, P. et al. (1993) "Diabodies": small bivalent and bispecific antibody fragments. *Proc Natl Acad Sci U S A* 90 (14), 6444-6448
- 26 Borsi, L. et al. (2002) Selective targeting of tumoral vasculature: comparison of different formats of an antibody (L19) to the ED-B domain of fibronectin. *Int J Cancer* 102 (1), 75-85
- 27 Wu, A.M. et al. (1996) Tumor localization of anti-CEA single-chain Fvs: improved targeting by non-covalent dimers. *Immunotechnology* 2 (1), 21-36
- 28 Pasche, N. and Neri, D. (2012) Immunocytokines: a novel class of potent armed antibodies. *Drug Discovery Today*
- 29 Rosenblum, M.G. et al. (1995) An antimelanoma immunotoxin containing recombinant human tumor necrosis factor: tissue disposition, pharmacokinetic, and therapeutic studies in xenograft models. *Cancer Immunol Immunother* 40 (5), 322-328

- 30 Rossi, E.A. et al. (2009) CD20-targeted tetrameric interferon-alpha, a novel and potent immunocytokine for the therapy of B-cell lymphomas. *Blood* 114 (18), 3864-3871
- 31 Rossi, E.A. et al. Preclinical studies on targeted delivery of multiple IFNalpha2b to HLA-DR in diverse hematologic cancers. *Blood* 118 (7), 1877-1884
- 32 Borsi, L. et al. (2003) Selective targeted delivery of TNFalpha to tumor blood vessels. *Blood* 102 (13), 4384-4392
- 33 Kaspar, M. et al. (2007) The antibody-mediated targeted delivery of interleukin-15 and GM-CSF to the tumor neovasculature inhibits tumor growth and metastasis. *Cancer Res* 67 (10), 4940-4948
- 34 Pasche, N. et al. (2011) Cloning and characterization of novel tumor-targeting immunocytokines based on murine IL7. *J Biotechnol* 154 (1), 84-92
- 35 Ebbinghaus, C. et al. (2005) Engineered vascular-targeting antibody-interferon-gamma fusion protein for cancer therapy. *Int J Cancer* 116 (2), 304-313
- 36 Holden, S.A. et al. (2001) Augmentation of antitumor activity of an antibody-interleukin 2 immunocytokine with chemotherapeutic agents. *Clin Cancer Res* 7 (9), 2862-2869
- 37 Marlind, J. et al. (2008) Antibody-mediated delivery of interleukin-2 to the stroma of breast cancer strongly enhances the potency of chemotherapy. *Clin Cancer Res* 14 (20), 6515-6524
- 38 Pedretti, M. et al. (2010) Combination of temozolomide with immunocytokine F16-IL2 for the treatment of glioblastoma. *Br J Cancer* 103 (6), 827-836
- 39 Schliemann, C. et al. (2009) Complete eradication of human B-cell lymphoma xenografts using rituximab in combination with the immunocytokine L19-IL2. *Blood* 113 (10), 2275-2283
- 40 Halin, C. et al. (2003) Synergistic therapeutic effects of a tumor targeting antibody fragment, fused to interleukin 12 and to tumor necrosis factor alpha. *Cancer Res* 63 (12), 3202-3210
- 41 Hornick, J.L. et al. (1999) Pretreatment with a monoclonal antibody/interleukin-2 fusion protein directed against DNA enhances the delivery of therapeutic molecules to solid tumors. *Clin Cancer Res* 5 (1), 51-60
- 42 Frey, K. et al. (2010) The immunocytokine F8-IL2 improves the therapeutic performance of sunitinib in a mouse model of renal cell carcinoma. *J Urol* 184 (6), 2540-2548
- 43 Balza, E. et al. (2006) Targeted delivery of tumor necrosis factor-alpha to tumor vessels induces a therapeutic T cell-mediated immune response that protects the host against syngeneic tumors of different histologic origin. *Clin Cancer Res* 12 (8), 2575-2582

- 44** Gillies, S.D. et al. (2002) Bi-functional cytokine fusion proteins for gene therapy and antibody-targeted treatment of cancer. *Cancer Immunol Immunother* 51 (8), 449-460
- 45** Johannsen, M. et al. (2010) The tumour-targeting human L19-IL2 immunocytokine: preclinical safety studies, phase I clinical trial in patients with solid tumours and expansion into patients with advanced renal cell carcinoma. *Eur J Cancer* 46 (16), 2926-2935
- 46** Eigentler, T.K. et al. (2011) A dose-escalation and signal-generating study of the immunocytokine L19-IL2 in combination with dacarbazine for the therapy of patients with metastatic melanoma. *Clin Cancer Res*
- 47** King, D.M. et al. (2004) Phase I clinical trial of the immunocytokine EMD 273063 in melanoma patients. *J Clin Oncol* 22 (22), 4463-4473
- 48** Ribas, A. et al. (2009) Phase I/II open-label study of the biologic effects of the interleukin-2 immunocytokine EMD 273063 (hu14.18-IL2) in patients with metastatic malignant melanoma. *J Transl Med* 7, 68
- 49** Osenga, K.L. et al. (2006) A phase I clinical trial of the hu14.18-IL2 (EMD 273063) as a treatment for children with refractory or recurrent neuroblastoma and melanoma: a study of the Children's Oncology Group. *Clin Cancer Res* 12 (6), 1750-1759
- 50** Shusterman, S. et al. Antitumor activity of hu14.18-IL2 in patients with relapsed/refractory neuroblastoma: a Children's Oncology Group (COG) phase II study. *J Clin Oncol* 28 (33), 4969-4975
- 51** Ko, Y.J. et al. (2004) Safety, pharmacokinetics, and biological pharmacodynamics of the immunocytokine EMD 273066 (huKS-IL2): results of a phase I trial in patients with prostate cancer. *J Immunother* 27 (3), 232-239
- 52** Yang, J.C. et al. (2003) Randomized study of high-dose and low-dose interleukin-2 in patients with metastatic renal cancer. *J Clin Oncol* 21 (16), 3127-3132
- 53** Rosenberg, S.A. et al. (1998) Durability of complete responses in patients with metastatic cancer treated with high-dose interleukin-2: identification of the antigens mediating response. *Ann Surg* 228 (3), 307-319
- 54** Johannsen, M. et al. The tumour-targeting human L19-IL2 immunocytokine: preclinical safety studies, phase I clinical trial in patients with solid tumours and expansion into patients with advanced renal cell carcinoma. *Eur J Cancer* 46 (16), 2926-2935

- 55 Kirchner, G.I. et al. (1998) Pharmacokinetics of recombinant human interleukin-2 in advanced renal cell carcinoma patients following subcutaneous application. *Br J Clin Pharmacol* 46 (1), 5-10
- 56 Rudman, S.M. et al. (2011) A phase 1 study of AS1409, a novel antibody-cytokine fusion protein, in patients with malignant melanoma or renal cell carcinoma. *Clin Cancer Res* 17 (7), 1998-2005
- 57 Tijink, B.M. et al. (2009) (124)I-L19-SIP for immuno-PET imaging of tumour vasculature and guidance of (131)I-L19-SIP radioimmunotherapy. *Eur J Nucl Med Mol Imaging* 36 (8), 1235-1244
- 58 Bassani-Sternberg, M. et al. Soluble plasma HLA peptidome as a potential source for cancer biomarkers. *Proc Natl Acad Sci U S A* 107 (44), 18769-18776
- 59 Namen, A.E. et al. (1988) Stimulation of B-cell progenitors by cloned murine interleukin-7. *Nature* 333 (6173), 571-573
- 60 Namen, A.E. et al. (1988) B cell precursor growth-promoting activity. Purification and characterization of a growth factor active on lymphocyte precursors. *J Exp Med* 167 (3), 988-1002
- 61 Fry, T.J. and Mackall, C.L. (2002) Interleukin-7: from bench to clinic. *Blood* 99 (11), 3892-3904
- 62 Conlon, P.J. et al. (1989) Murine thymocytes proliferate in direct response to interleukin-7. *Blood* 74 (4), 1368-1373
- 63 Morrissey, P.J. et al. (1989) Recombinant interleukin 7, pre-B cell growth factor, has costimulatory activity on purified mature T cells. *J Exp Med* 169 (3), 707-716
- 64 Chazen, G.D. et al. (1989) Interleukin 7 is a T-cell growth factor. *Proc Natl Acad Sci U S A* 86 (15), 5923-5927
- 65 Borger, P. et al. (1996) IL-7 differentially modulates the expression of IFN-gamma and IL-4 in activated human T lymphocytes by transcriptional and post-transcriptional mechanisms. *J Immunol* 156 (4), 1333-1338
- 66 Gringhuis, S.I. et al. (1997) Interleukin-7 upregulates the interleukin-2-gene expression in activated human T lymphocytes at the transcriptional level by enhancing the DNA binding activities of both nuclear factor of activated T cells and activator protein-1. *Blood* 90 (7), 2690-2700
- 67 Vella, A.T. et al. (1998) Cytokine-induced survival of activated T cells in vitro and in vivo. *Proc Natl Acad Sci U S A* 95 (7), 3810-3815

- 68 Komschlies, K.L. et al. (1994) Administration of recombinant human IL-7 to mice alters the composition of B-lineage cells and T cell subsets, enhances T cell function, and induces regression of established metastases. *J Immunol* 152 (12), 5776-5784
- 69 Hock, H. et al. (1991) Interleukin 7 induces CD4+ T cell-dependent tumor rejection. *J Exp Med* 174 (6), 1291-1298
- 70 Miller, A.R. et al. (1993) Transduction of human melanoma cell lines with the human interleukin-7 gene using retroviral-mediated gene transfer: comparison of immunologic properties with interleukin-2. *Blood* 82 (12), 3686-3694
- 71 Sharma, S. et al. (2003) Interleukin-7 gene-modified dendritic cells reduce pulmonary tumor burden in spontaneous murine bronchoalveolar cell carcinoma. *Hum Gene Ther* 14 (16), 1511-1524
- 72 Sportes, C. et al. (2010) Phase I study of recombinant human interleukin-7 administration in subjects with refractory malignancy. *Clin Cancer Res* 16 (2), 727-735
- 73 Cosenza, L. et al. (1997) Disulfide bond assignment in human interleukin-7 by matrix-assisted laser desorption/ionization mass spectroscopy and site-directed cysteine to serine mutational analysis. *J Biol Chem* 272 (52), 32995-33000
- 74 Wolf, S.F. et al. (1991) Cloning of cDNA for natural killer cell stimulatory factor, a heterodimeric cytokine with multiple biologic effects on T and natural killer cells. *J Immunol* 146 (9), 3074-3081
- 75 Magram, J. et al. (1996) IL-12-deficient mice are defective in IFN gamma production and type 1 cytokine responses. *Immunity* 4 (5), 471-481
- 76 Manetti, R. et al. (1993) Natural killer cell stimulatory factor (interleukin 12 [IL-12]) induces T helper type 1 (Th1)-specific immune responses and inhibits the development of IL-4-producing Th cells. *J Exp Med* 177 (4), 1199-1204
- 77 Schmitt, E. et al. (1994) Differential effects of interleukin-12 on the development of naive mouse CD4+ T cells. *Eur J Immunol* 24 (2), 343-347
- 78 Schmitt, E. et al. (1994) T helper type 1 development of naive CD4+ T cells requires the coordinate action of interleukin-12 and interferon-gamma and is inhibited by transforming growth factor-beta. *Eur J Immunol* 24 (4), 793-798
- 79 Sypek, J.P. et al. (1993) Resolution of cutaneous leishmaniasis: interleukin 12 initiates a protective T helper type 1 immune response. *J Exp Med* 177 (6), 1797-1802

- 80** Murphy, E.E. et al. (1994) B7 and interleukin 12 cooperate for proliferation and interferon gamma production by mouse T helper clones that are unresponsive to B7 costimulation. *J Exp Med* 180 (1), 223-231
- 81** Curtsinger, J.M. et al. (2003) Signal 3 determines tolerance versus full activation of naive CD8 T cells: dissociating proliferation and development of effector function. *J Exp Med* 197 (9), 1141-1151
- 82** Yoo, J.K. et al. (2002) IL-12 provides proliferation and survival signals to murine CD4+ T cells through phosphatidylinositol 3-kinase/Akt signaling pathway. *J Immunol* 169 (7), 3637-3643
- 83** Colombo, M.P. and Trinchieri, G. (2002) Interleukin-12 in anti-tumor immunity and immunotherapy. *Cytokine Growth Factor Rev* 13 (2), 155-168
- 84** Brunda, M.J. et al. (1993) Antitumor and antimetastatic activity of interleukin 12 against murine tumors. *J Exp Med* 178 (4), 1223-1230
- 85** Atkins, M.B. et al. (1997) Phase I evaluation of intravenous recombinant human interleukin 12 in patients with advanced malignancies. *Clin Cancer Res* 3 (3), 409-417
- 86** Bajetta, E. et al. (1998) Pilot study of subcutaneous recombinant human interleukin 12 in metastatic melanoma. *Clin Cancer Res* 4 (1), 75-85
- 87** Gollob, J.A. et al. (2000) Phase I trial of twice-weekly intravenous interleukin 12 in patients with metastatic renal cell cancer or malignant melanoma: ability to maintain IFN-gamma induction is associated with clinical response. *Clin Cancer Res* 6 (5), 1678-1692
- 88** Motzer, R.J. et al. (1998) Phase I trial of subcutaneous recombinant human interleukin-12 in patients with advanced renal cell carcinoma. *Clin Cancer Res* 4 (5), 1183-1191
- 89** Motzer, R.J. et al. (2001) Randomized multicenter phase II trial of subcutaneous recombinant human interleukin-12 versus interferon-alpha 2a for patients with advanced renal cell carcinoma. *J Interferon Cytokine Res* 21 (4), 257-263
- 90** Lenzi, R. et al. (2007) Phase II study of intraperitoneal recombinant interleukin-12 (rhIL-12) in patients with peritoneal carcinomatosis (residual disease < 1 cm) associated with ovarian cancer or primary peritoneal carcinoma. *J Transl Med* 5, 66
- 91** Lenzi, R. et al. (2002) Phase I study of intraperitoneal recombinant human interleukin 12 in patients with Mullerian carcinoma, gastrointestinal primary malignancies, and mesothelioma. *Clin Cancer Res* 8 (12), 3686-3695

- 92** Wadler, S. et al. (2004) A phase II trial of interleukin-12 in patients with advanced cervical cancer: clinical and immunologic correlates. Eastern Cooperative Oncology Group study E1E96. *Gynecol Oncol* 92 (3), 957-964
- 93** Weiss, G.R. et al. (2003) Phase 1 study of the intravesical administration of recombinant human interleukin-12 in patients with recurrent superficial transitional cell carcinoma of the bladder. *J Immunother* 26 (4), 343-348
- 94** Rook, A.H. et al. (1999) Interleukin-12 therapy of cutaneous T-cell lymphoma induces lesion regression and cytotoxic T-cell responses. *Blood* 94 (3), 902-908
- 95** Little, R.F. et al. (2006) Activity of subcutaneous interleukin-12 in AIDS-related Kaposi sarcoma. *Blood* 107 (12), 4650-4657
- 96** Younes, A. et al. (2004) Phase II clinical trial of interleukin-12 in patients with relapsed and refractory non-Hodgkin's lymphoma and Hodgkin's disease. *Clin Cancer Res* 10 (16), 5432-5438
- 97** Pini, A. et al. (1998) Design and use of a phage display library. Human antibodies with subnanomolar affinity against a marker of angiogenesis eluted from a two-dimensional gel. *J Biol Chem* 273 (34), 21769-21776
- 98** Gafner, V. et al. (2006) An engineered antibody-interleukin-12 fusion protein with enhanced tumor vascular targeting properties. *Int J Cancer* 119 (9), 2205-2212
- 99** Somavilla, R. et al. (2010) Expression, engineering and characterization of the tumor-targeting heterodimeric immunocytokine F8-IL12. *Protein Eng Des Sel* 23 (8), 653-661
- 100** Lo, K.M. et al. (2007) huBC1-IL12, an immunocytokine which targets EDB-containing oncofetal fibronectin in tumors and tumor vasculature, shows potent anti-tumor activity in human tumor models. *Cancer Immunol Immunother* 56 (4), 447-457
- 101** Carnemolla, B. et al. (1992) The inclusion of the type III repeat ED-B in the fibronectin molecule generates conformational modifications that unmask a cryptic sequence. *J Biol Chem* 267 (34), 24689-24692
- 102** Gaffen, S.L. (2008) An overview of IL-17 function and signaling. *Cytokine* 43 (3), 402-407
- 103** Yu, J.J. and Gaffen, S.L. (2008) Interleukin-17: a novel inflammatory cytokine that bridges innate and adaptive immunity. *Front Biosci* 13, 170-177
- 104** Rouvier, E. et al. (1993) CTLA-8, cloned from an activated T cell, bearing AU-rich messenger RNA instability sequences, and homologous to a herpesvirus saimiri gene. *J Immunol* 150 (12), 5445-5456

- 105** Yao, Z. et al. (1995) Human IL-17: a novel cytokine derived from T cells. *J Immunol* 155 (12), 5483-5486
- 106** Fossiez, F. et al. (1996) T cell interleukin-17 induces stromal cells to produce proinflammatory and hematopoietic cytokines. *J Exp Med* 183 (6), 2593-2603
- 107** Steinman, L. (2007) A brief history of T(H)17, the first major revision in the T(H)1/T(H)2 hypothesis of T cell-mediated tissue damage. *Nat Med* 13 (2), 139-145
- 108** McGeachy, M.J. et al. (2007) TGF-beta and IL-6 drive the production of IL-17 and IL-10 by T cells and restrain T(H)-17 cell-mediated pathology. *Nat Immunol* 8 (12), 1390-1397
- 109** Liu, X.K. et al. (2005) Signaling through the murine T cell receptor induces IL-17 production in the absence of costimulation, IL-23 or dendritic cells. *Mol Cells* 20 (3), 339-347
- 110** Rachitskaya, A.V. et al. (2008) Cutting edge: NKT cells constitutively express IL-23 receptor and RORgammat and rapidly produce IL-17 upon receptor ligation in an IL-6-independent fashion. *J Immunol* 180 (8), 5167-5171
- 111** Stark, M.A. et al. (2005) Phagocytosis of apoptotic neutrophils regulates granulopoiesis via IL-23 and IL-17. *Immunity* 22 (3), 285-294
- 112** Harrington, L.E. et al. (2005) Interleukin 17-producing CD4+ effector T cells develop via a lineage distinct from the T helper type 1 and 2 lineages. *Nat Immunol* 6 (11), 1123-1132
- 113** Park, H. et al. (2005) A distinct lineage of CD4 T cells regulates tissue inflammation by producing interleukin 17. *Nat Immunol* 6 (11), 1133-1141
- 114** Stumhofer, J.S. et al. (2006) Interleukin 27 negatively regulates the development of interleukin 17-producing T helper cells during chronic inflammation of the central nervous system. *Nat Immunol* 7 (9), 937-945
- 115** Shen, F. et al. (2006) Identification of common transcriptional regulatory elements in interleukin-17 target genes. *J Biol Chem* 281 (34), 24138-24148
- 116** Lubberts, E. (2008) IL-17/Th17 targeting: on the road to prevent chronic destructive arthritis? *Cytokine* 41 (2), 84-91
- 117** Lubberts, E. et al. (2004) Treatment with a neutralizing anti-murine interleukin-17 antibody after the onset of collagen-induced arthritis reduces joint inflammation, cartilage destruction, and bone erosion. *Arthritis Rheum* 50 (2), 650-659
- 118** Nakae, S. et al. (2003) Suppression of immune induction of collagen-induced arthritis in IL-17-deficient mice. *J Immunol* 171 (11), 6173-6177

- 119** Numasaki, M. et al. (2005) IL-17 enhances the net angiogenic activity and in vivo growth of human non-small cell lung cancer in SCID mice through promoting CXCR-2-dependent angiogenesis. *J Immunol* 175 (9), 6177-6189
- 120** Numasaki, M. et al. (2003) Interleukin-17 promotes angiogenesis and tumor growth. *Blood* 101 (7), 2620-2627
- 121** Murugaiyan, G. and Saha, B. (2009) Protumor vs antitumor functions of IL-17. *J Immunol* 183 (7), 4169-4175
- 122** Tartour, E. et al. (1999) Interleukin 17, a T-cell-derived cytokine, promotes tumorigenicity of human cervical tumors in nude mice. *Cancer Res* 59 (15), 3698-3704
- 123** Benchetrit, F. et al. (2002) Interleukin-17 inhibits tumor cell growth by means of a T-cell-dependent mechanism. *Blood* 99 (6), 2114-2121
- 124** Kryczek, I. et al. (2009) Endogenous IL-17 contributes to reduced tumor growth and metastasis. *Blood* 114 (2), 357-359
- 125** Ngiow, S.F. et al. (2010) Does IL-17 suppress tumor growth? *Blood* 115 (12), 2554-2555; author reply 2556-2557
- 126** Dinarello, C.A. (1999) Interleukin-18. *Methods* 19 (1), 121-132
- 127** Ushio, S. et al. (1996) Cloning of the cDNA for human IFN-gamma-inducing factor, expression in *Escherichia coli*, and studies on the biologic activities of the protein. *J Immunol* 156 (11), 4274-4279
- 128** Gu, Y. et al. (1997) Activation of interferon-gamma inducing factor mediated by interleukin-1beta converting enzyme. *Science* 275 (5297), 206-209
- 129** Gracie, J.A. et al. (2003) Interleukin-18. *J Leukoc Biol* 73 (2), 213-224
- 130** Gracie, J.A. et al. (1999) A proinflammatory role for IL-18 in rheumatoid arthritis. *J Clin Invest* 104 (10), 1393-1401
- 131** Leung, B.P. et al. (2001) A role for IL-18 in neutrophil activation. *J Immunol* 167 (5), 2879-2886
- 132** Ahn, H.J. et al. (1997) A mechanism underlying synergy between IL-12 and IFN-gamma-inducing factor in enhanced production of IFN-gamma. *J Immunol* 159 (5), 2125-2131
- 133** Munder, M. et al. (1998) Murine macrophages secrete interferon gamma upon combined stimulation with interleukin (IL)-12 and IL-18: A novel pathway of autocrine macrophage activation. *J Exp Med* 187 (12), 2103-2108

- 134** Micallef, M.J. et al. (1997) In vivo antitumor effects of murine interferon-gamma-inducing factor/interleukin-18 in mice bearing syngeneic Meth A sarcoma malignant ascites. *Cancer Immunol Immunother* 43 (6), 361-367
- 135** Osaki, T. et al. (1998) IFN-gamma-inducing factor/IL-18 administration mediates IFN-gamma- and IL-12-independent antitumor effects. *J Immunol* 160 (4), 1742-1749
- 136** Yamashita, K. et al. (2002) Interleukin-18 inhibits lodging and subsequent growth of human multiple myeloma cells in the bone marrow. *Oncol Rep* 9 (6), 1237-1244
- 137** Okamoto, T. et al. (2004) Inhibition by interleukin-18 of the growth of Dunn osteosarcoma cells. *J Interferon Cytokine Res* 24 (3), 161-167
- 138** Akamatsu, S. et al. (2002) Antitumor activity of interleukin-18 against the murine T-cell leukemia/lymphoma EL-4 in syngeneic mice. *J Immunother* 25 Suppl 1, S28-34
- 139** Robertson, M.J. et al. (2006) Clinical and biological effects of recombinant human interleukin-18 administered by intravenous infusion to patients with advanced cancer. *Clin Cancer Res* 12 (14 Pt 1), 4265-4273
- 140** Robertson, M.J. et al. (2008) A dose-escalation study of recombinant human interleukin-18 using two different schedules of administration in patients with cancer. *Clin Cancer Res* 14 (11), 3462-3469
- 141** Tarhini, A.A. et al. (2009) A phase 2, randomized study of SB-485232, rhIL-18, in patients with previously untreated metastatic melanoma. *Cancer* 115 (4), 859-868
- 142** Helguera, G. et al. (2002) Antibody-cytokine fusion proteins: harnessing the combined power of cytokines and antibodies for cancer therapy. *Clin Immunol* 105 (3), 233-246
- 143** Schliemann, C. and Neri, D. (2007) Antibody-based targeting of the tumor vasculature. *Biochim Biophys Acta* 1776 (2), 175-192
- 144** Villa, A. et al. (2008) A high-affinity human monoclonal antibody specific to the alternatively spliced EDA domain of fibronectin efficiently targets tumor neo-vasculature in vivo. *Int J Cancer* 122 (11), 2405-2413
- 145** Frey, K. et al. (2011) Antibody-based targeting of interferon-alpha to the tumor neovasculature: a critical evaluation. *Integr Biol (Camb)*
- 146** Pasche, N. et al. (2011) The targeted delivery of IL17 to the mouse neo-vasculature enhances angiogenesis but does not reduce tumor growth rate. *Angiogenesis*
- 147** Pasche, N. et al. The antibody-based delivery of interleukin-12 to the tumor neo-vasculature eradicates cancer in combination with paclitaxel. *Submitted*

- 148** Moschetta, M. et al. (2012) Paclitaxel enhances the therapeutic efficacy of F8 antibody-interleukin-2 conjugate (F8-IL2) to EDA-fibronectin positive human melanoma xenografts. *Cancer Res*
- 149** Silacci, M. et al. (2005) Design, construction, and characterization of a large synthetic human antibody phage display library. *Proteomics* 5 (9), 2340-2350
- 150** Muller, N. et al. (2007) Scalable transient gene expression in Chinese hamster ovary cells in instrumented and non-instrumented cultivation systems. *Biotechnol Lett* 29 (5), 703-711
- 151** Senter, P.D. (2009) Potent antibody drug conjugates for cancer therapy. *Curr Opin Chem Biol* 13 (3), 235-244
- 152** Steiner, M. and Neri, D. (2011) Antibody-radionuclide conjugates for cancer therapy: historical considerations and new trends. *Clin Cancer Res* 17 (20), 6406-6416
- 153** Carter, P. (2001) Improving the efficacy of antibody-based cancer therapies. *Nat Rev Cancer* 1 (2), 118-129
- 154** Gillies, S.D. et al. (2005) An anti-CD20-IL-2 immunocytokine is highly efficacious in a SCID mouse model of established human B lymphoma. *Blood* 105 (10), 3972-3978
- 155** Liu, Y. et al. (2006) The antimelanoma immunocytokine scFvMEL/TNF shows reduced toxicity and potent antitumor activity against human tumor xenografts. *Neoplasia* 8 (5), 384-393
- 156** Tarli, L. et al. (1999) A high-affinity human antibody that targets tumoral blood vessels. *Blood* 94 (1), 192-198
- 157** Dor, Y. et al. (2003) Induction of vascular networks in adult organs: implications to proangiogenic therapy. *Ann N Y Acad Sci* 995, 208-216
- 158** Quezada, S.A. et al. (2010) Tumor-reactive CD4(+) T cells develop cytotoxic activity and eradicate large established melanoma after transfer into lymphopenic hosts. *J Exp Med* 207 (3), 637-650
- 159** Yang, X. et al. (2006) Targeted in vivo expression of IFN-gamma-inducible protein 10 induces specific antitumor activity. *J Leukoc Biol* 80 (6), 1434-1444
- 160** Trachsel, E. et al. (2007) A human mAb specific to oncofetal fibronectin selectively targets chronic skin inflammation in vivo. *J Invest Dermatol* 127 (4), 881-886
- 161** Trachsel, E. et al. (2007) Antibody-mediated delivery of IL-10 inhibits the progression of established collagen-induced arthritis. *Arthritis Res Ther* 9 (1), R9
- 162** Schwager, K. et al. (2011) The antibody-mediated targeted delivery of interleukin-10 inhibits endometriosis in a syngeneic mouse model. *Hum Reprod* 26 (9), 2344-2352

- 163** Dietrich, T. et al. (2012) Local delivery of IL-2 reduces atherosclerosis via expansion of regulatory T cells. *Atherosclerosis*
- 164** Frey, K. et al. (2011) Different patterns of fibronectin and tenascin-C splice variants expression in primary and metastatic melanoma lesions. *Exp Dermatol* 20 (8), 685-688
- 165** Schliemann, C. et al. (2009) Three clinical-stage tumor targeting antibodies reveal differential expression of oncofetal fibronectin and tenascin-C isoforms in human lymphoma. *Leuk Res* 33 (12), 1718-1722
- 166** Fiechter, M. et al. Comparative in vivo analysis of the atherosclerotic plaque targeting properties of eight human monoclonal antibodies. *Atherosclerosis* 214 (2), 325-330
- 167** Pedretti, M. et al. (2010) Comparative immunohistochemical staining of atherosclerotic plaques using F16, F8 and L19: Three clinical-grade fully human antibodies. *Atherosclerosis* 208 (2), 382-389
- 168** Bauer, S. et al. (2004) Targeted bioactivity of membrane-anchored TNF by an antibody-derived TNF fusion protein. *J Immunol* 172 (6), 3930-3939
- 169** Bauer, S. et al. (2009) Targeted therapy of renal cell carcinoma: synergistic activity of cG250-TNF and IFN γ . *Int J Cancer* 125 (1), 115-123
- 170** Liu, Y. et al. (2004) Recombinant single-chain antibody fusion construct targeting human melanoma cells and containing tumor necrosis factor. *Int J Cancer* 108 (4), 549-557
- 171** Cooke, S.P. et al. (2002) In vivo tumor delivery of a recombinant single chain Fv::tumor necrosis factor- α fusion [correction of factor: a fusion] protein. *Bioconjug Chem* 13 (1), 7-15
- 172** Sharifi, J. et al. (2002) Generation of human interferon gamma and tumor Necrosis factor alpha chimeric TNT-3 fusion proteins. *Hybrid Hybridomics* 21 (6), 421-432
- 173** Christ, O. et al. (2001) Efficacy of local versus systemic application of antibody-cytokine fusion proteins in tumor therapy. *Clin Cancer Res* 7 (4), 985-998
- 174** Scherf, U. et al. (1996) Cytotoxic and antitumor activity of a recombinant tumor necrosis factor-B1(Fv) fusion protein on LeY antigen-expressing human cancer cells. *Clin Cancer Res* 2 (9), 1523-1531
- 175** Dela Cruz, J.S. et al. (2000) Recombinant anti-human HER2/neu IgG3-(GM-CSF) fusion protein retains antigen specificity and cytokine function and demonstrates antitumor activity. *J Immunol* 165 (9), 5112-5121

- 176** Hornick, J.L. et al. (1997) Chimeric CLL-1 antibody fusion proteins containing granulocyte-macrophage colony-stimulating factor or interleukin-2 with specificity for B-cell malignancies exhibit enhanced effector functions while retaining tumor targeting properties. *Blood* 89 (12), 4437-4447
- 177** Dolman, C.S. et al. (1998) Suppression of human prostate carcinoma metastases in severe combined immunodeficient mice by interleukin 2 immunocytokine therapy. *Clin Cancer Res* 4 (10), 2551-2557
- 178** Becker, J.C. et al. (1996) Long-lived and transferable tumor immunity in mice after targeted interleukin-2 therapy. *J Clin Invest* 98 (12), 2801-2804
- 179** Lode, H.N. et al. (1997) Targeted interleukin-2 therapy for spontaneous neuroblastoma metastases to bone marrow. *J Natl Cancer Inst* 89 (21), 1586-1594
- 180** Neal, Z.C. et al. (2004) Enhanced activity of hu14.18-IL2 immunocytokine against murine NXS2 neuroblastoma when combined with interleukin 2 therapy. *Clin Cancer Res* 10 (14), 4839-4847
- 181** Pancook, J.D. et al. (1996) Eradication of established hepatic human neuroblastoma metastases in mice with severe combined immunodeficiency by antibody-targeted interleukin-2. *Cancer Immunol Immunother* 42 (2), 88-92
- 182** Sabzevari, H. et al. (1994) A recombinant antibody-interleukin 2 fusion protein suppresses growth of hepatic human neuroblastoma metastases in severe combined immunodeficiency mice. *Proc Natl Acad Sci U S A* 91 (20), 9626-9630
- 183** Penichet, M.L. et al. (2001) A recombinant IgG3-(IL-2) fusion protein for the treatment of human HER2/neu expressing tumors. *Hum Antibodies* 10 (1), 43-49
- 184** Xu, X. et al. (2000) Targeting and therapy of carcinoembryonic antigen-expressing tumors in transgenic mice with an antibody-interleukin 2 fusion protein. *Cancer Res* 60 (16), 4475-4484
- 185** Matsumoto, H. et al. (2002) Targeting of interleukin-2 to human MK-1-expressing carcinoma by fusion with a single-chain Fv of anti-MK-1 antibody. *Anticancer Res* 22 (4), 2001-2007
- 186** Melani, C. et al. (1998) Targeting of interleukin 2 to human ovarian carcinoma by fusion with a single-chain Fv of antifolate receptor antibody. *Cancer Res* 58 (18), 4146-4154
- 187** Huang, X. et al. (2011) Enhancing the potency of a whole-cell breast cancer vaccine in mice with an antibody-IL-2 immunocytokine that targets exposed phosphatidylserine. *Vaccine* 29 (29-30), 4785-4793
- 188** Gillies, S.D. et al. A low-toxicity IL-2-based immunocytokine retains antitumor activity despite its high degree of IL-2 receptor selectivity. *Clin Cancer Res* 17 (11), 3673-3685

- 189** Li, J. et al. (2004) chTNT-3/hu IL-12 fusion protein for the immunotherapy of experimental solid tumors. *Hybrid Hybridomics* 23 (1), 1-10
- 190** Gillies, S.D. et al. (1998) Antibody-IL-12 fusion proteins are effective in SCID mouse models of prostate and colon carcinoma metastases. *J Immunol* 160 (12), 6195-6203
- 191** Peng, L.S. et al. (2001) Mechanism of antitumor activity of a single-chain interleukin-12 IgG3 antibody fusion protein (mscIL-12.her2.IgG3). *J Interferon Cytokine Res* 21 (9), 709-720
- 192** Peng, L.S. et al. (1999) A single-chain IL-12 IgG3 antibody fusion protein retains antibody specificity and IL-12 bioactivity and demonstrates antitumor activity. *J Immunol* 163 (1), 250-258
- 193** Xuan, C. et al. (2010) Targeted delivery of interferon-alpha via fusion to anti-CD20 results in potent antitumor activity against B-cell lymphoma. *Blood* 115 (14), 2864-2871
- 194** Huang, T.H. et al. (2007) Targeting IFN-alpha to B cell lymphoma by a tumor-specific antibody elicits potent antitumor activities. *J Immunol* 179 (10), 6881-6888
- 195** Mizokami, M.M. et al. (2003) Chimeric TNT-3 antibody/murine interferon-gamma fusion protein for the immunotherapy of solid malignancies. *Hybrid Hybridomics* 22 (4), 197-207

9. ACKNOWLEDGMENTS

First of all, I would like to express my sincere gratitude to my supervisor Prof. Dr. Dario Neri for the great opportunity to perform my PhD in his laboratory, to work on such interesting projects and for supporting and encouraging me during my thesis.

I also thank Prof. Dr. Cornelia Halin-Winter for having kindly accepted to be my co-examiner.

Many thanks go to Prof. Dr. Marra for providing the NIH 3T3 cell line.

I am grateful to current and former members of the Neri Group and Philochem for the nice atmosphere and the pleasant moments spent together. In particular, for their scientific contribution and support during my PhD thesis I would like to thank Dr. Sarah Wulhfard, Dr. Roberto Somavilla and Dr. Alessandra Villa. Moreover, I thank Elena Perrino, Dr. Katharina Frey, Dr. Eveline Trachsel and MD Michael Fiechter for their help with animal experiments.

I am thankful to my master students Janine Woytschak and Elisa Carugati, who contributed to the successful development of my projects.

I also would like to thank my friends that have always supported and encouraged me throughout my PhD thesis. In particular many thanks to Sarah, Andrea, Elena, Roberto, Filippo, Alessandra, Francesca, Giulio, Yanela, Luca, Anita and Manuela.

A special thank goes to my parents and to my sister for their love, support and never ending help.

Finally, I would like to express my deepest gratitude to Mattia who has not only encouraged and motivated me during my thesis, but who was also a great help for me during animal experiments.